



# Formation, antimicrobial activity, and biomedical performance of plant-based nanoparticles: a review

Ngoan Thi Thao Nguyen<sup>1,2</sup> · Luan Minh Nguyen<sup>1,2</sup> · Thuy Thi Thanh Nguyen<sup>2,3</sup> · Thuong Thi Nguyen<sup>1,4</sup> · Duyen Thi Cam Nguyen<sup>1,4</sup> · Thuan Van Tran<sup>1,4</sup>

Received: 16 November 2021 / Accepted: 24 February 2022 / Published online: 25 March 2022  
© The Author(s), under exclusive licence to Springer Nature Switzerland AG 2022

## Abstract

Because many engineered nanoparticles are toxic, there is a need for methods to fabricate safe nanoparticles such as plant-based nanoparticles. Indeed, plant extracts contain flavonoids, amino acids, proteins, polysaccharides, enzymes, polyphenols, steroids, and reducing sugars that facilitate the reduction, formation, and stabilization of nanoparticles. Moreover, synthesizing nanoparticles from plant extracts is fast, safe, and cost-effective because it does not consume much energy, and non-toxic derivatives are generated. These nanoparticles have diverse and unique properties of interest for applications in many fields. Here, we review the synthesis of metal/metal oxide nanoparticles with plant extracts. These nanoparticles display antibacterial, antifungal, anticancer, and antioxidant properties. Plant-based nanoparticles are also useful for medical diagnosis and drug delivery.

**Keywords** Nanoparticles · Green synthesis · Plant extract · Phytochemical compounds · Biomedical applications

## Abbreviations

UV–Vis	Ultraviolet–visible	DFT	Density functional theory
FT-IR	Fourier transform infrared	ROS	Reactive oxygen species
SEM	Scanning electron microscope	VB	The valence band
TEM	Transmission electron microscopy	CB	The conduction band
AFM	Atomic force microscope	CT	Computerized tomography scan
XRD	X-Ray diffraction	MRI	Magnetic resonance imaging
EDS	Energy-dispersive spectroscopy	DPPH	2-Diphenyl-1-picrylhydrazyl
BJH	Barrett, Joyner, and Halenda	MIC	Minimum inhibitory concentration
		MBC	Minimum bactericidal concentration
		IC50	Half-maximal inhibitory concentration
		AGS	Human gastric adenocarcinoma cell line
		HT-29	Human colorectal adenocarcinoma cell line
		PANC-1	Human pancreas ductal adenocarcinoma cell line
		HepG2	Human liver cancer cell line
		MCF-7	Human breast cancer cell line
		AIDS	Acquired immunodeficiency syndrome
		GSH	Glutathione
		A549	Human lung cancer cell line

✉ Duyen Thi Cam Nguyen  
ntcduyen@ntt.edu.vn

✉ Thuan Van Tran  
tranuv@gmail.com; tranvt@ntt.edu.vn;  
ttran@gradcenter.cuny.edu

<sup>1</sup> Institute of Environmental Technology and Sustainable Development, Nguyen Tat Thanh University, 298-300A Nguyen Tat Thanh, District 4, Ho Chi Minh City 755414, Vietnam

<sup>2</sup> Department of Chemical Engineering and Processing, Nong Lam University, Thu Duc District, Ho Chi Minh City 700000, Vietnam

<sup>3</sup> Faculty of Science, Nong Lam University, Thu Duc District, Ho Chi Minh City 700000, Vietnam

<sup>4</sup> NTT Hi-Tech Institute, Nguyen Tat Thanh University, 298-300A Nguyen Tat Thanh, District 4, Ho Chi Minh City 755414, Vietnam

## Introduction

Nanotechnology is mainly related to the design, synthesis, structural analysis, and applications of materials with the sizes less than 100 nm (Mohamad et al. 2013). In recent

years, nanomaterials have been extensively discovered with unique properties and brilliant capabilities since they pave the way for developing multidisciplinary researches, and applying for solving many practical problems. Indeed, they have brought many advantages and desirable prospects for human life such as medicine, pharmaceuticals, agriculture, environment, catalysis, food, cosmetics, and electronics (Ghotekar et al. 2020). The main reason may rely on their tiny size, diverse structure, and many biochemical and physicochemical properties, which are suitable for many different fields. Among them, metallic/metal oxide nanoparticles are considered to be the most superior, possibly thanks to their large surface area to volume ratio, high biocompatibility, tunable synthesis, and high stability (Ahmed et al. 2016). This leads to the huge interest of researchers in the development and synthesis of nanoparticles.

To acquire the purposes of green synthesis and sustainable development, various approaches are still essentially considered. Physical and chemical synthesis methods are not necessarily optimal solutions due to many shortcomings of energy consumption, environmental pollution, and high risks for human health (Mohamad et al. 2013). Twelve principles of green chemistry are guidelines for researchers to take new steps toward green synthesis methods (Ivanković 2017). Green synthesis methods mainly aim to bring more environmentally friendly, healthily safe, and performance benefits than physical or chemical methods (Ahmed et al. 2016). Indeed, the green synthesis is highly preferable because this approach uses raw materials that are locally available, low-cost, and easy to collect. In particular, they considerably save the production cost of nanoparticles due to energy saving and simple routes without complicated equipment and machines (Cuong et al. 2022). There are three major biosynthetic pathways for nanoparticles, specifically from microorganisms, biomolecules, and plants. During the biogenic synthesis of nanoparticles, natural compounds found available in the plant and microbial extracts act as reducing and stabilizing agents. These functional components allow to convert metal sources into nanoparticles (Dabhane et al. 2021). Although the green synthesis methods from microorganisms and biomolecules can bring certain successes, there are still many limitations and challenges in the production of nanoparticles. For example, these methods necessarily require a series of technically and safely serious conditions, whereas the rate of the overall process is very slow to suit for large-scale nanoparticles production (Ghotekar et al. 2021).

Plant extracts may be the best method for the biosynthesis of nanoparticles which can produce nanoparticles in larger amount within a short time with high efficiency and low production cost (Srikar et al. 2016). Plants are prevalently present in ecosystems and can be collected easily. They contain an amount of phytochemicals that can replace highly toxic, expensive, and environmentally

harmful chemical reducing agents such as sodium citrate, sodium borohydride ( $\text{NaBH}_4$ ), and ascorbate (Ahmed et al. 2016). Indeed, many studies indicated that phytochemicals such as polysaccharides, flavonoids, phenolic acids, and quercetins in plant extracts are capable of excellently reducing metal ions, e.g.,  $\text{Ag}^+$ ,  $\text{Cu}^{2+}$ , and  $\text{Au}^{3+}$  (Agarwal et al. 2017; Ong et al. 2018; Jadoun et al. 2021). Moreover, they can exhibit many capping, stabilizing, and chelating functions during the formation of nanoparticles. These biocompounds are also easily extracted from different plant parts such as leaves, flowers, stems, roots and other parts of plants, leading to the superiority of plants for the biosynthesis of nanoparticles (Beyene et al. 2017).

In addition to the highly effective green synthesis, plant synthesized nanoparticles make great contribution to the different fields. For water treatment, they can catalyze reactions that degrade toxic pollutants from the aquatic environment (Veisi et al. 2016; Rasheed et al. 2019; Pakzad et al. 2020). With their small size, high biocompatibility, high surface area, excellent stability, good versatility, and many outstanding capabilities, green nanoparticles are suitable for many medical applications such as antibacterial, antifungal, anti-cancer, and treatment of various diseases (Narendhran and Sivaraj 2016; Pansambal et al. 2017; Qasim Nasar et al. 2019; Youssif et al. 2019). For therapeutic effects, nanoparticles have discovered with their potentials for biomedical diagnostics and drugs delivery (Fazal et al. 2014; Sriramulu et al. 2018). Biosynthesized nanoparticles significantly contribute in the advancement of biomedical technology and environmental remediation.

Although the green synthesis of nanoparticles using plant extracts and their antimicrobial performance has been overviewed in the past literatures, their formation and antimicrobial mechanisms were not still insightful. Moreover, a very limited number of previous works profoundly elucidated the biomedical applications involving drug delivery, medical diagnostics, and antiaging of green nanoparticles. These potentials, in our view, are very fascinating and worth considered to widen the scope of the green nanoparticles. In this work, therefore, we aim to overview the green routes for synthesizing nanoparticles and place a great emphasis on the botanical route owing to the clear benignity, safety, cost-effectiveness, and high efficiency of plants (Fig. 1). Botanically synthesized nanoparticles are systematically elucidated from how they are synthesized to their superior applications in antibacterial, antifungal, anti-cancer, and biomedical applications. More importantly, the specific mechanisms in each application are also better clarified and profoundly discussed. Ultimately, the knowledge gaps, limitations, and challenges and prospects are pointed out to orientate further studies.

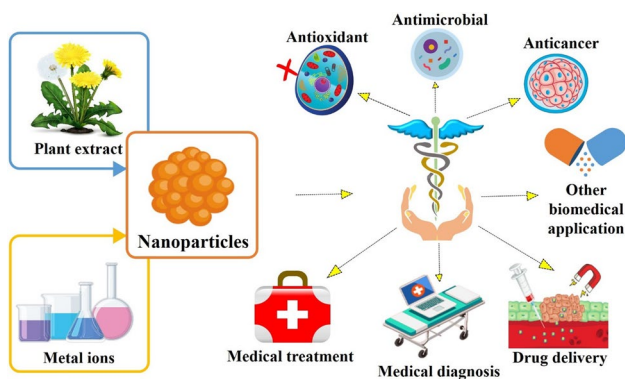


**Fig. 1** Biosynthesis of nanoparticles from plant extract for biomedical applications

## Synthesis of nanoparticles

### General strategy

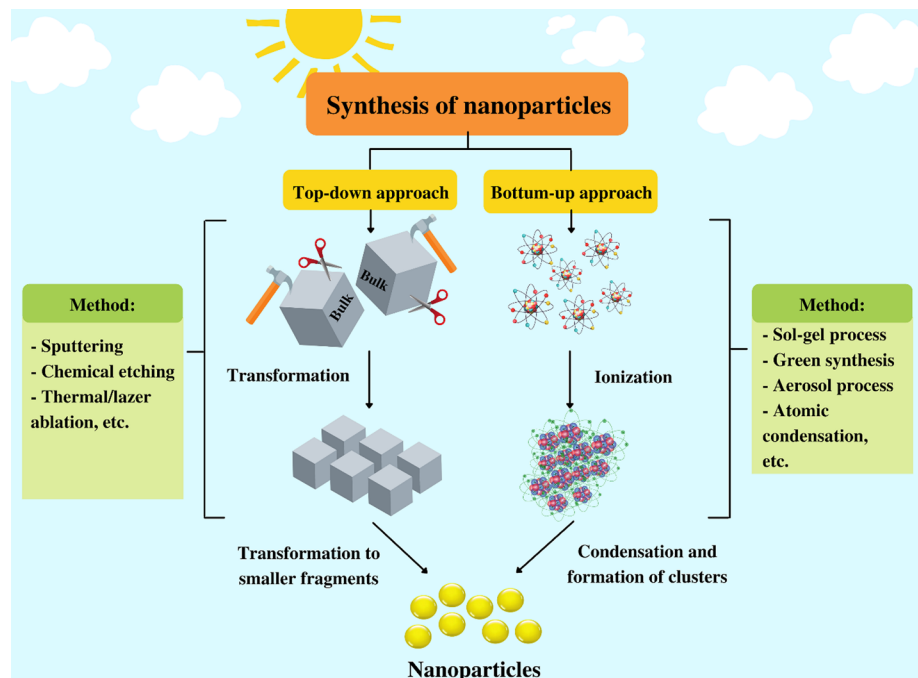
The unique properties of nanoparticles have fueled the research activities, yielding a wide range of practical utilizations including chemical sensing, heterogeneous catalysis, environmental remediation, nanotechnology, biomedical engineering, and agriculture. There is an increasing demand for tailoring and developing nanoparticles in the simplest pathway. At present, nanoparticles are synthesized by two different routes: "top-down" and "bottom-up" (Fig. 2). The former process is to reduce the size of the original bulk materials to new nano-sized ones through

some common methods such as sputtering, chemical etching, and so forth (Jadoun et al. 2021). The latter process is the use of atoms, molecules to assemble or splice small particles together into a nano-sized material through some common methods such as the sol-gel process, green synthesis, and so forth (Rath et al. 2014). Synthesizing nanoparticles can be mainly conducted using chemical, physical and biological approaches. The following sections will vigorously articulate the strengths and weaknesses of each approach.

### Physical methods

To synthesize nanoparticles, there are some widely used physical methods such as high-energy ball milling, electrospraying, laser ablation, physical vapor deposition, melt mixing, inert gas condensation, laser pyrolysis, and flash spray pyrolysis (Dhand et al. 2015; Vishnukumar et al. 2017). These methods mostly belong to the top-down approach by using mechanical energy or electrical energy to grind materials into small-size nanoparticles (Dhand et al. 2015). Two of the most noteworthy methods are evaporation and condensation, carried out in a tube furnace to produce metallic nanoparticles at atmospheric pressure (Abbasi et al. 2014). Although the physical methods are eco-friendly because they do not use toxic chemical substances, the grinding of materials is considerably energy-consuming and requires elaborate equipment, leading to high production cost, and difficulty of systematical scalability (Iravani et al. 2014).

**Fig. 2** Synthesis of nanoparticles by top-down and bottom-up methods



## Chemical methods

The chemical methods are widely used to synthesize nanoparticles, involving sol–gel, hydrothermal, microemulsion, chemical reduction, and precipitation (Jamkhande et al. 2019). Among them, sol–gel is the most commonly used technique due to tunable implementation and high-yield production. Metal precursors and chemical reducing agents are used for the synthesis (Abinaya et al. 2021). However, chemical techniques not only increase the cost of production but also impose the burden of hazardous waste on the environment and human health (Bandeira et al. 2020). To solve this drawback, the green synthesis of nanoparticles from biological methods has paid great attention during the past decades.

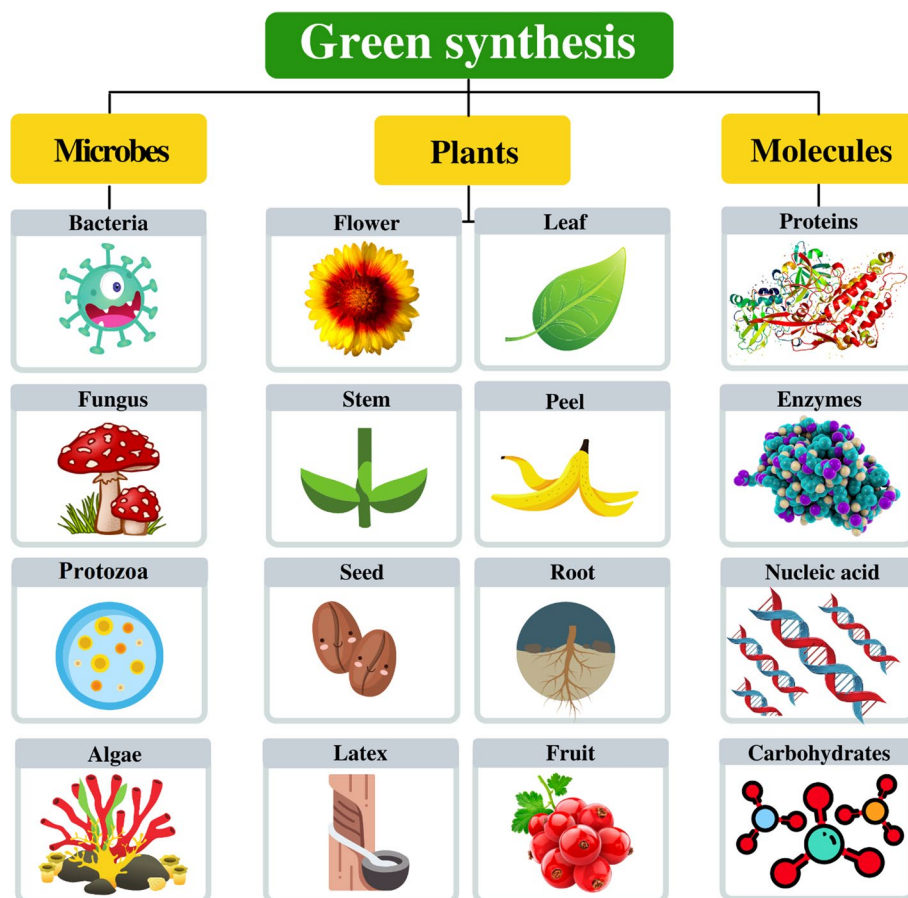
## Biological methods

Biological methods adopt bioreducing agents from microbes, e.g., bacteria, fungus, algae and protozoa, biomolecules or macromolecules, e.g., proteins, enzymes, nucleic acids and carbohydrates, and plant extracts to synthesize nanoparticles (Fig. 3). The use of these biological substrates is intended to replace toxic chemical reductants and chemical stabilizers

(Abinaya et al. 2021). Biological methods have also many advantages over chemical methods since they are more benign and highly biocompatible. Indeed, microorganisms can secrete enzymes that play a role in reducing and stabilizing metal nanoparticles. However, the microbial synthesis of nanoparticles presents more obstacles than other biological methods because it exhibits a range of difficulties in culturing and maintaining microbial growth (Srikar et al. 2016). In terms of biomolecules for synthesizing nanoparticles, enzymes are the representatives which can bind with metal ions and reduce them to form nanoparticles. They can bind with metal ions and reduce them to form nanoparticles. The main limitation of the biomolecules-mediated synthesis is, however, the poor stability of nanoparticles and prolonged duration (Palomo 2019).

Meanwhile, plant extract-mediated synthesis discloses some large advantages because various phytochemicals presenting in the plant extracts (e.g., polyphenols, alkaloids, flavonoids, and alcoholic) possibly act as biocapping and bioreducing agents in the fabrication process, enhancing the stability of the nanoparticles (Lee et al. 2014; Ikram 2015). For example, Rafique et al. (2017) showed that plant extracts to synthesize nanoparticles bring higher efficiency, easy handling, safer and rapid than other biological methods.

**Fig. 3** Green synthesis of nanoparticles using microbes, plant tissues, and biomolecules





Phytochemicals are usually extracted from different parts of plants involving leaves, flowers, roots, seeds, stems, bark, peel, and latex. These compounds have long been known to be excellent antioxidants, thus they are utilized in the reduction process to synthesize various nanoparticles. Singh et al. (2019a, b, c) demonstrated that MgO nanoparticles are formed under the role of phytochemicals as antioxidants. In other words, these phytochemicals are capable of converting the metallic precursors into respective nanoparticles. As another demonstration, Kesharwani et al. (2009) proved that amino acids, alkaloids, polysaccharides, reducing sugar compounds participated in reducing  $\text{Ag}^+$  to  $\text{Ag}^0$ .

In addition to the main role as a reducing agent, the chemical compositions in plant extract also aid to prolong the life of nanoparticles by coverage of nanoparticles, and thus increasing their stability. For example, Dubey et al. (2009) took advantage of flavonoid and terpenoid compounds in *E. hybrida* extract for the longer stability of the silver nanoparticles. Mittal et al. (2013) confirmed the presence of quinol and chlorophyll pigments in the plant extract is accountable for the stabilization of such nanoparticles. More interestingly, the chemical compositions also hinder the agglomeration of nanoparticles during the synthesis, leading to good dispersion and more active sites (Abinaya et al. 2021). Besides, the concentration of extract along with other fabrication conditions such as temperature, pH, or time directly affects the size of nanoparticles. Elemike et al. (2017a, b) investigated the potential of *L. africanum* extracts for synthesizing Ag nanoparticles. The results showed that Ag nanoparticles acquired a smaller size (8–35 nm) upon the optimal pH range from 6.8 to 7 and the temperature of 65 °C. At the concentration ratio of leaf extract/ionic salt solution (1:10), the nanoparticle formation rate was the fastest. From the above arguments, plant extracts can be excellent reducing agents for the synthesis of nanoparticles with high stability, low clustering, and good dispersibility.

## Chemical composition of plants

As mentioned, plant extracts bring many benefits and effectiveness to the synthesis of nanoparticles, which could be thanks to the intrinsic presence of phytochemicals such as polyphenols, flavonoids, sugars, terpenes, and so forth originated from the plant species. Phytochemicals can exist in different tissues of the plant such as leaves, flowers, roots, stems, seeds, pods, resins, and bark (Vishnukumar et al. 2018). Table 1 shows the types of phytochemicals presenting in different plant parts. In general, flavonoids, phenolics, quercetin, and terpenoids are main phytochemicals in most plants. They contribute essentially to the reduction, capping and stabilization of nanoparticles during synthesis. For example, Pansambal et al. (2017) confirmed that

polyphenols, saponins, flavonoids, coumarins, volatile oils, tannins, and sterols from *A. hispidum* act as capping and chelating agents for the synthesis of CuO nanoparticles. Sundararajan and Ranjitha Kumari (2017) proved the major role of polyphenols and flavonoids in *A. vulgaris* leaf as a bio-capping agent for Au nanoparticles synthesis. In another study, Khan et al. (2020) discovered that the presence of kaempferol, quercetin, caffeic acid, dihydrokaempferol in *P. undulata* extract showed as effective metal reducing agents during the formation of Au and Ag nanoparticles. Chandraker et al. (2019) published that the leaves of *A. conyzoides* contain alkaloids, flavonoids, terpenoids, saponins, tannins, which are all capable of reducing, capping and stabilizing Ag nanoparticles. Among them, tannin and tannic acid are prominent phytochemicals for the efficient reduction process. These studies showed the importance of phytochemicals in plant extracts for the synthesis of nanoparticles.

## Role of phytochemicals for nanoparticles biosynthesis

The presence of the phytochemicals from plant extract can benefit the adsorptive, catalytic, biomedical, and biocompatible properties of nanoparticles. For the adsorptive activity, the phytochemicals enrich the surface of nanoparticles by providing new functional groups (Abdullah et al. 2021). Thus, they enhance the surface functionalization and create more physicochemical interactions (e.g., electrostatic interaction,  $\pi$ - $\pi$  interaction, hydrogen bonding, and so forth) (Wu et al. 2020). For example, Hammad and Asaad (2021) recently compared the methylene blue dye sorption affinity between biologically and chemically synthesized FeO nanoparticles. In this study, iron nanoparticles material produced from *C. vulgaris* extract exhibited a higher surface area (85.7 m<sup>2</sup>/g) than the one (71.6 m<sup>2</sup>/g) produced by the chemical precipitation method. The authors implicated that the phytochemicals from *C. vulgaris* significantly reduced the particle size (4.47 nm) of FeO nanoparticles in comparison with the chemical synthesis case (9.07 nm). More importantly, the maximum dye adsorption capacity obtained by biologically synthesized FeO nanoparticles (29.14 mg/g) was significantly higher than that of chemically synthesized ones (19.08 mg/g). This confirmed the main role of phytochemicals in enhancing the surface functionalization and improving the adsorption performance.

For the catalytic activity, the presence of phytochemicals aids in lowering the band gap energy of the nanomaterials (Muthuvel et al. 2020a). This results in decreasing the electron-splitting activation energy, promoting the rapid and efficient separation of electrons, and facilitating the formation of reactive oxygen species ( $\cdot\text{OH}$ ,  $\cdot\text{O}_2^-$ ,  $\text{H}_2\text{O}_2$ ) (Khan et al. 2019). In addition, the phytochemicals on the surface of the

**Table 1** Phytochemicals present in different parts of the plant, for the synthesis of nanoparticles

Plant (common name)	Plant tissues	Nanoparticles	Phytochemicals	References
<i>C. pumilio</i>	Aerial	Ag	Polyphenols, flavonoid, rutin, quercetin, myricetin, kaempferol and gallic acid	(Mostafa et al. 2019)
<i>A. hispidum</i> (Bristly starbur)	Leaf	CuO	Saponins, coumarins, phenols, flavonoids, volatile oils, tannins and sterols	(Pansambal et al. 2017)
<i>A. vulgaris</i> (Mugwort)	Leaf	Au	Polyphenols, flavonoids and terpenoid	(Sundararajan and Ranjitha Kumari 2017)
<i>P. undulata</i> (False fleabane)	Aerial	Au, Ag, Au–Ag	Kaempferol, quercetin, caffeic acid, dihydrokaempferol	(Khan et al. 2020)
<i>A. conyzoides</i> (Billygoat –weed)	Leaf	Ag	Alkaloids, flavonoids, terpenoids, saponins, cardiac glycosides, resins, steroids, phenols, amino acid	(Chandraker et al. 2019)
<i>A. hispidum</i> (Bristly starbur)	Leaf	Ag	Saponins, coumarins, phenols, flavonoids, volatile oils, tannins and sterols	(Ghotekar et al. 2019)
<i>P. vulgaris</i> (False fleabane)	Flower, leaf, and stems	AgCl	Polyphenols, flavonoid, amino acid, alcohols	(Sharifi-Rad and Pohl 2020)
<i>C. intybus</i> (Chicory)	Leaf	Ag	Terpenoids and phenols	(Behboodi et al. 2019)
<i>S. indicus</i> (East Indian globe thistle)	Leaf	Au	Isoflavone, glycosides, protein	(Balalakshmi et al. 2017)
<i>V. amygdalina</i> (Bitter leaf)	Leaf	Zn <sub>1-x</sub> Cu <sub>x</sub> O	Flavonoids, glycosides, saponins, and alkaloids	(Okeke et al. 2020)
<i>O. genistifolia</i> (Klein perdekaroo)	Leaf	Ag/AgCl	Polyphenols, ancaloid, tannin, flavonoid, saponin, glycoside, terpenoids, steroid, protein, carbohydrate	(Okaiyeto et al. 2019)
<i>X. strumerium</i> (Rough cocklebur)	Leaf	Ag	Alkaloid, flavonoid and terpenoid	(Mittal et al. 2017)
<i>A. pseudocotula</i> (Common chamomile)	Aerial	Fe <sub>3</sub> O <sub>4</sub>	Fatty acids, sesquiterpenoids, diterpenoids, polyphenols compounds, coumarins and terpenoids	(Abdullah et al. 2018)
<i>A. annua</i> (Sweet wormwood)	Stem, bark	ZnO	Terpenoids, flavonoids, caffeoylquinic acids, coumarins, acetylenes and sterols	(Wang et al. 2020)
<i>P. leubnitziae</i> (Stinkbush)	Whole plant	Ag	Flavonoids and alkaloids	(Mofolo et al. 2020)
<i>W. chinensis</i> (Sphagneticola calendulacea)	Leaf	Ag	Polyphenols, flavonoids, triterpenoids, wedelolactones	(Paul Das et al. 2018)
<i>A. factorovskyi</i>	Leaf	Ag	Polyphenols and terpenoids	(Al-Otibi et al. 2020)
<i>A. ciniformis</i>	Leaf	Ag	Alcohols, phenols, alkaloids, tannins, terpenes and terpenoids	(Aslany et al. 2020)
<i>V. amygdalina</i> (Bitter leaf)	Leaf	MnO <sub>2</sub>	Flavonoids, alkaloids, steroids, terpenoids, glycosides, tannins, phenols, saponins	(Dessie et al. 2020)
<i>S. costus</i> (Putchuk)	Root	MgO	Sesquiterpenes, alkaloid, triterpenes, lignans and tannin	(Alavi and Karimi 2017a)

nanoparticles also hinder the electron recombination process (Ganesan et al. 2020). For example, *S. nigrum*-derived ZnO nanoparticles yielded high efficiency of 98.89%, compared with 81.94% of chemically produced ZnO nanoparticles for the photocatalytic degradation of methylene blue (Muthuvel et al. 2020b). In another study, Abdullah et al. (2021) indicated the excellent photocatalytic ability of ZnO

nanoparticles biofabricated from *M. acuminata* peel for degrading basic blue 100%, while that of chemically synthesized ZnO nanoparticles obtained only 87.71%.

For the biomedical activity, the phytochemicals such as phenolic and flavonoid compound act a capping layer around the nanoparticles, leading to their high durability in contact with bacterial surfaces (Muthuvel et al. 2020a). These

phytochemicals diversify the surface chemistry of nanoparticles, increasing their binding to bacterial cells through electrostatic interactions (Nithya and Kalyanasundharam 2019). Also, they were more capable of supporting the nanoparticles to generate reactive oxygen species than those synthesized by chemical methods (Virmani et al. 2020). In addition, Muthuvel et al. (2020a) pointed that some phytochemicals in plant extracts such as terpenoids, tannins, flavonoids, alkaloids, carbohydrates, saponins have high bactericidal abilities. Accordingly, the inhibition zones of chemical CuO nanoparticles for *B. subtilis* and *E. coli* were 2 and 3 mm, respectively, considerably lower than those (11 and 12 mm) of CuO nanoparticles produced from *S. nigrum* leaves. Nithya and Kalyanasundharam (2019) synthesized ZnO nanoparticles from *C. halicacabum* with inhibition zones for *S. aureus* and *P. aeruginosa* about 20 and 19 mm, while the chemically synthesized ones acquired only 13 and 12 mm, respectively. This may be due to alkaloids acting as a capping agent to bind nanoparticles with the bacterial surface. In another study, Ni nanoparticles from *D. gangeticum* exhibited the inhibition zone of 5.67 mm, compared with 5.14 mm of chemical ZnO nanoparticles against *S. aureus* (Sudhasree et al. 2014). In terms of anticancer activity, Virmani et al. (2020) proved the contribution of phytochemicals in bioactivity of Au nanoparticles. The survey was carried out for HeLa cells with 50% cell viability for green Au nanoparticles and 80% for chemical Au nanoparticles. These findings pave the way for the next steps of nanoparticles from plant extracts in biomedical applications.

For the biocompatibility, Amooaghaie et al. (2015) demonstrated non-toxic phytochemicals coating around the nanoparticles to both reduce the toxicity of nanoparticles and improve their biocompatibility. In this study, Ag nanoparticles produced from *N. sativa* gave the rate of apoptosis in bone stem cells of mice 11 times lower than that of chemical Ag nanoparticles, indicating less cytotoxicity and better biocompatibility of green nanoparticles. Dowlath et al. (2021) performed the investigation for peripheral blood mononuclear cells and compared the biocompatibility of two types of FeO nanoparticles synthesized from *C. halicacabum* and the chemical method. The results showed that the cell viability of green FeO nanoparticles was 84.04%, significantly higher than that of chemical FeO nanoparticles. With promising biocompatibility findings, nanoparticles are suitable for biomedical applications in drug delivery, diagnosis, and treatment of diseases.

For stability, thanks to the coating by phytochemicals, green nanoparticles are more stable than chemically synthesized ones. To elucidate more, the zeta potential of nanoparticles can be measured. If the zeta potential of nanoparticles receives a more negative or positive value, they repel each other more strongly; hence, exhibiting lower clustering and higher stability. Normally, nanoparticles with the

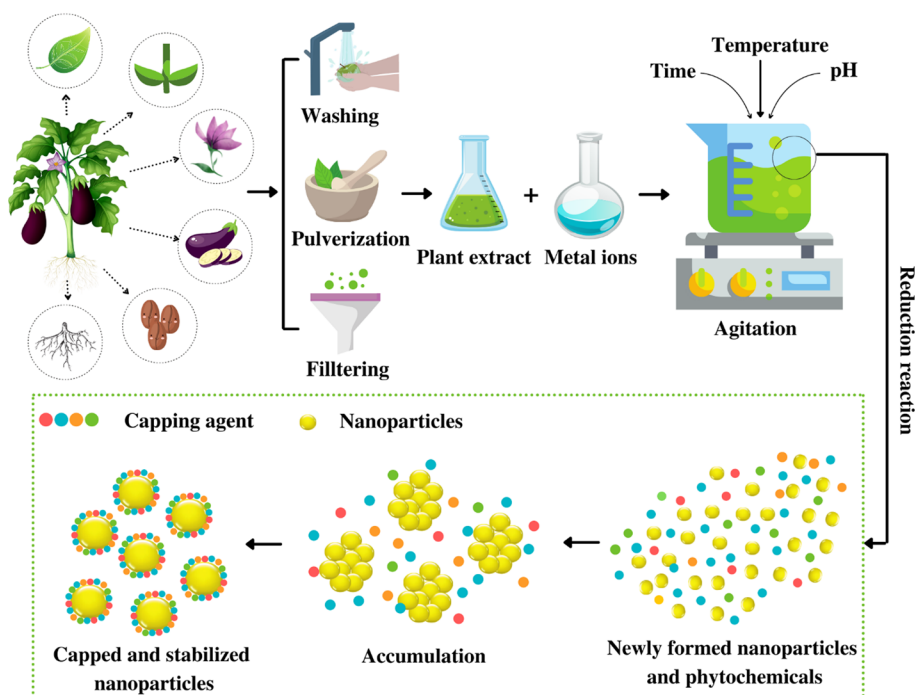
zeta potential was more negative than  $-30$  or more positive than  $30$  stabilize well (Jameel et al. 2020). It was found the zeta potential of Pt nanoparticles from *P. farcta* was higher negative ( $-34.6$  mV) than that of chemically produced ones ( $-15.6$  mV). At the same trend, Nithya and Kalyanasundharam (2019) found the zeta potential obtained at  $-32.06$  and  $-17.89$  mV for ZnO nanoparticles from *C. halicacabum*, and chemical method, respectively. The above outcomes made the deduction of higher stability of green nanoparticles than that of chemically produced ones. Mousavi-Khattat et al. (2018) observed the change of durability on zeta potential histograms between green and chemical Ag nanoparticles. They found the remarkable stability of the green Ag nanoparticles after 2 months. Thus, the phytochemicals enhanced the stability and the long shelf life of nanoparticles, enabling them to apply intensively. To sum up, phytochemicals have supplied many benefits for nanoparticles in terms of adsorptive, catalytic, biomedical, stability, and biocompatible properties.

## Mechanisms for fabricating nanoparticles using plant extracts

### Ag, Au, and Pt nanoparticles

The general mechanism of synthesizing the Ag, Au, and Pt nanoparticles from plant extracts is the bioreduction by biomolecules originating from plants (Fig. 4). Plant extracts often contain functional groups (e.g., carbonyl, hydroxyl, and amine) to react with metal ions and reduce these to nanoparticles with different shapes and sizes. For example, some compounds involving flavonoids, protein, sugars and terpenoids or other bioactive substances possibly participated in the reduction in  $\text{Ag}^+$  to  $\text{Ag}^0$  (Borase et al. 2014). This was demonstrated by evaluating the significant change in the content of sugars and flavonoids before and after the reduction reaction. Ghotekar et al. (2018) determined the components of *L. leucocephala* leaf extract including tannins, saponins, carbohydrates, coumarins, steroids, flavonoids, phenols, and amino acids. Thanks to the antioxidant groups of polyphenols in *L. leucocephala* extract, Ag nanoparticles could be formed through the reduction in  $\text{Ag}^+$ . In addition, the authors demonstrated that various substances such as gallic acid,  $\beta$ -sitosterol, mimosine, caffeic acid, and chrysoenol also play a key role in stabilizing the of Ag nanoparticles. In addition, Zheng et al. (2013) revealed that the reduction in Pt(II) into Pt(0) nanoparticles was dependent on many factors such as temperature, reducing sugars, flavonoid contents. Another research also showed that plant extracts exhibited a possible mechanism for the reduction and stabilization of the chloroaurate ions ( $\text{AuCl}_4^-$ ) to Au nanoparticles (Huang et al. 2011).

**Fig. 4** Mechanism of synthesis of nanoparticles from plant extracts



## Cu nanoparticles

Murthy et al. (2020) documented the synthesis of Cu nanoparticles from *H. abyssinica* plant extracts. Phenolic compounds, anthraquinone glycosides, and tannins, which are known to be high antioxidants, bind to  $\text{Cu}^{2+}$  ions in the precursor salt solution  $\text{Cu}(\text{NO}_3)_2$  and reduce to the  $\text{Cu}^0$  form. After the reduction, these biomolecules played a fundamental role in enveloping and stabilizing the Cu nanoparticles. In another study, Naghdi et al. (2018) speculated that the concise mechanism with the incorporation of quercetin, a polyphenol found in *C. reflexa* leaf extract for the formation of Cu nanoparticles. Firstly,  $\text{Cu}^{2+}$  would oxidize quercetin, forming the intermediate Cu(I)–quinone complex. Cu(I) in this complex continued to oxidize quercetin again to form Cu nanoparticles and quinone compounds. Cu nanoparticles could be highly stabilized with the encapsulation of phytochemicals in the extract. As a consequence, the ratio between  $\text{Cu}^{2+}$  and plant extract concentration affect the formation of Cu nanoparticles. Indeed, Nagar and Devra (2018) suggested that the precursor salt concentration could significantly affect the shape and particle size of the Cu nanoparticles biosynthesized from *A. indica* leaf extract. Specifically, when the concentration of  $\text{CuCl}_2$  increased from  $6 \times 10^{-3}$  mol/L to  $7.5 \times 10^{-3}$  mol/L, the particle size also increased from 48.01 to 78.51 nm, respectively. The authors explain that a higher amount of  $\text{CuCl}_2$  will supply larger amount of nucleus, leading to a higher degree of agglomeration of Cu nanoparticles.

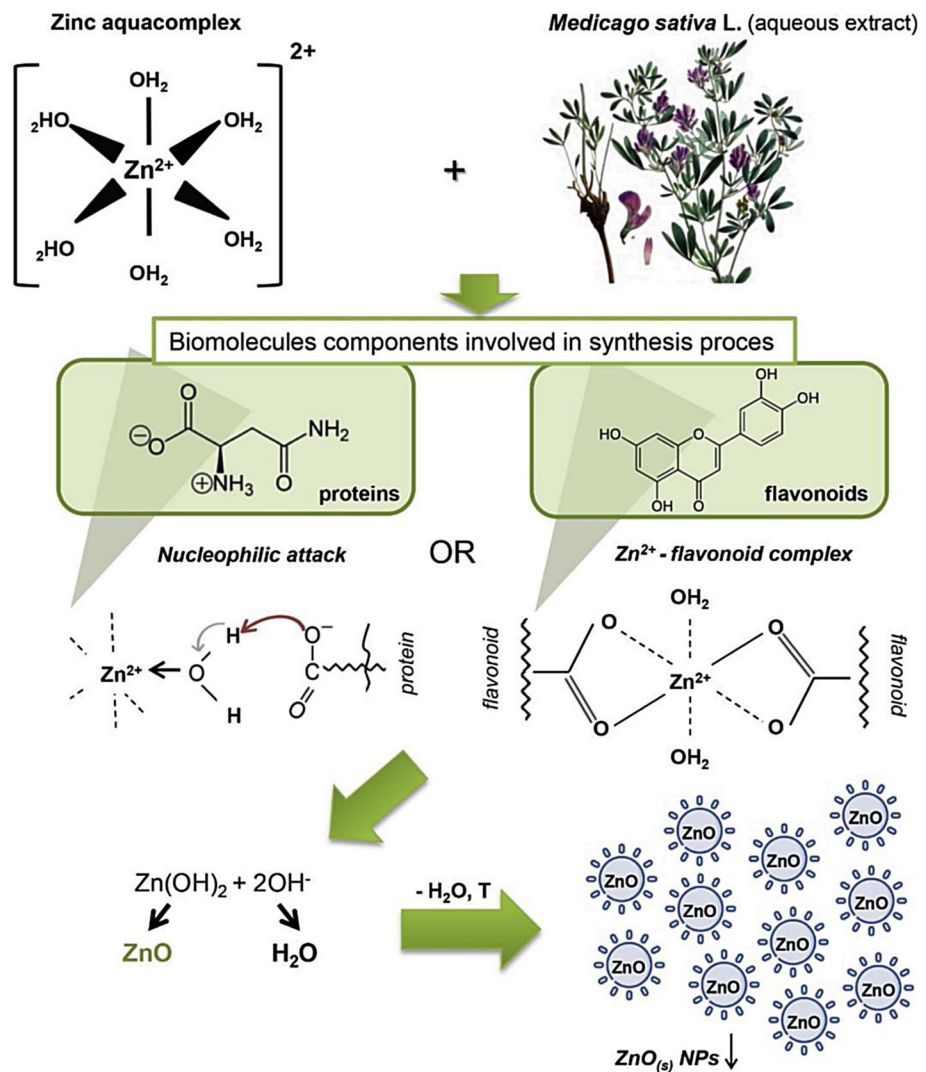
## ZnO nanoparticles

The mechanism of forming other green oxide metal nanoparticles such as ZnO nanoparticles is also significantly dependent on phytochemicals in plant extracts. Król et al. (2019) studied ZnO nanoparticle fusion with the aid of biomolecules from *M. sativa* extract. Zinc aqua complex can exchange with their water molecules when binding to protein ligands due to the coordination chemistry of zinc. On the other hand, flavonoids (e.g., quercetin, rutin and galangin) can chelate with  $\text{Zn}^{2+}$  ions through specific metal ion binding sites (Fig. 5). The Zn–flavonoid complex was formed and calcined at high temperature to form ZnO nanoparticles. In another study, Kumar et al. (2014) demonstrated that phytochemicals such as flavonoids, limonoids, and carotenoids containing free  $-\text{OH}$  and  $-\text{COOH}$  can react with  $\text{ZnSO}_4$  to form the Zn–(flavonoid, limonoids, carotenoid) complex. This complex is then transferred into a furnace at  $150^\circ\text{C}$  to produce ZnO nanoparticles.

Many operating factors also have a great impact on their morphology and particles size. Take temperature as an example, Hassan Basri et al. (2020) studied the effect of synthesis temperature on the morphology of ZnO nanoparticles produced from the pineapple peel extract. At the synthesis temperature of  $60^\circ\text{C}$ , the as-obtained ZnO nanoparticles produced a combination of spherical and rod-shaped structures. Meanwhile, the synthesis condition at  $28^\circ\text{C}$  produced ZnO nanoparticles with a spherical flower-shaped structure. Considering another factor such as extraction concentration, green ZnO particles tended to decrease the size as the



**Fig. 5** Formation mechanism of ZnO nanoparticles from *M. sativa* extract through the complexation of zinc and flavonoid or nucleophilic attack. Reproduced with the permission of Elsevier from the reference (Król et al. 2019)



extract concentration increased. Indeed, Soto-Robles et al. (2019) showed that the particle size of ZnO nanoparticles was 5–12 nm in the condition using 8% concentration of *H. sabdariffa* extract, compared with 20–40 nm for 1% concentration condition. As a consequence, the control of operating factors such as temperature and extraction concentration is substantial to produce the green nanoparticles with expectable properties.

### MgO nanoparticles

The synthesis mechanism of MgO nanoparticles is also based on the biocapping and chelating mechanism of biomolecules in plant extracts. Specifically, Mg<sup>2+</sup> ions in the precursor can be chelated with biomolecules to form complexes with metals (Singh et al. 2019a). Isoleucine acid is a phytochemical originating from *L. acidissima* fruit extract and accounts for forming MgO nanoparticles with high stability (Nijalingappa et al. 2019). In this study, the

isoleucine–MgO complex was formed after the binding of magnesium nitrate to isoleucine acid. Next, the complex was calcined at high temperature (500–800 °C) so that MgO nanoparticles could be formed with good dispersion and high stability. Suresh et al. (2018) described the possible mechanism of MgO nanoparticles synthesis from insulin plant extracts as follows: (i) diosgenin in the extract reacts with magnesium nitrate salt solution to form complexes with weak hydrogen bonds; (ii) treat this complex at a temperature of about 80 °C to form the precipitation in the form of hydroxide; (iii) the product MgO nanoparticles was created by calcination at 450 °C.

Considering the operating factors, the structure of MgO can be significantly contingent on the pH of the extract solution. In a recent study, Jeevanandam et al. (2020) found that the higher the pH was, the more negative the zeta potential value of MgO nanoparticles had. This means that the stabilization of green MgO nanoparticles increased. By contrast, an unfavorable condition of pH can lead to an increase in the

agglomeration of the MgO nanoparticles, thereby, increasing their particle size. Indeed, the authors reported the characteristic results of MgO nanoparticles at various pH values. At pH 3, hexagonal MgO nanoparticle size was determined to be smaller than 44 nm, but at pH 5 and pH 8, their sizes were higher, at 50.75 and 58.77 nm, respectively. As such, the adjustment of pH is an important step to drive the structure of green MgO nanoparticles.

## CuO nanoparticles

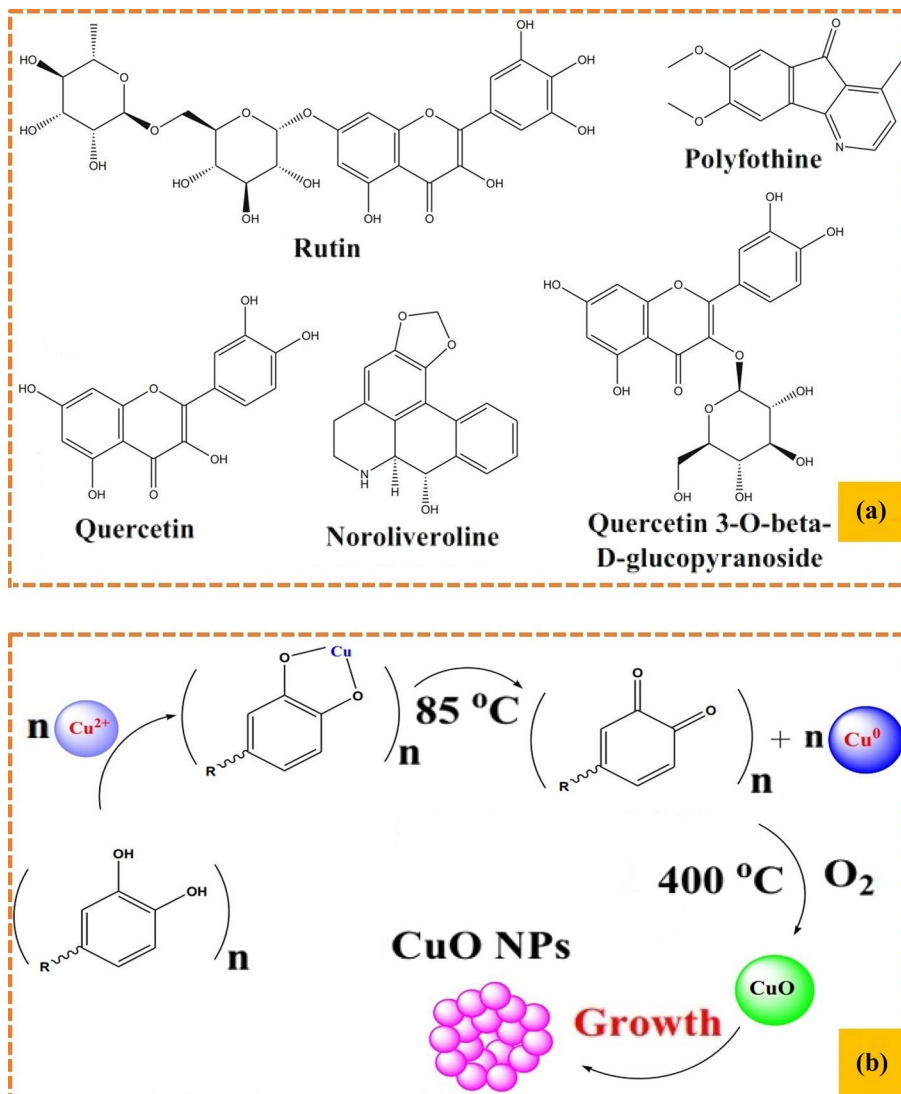
For the synthesis of CuO nanoparticles, the process can be supplemented with an additional step by the calcination at a high temperature under oxygen atmosphere (Fig. 6). This condition allows to convert zero-valent Cu into CuO nanoparticles. For instance, Nagore et al. (2021) demonstrated natural biomolecules present in *P. longifolia* leaf extract could be chelated with  $\text{Cu}^{2+}$  at 85 °C so that the chemical

components bonded with  $\text{Cu}^{2+}$  ions. The authors determined these compounds including saponins, flavonoids, tannins, polyphenols, steroids, and alkaloids. After the chelating process, the complex could be calcinated at 400 °C in a furnace in the presence of air flow. As a consequence, the CuO crystals are formed. The study also confirmed the important role of phytochemicals in the synthesis of CuO nanoparticles.

## Characterization of nanoparticles

Nanoparticles have characteristics in terms of shape, size, surface area, or dispersion. The methods of analyzing the structure of nanoparticles involve a variety of techniques such as UV–Vis spectroscopy, Fourier transform infrared spectroscopy (FT–IR), scanning electron microscopy (SEM), transmission electron microscopy (TEM), energy-dispersive spectroscopy (EDS), and so forth (Fig. 7). State-of-the-art

**Fig. 6** Main compounds such as rutin, polyfothine, quercetin and noroliveroline in *P. longifolia* leaf extract (a); plausible mechanism of green synthesis of CuO nanoparticles using phytochemicals from the *P. longifolia* leaf extract (b). Reprinted with the permission of Springer Nature from the reference (Nagore et al. 2021)



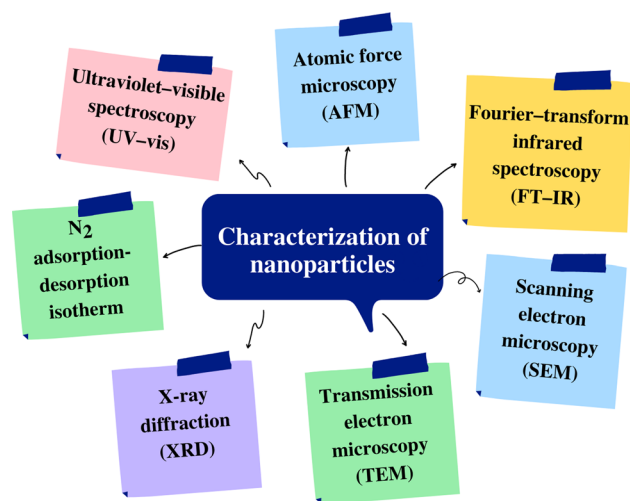


**Fig. 7** Characteristic techniques for determining the structure of nanoparticles

structural characterization techniques have greatly supported the study of the synthesis of nanoparticles as well as the observation and determination of the characteristics of the nanoparticles. Table 2 lists the characterization of nanoparticles biosynthesized from plant extracts.

### Ultraviolet–visible spectroscopy

Ultraviolet–visible (UV–Vis) spectroscopy is a substantial technique to determine optical properties, the generation and stability of nanoparticles (Förster 2004). This technique is a simple, easy to use, fast, sensitive and selective technique. It involves quantifying the amount of ultraviolet or visible radiation absorbed by a component in a solution (Rajeshkumar and Bharath 2017). When a sample solution containing only the crude extract was added, no typical peak was present. Meanwhile, the botanically synthesized nanoparticle sample gave the typical peaks at the different wavelength region. Table 2 shows some characteristic properties of nanoparticles synthesized from different parts of various plants. Accordingly, the adsorption band of Ag nanoparticles is ranged from 417 to 448 nm (Francis et al. 2018; Yazdi et al. 2019; Ahn et al. 2019; Seifpour et al. 2020). For CuO nanoparticles, the maximum wavelength ranges between 236 and 670 nm (Pansambal et al. 2017; Muthamil Selvan et al. 2018; Nordin and Shamsuddin 2019; Singh et al. 2019c). In addition, MgO and ZnO nanoparticles exhibit the typical summit at the wavelengths of 250–300 nm, and 420–330 nm, respectively (Alavi and Karimi 2017a; Dobrucka 2018; Hameed et al. 2019; Wang et al. 2020; Rajapriya et al. 2020). In addition to demonstrating the presence of nanoparticles synthesized from plant extracts, UV–Vis spectrum can also confirm their stability. By monitoring the UV–Vis spectra of

the samples after regular periods, the position of the peaks is mostly constant, indicating high stability of the nanoparticles (Fig. 8a). Many works revealed that the nanoparticles have high stability up to many days or many months (Balashanmugam and Pudupalayam Thangavelu 2015).

### N<sub>2</sub> adsorption–desorption isotherm

The nitrogen adsorption–desorption isotherm is used to measure the amount of N<sub>2</sub> that adsorbs onto the nanoparticles surface. This reflects the plot of relative pressure versus volume of nitrogen at the temperature 77 K (Fig. 8b). Based on N<sub>2</sub> adsorption–desorption isotherm, the surface area can be determined by Barrett–Joyner–Halenda (BJH) or density functional theory (DFT) method. The surface area of nanoparticles can be well beneficial for explaining the catalytic, adsorption and different properties. Many studies reported that nanoparticles produced from plant extract exhibited the large surface area (52.6–137.4 m<sup>2</sup>/g) (Stan et al. 2017; Singh et al. 2019c; Sethy et al. 2020; Lakshminarayanan et al. 2021). It can be understood that phytochemicals in plant extracts reduce the aggregation of newborn nanoparticles, thereby increasing their surface area, which contributes to the excellent properties and applications of nanoparticles.

### Fourier transform infrared spectroscopy

Fourier transform infrared (FT–IR) spectroscopy is used to learn about the surface chemistry of nanoparticles. Specifically, this technique can detect functional groups derived from biomolecules, which contribute to the synthesis of nanoparticles. The resulting spectrum exhibits absorption and transmission by generating a sample molecular fingerprint, which changes the identity of the sample (Rajeshkumar and Bharath 2017). Yazdi et al. (2019) detected many functional groups existing in the surface of Ag nanoparticles produced from *H. trichophylla* flower extract, involving O–H (3397–3410 cm<sup>-1</sup>), C–H (2921 and 2847 cm<sup>-1</sup>), C–N (1626 cm<sup>-1</sup>), N–O (1385 cm<sup>-1</sup>), and so forth. Sundararajan and Ranjitha Kumari (2017) reported the presence of a wide range of chemical bonds belonging to alcohols, alkanes, aldehydes, and amines on the surface of Au nanoparticles synthesized from *A. vulgaris* extract. These evidences may provide the main hypothesis for the existence of phytochemicals that take part in the formation of nanoparticles.

### Scanning electron microscopy

The morphology of nanoparticles is very diverse and important to better understand the structure of nanoparticles. While the atomic force microscopy (AFM) technique produces three-dimensional images with many visualizations (Falsafi et al. 2020), scanning electron microscopy (SEM)

Table 2 Characterization of nanoparticles biosynthesized from plant extracts

Plant name (common name)	Part	NPs	$\lambda_{\max}$ (nm)	Particle size (nm)	Morphology	Chemical bonds	References
<i>A. haussknechtii</i>	Leaf	Ag, Cu, TiO <sub>2</sub>	340–350 (Ag), 200–300 (Cu), 400 (TiO <sub>2</sub> )	10.69 (Ag), 35.36 (Cu), 92.58 (TiO <sub>2</sub> )	Irregular (Ag), spherical (Cu, TiO <sub>2</sub> )	N–H, C–H, C=C, C–H, C–Cl, C–O, C–Cl	(Alavi and Karimi 2017b)
<i>H. trichophylla</i>	Flower	Ag	448	20–50	Spherical	O–H, C–N, C–C, N–O, C–N, C–Br	(Yazdi et al. 2019)
<i>T. farfara</i> (Coltsfoot)	Flower	Ag, Au	416 (Ag), 538 (Au)	13.57 (Ag), 18.20 (Au)	Spherical	Not reported	(Lee et al. 2019)
<i>E. scaber</i> (Elephant's foot)	Leaf	Ag	420	37.86	Spherical	O–H, C=O, C=C	(Francis et al. 2018)
<i>C. cernuum</i>	Whole plant	Ag	430	13.0	Spherical	Not reported	(Ahn et al. 2019)
<i>S. nodiflora</i> (Node-weed)	Leaf	Ag, Au	413 (Ag), 535 (Au)	19.4 (Ag), 22.01 (Au)	Spherical (Ag), Spherical, triangular (Au)	–OH, C=O, –C–O–C, C–O	(Vijayan et al. 2018)
<i>T. officinale</i> (Dandelion)	Leaf	Co	464	50–100	Spherical	–OH, C–H, –C=O–, C–N, C–O	(Rasheed et al. 2019)
<i>T. collinus</i> (Goats-beard)	Whole plant	Ag	400	7–18	Spherical	–OH, –NH, C–O, –NH <sub>2</sub> , C–C	(Seiffipour et al. 2020)
<i>S. quettense</i> (Podlech)	Whole plant	Ag	448	48.40–55.35	Spherical	N–H, O–H, C–O, –C–H, C≡N, C=C–, C–O, C–N	(Qasim Násar et al. 2019)
<i>G. tournefortii</i> (Tumbleweed)	Leaf	Au	528	40–45	Spherical	C=C, C=O, –C–O, –C–O–C	(Zhaheh et al. 2019)
<i>C. pumilio</i>	Aerial parts	Ag	446	6–8	Spherical	O–H, –CH, C=O, C–O–C, C=O	(Mostafa et al. 2019)
<i>A. hispidum</i> (Bristly starbur)	Leaf	CuO	390	5–25	Spherical	C–H, C=C, O–H, C–O, Cu–O	(Pansambal et al. 2017)
<i>A. vulgaris</i> (Mugwort)	Leaf	Au	560	12.0	Spherical, triangular, hexagonal	O–H, C–H, N–H, C–N, C–O	(Sundarajan and Ranjitha Kumari 2017)
<i>Pulicaria undulata</i> L. (False Fleabane)	Aerial parts	Au, Ag, Au–Ag	430 (Au), 540 (Ag), 490 (Au–Ag)	10–20	Spherical	O–H, C–H, C–C, C–O	(Khan et al. 2020)
<i>A. conyzoides</i> (Bilgoat –weed)	Leaf	Ag	443	14–48	Spherical	N–H, C–H, C=O, C–OH	(Chandraker et al. 2019)
<i>A. hispidum</i> (Bristly starbur)	Leaf	Ag	417	25–45	Quasi-spherical	–OH, C–H, C=O, C–O	(Ghotekar et al. 2019)
<i>P. vulgaris</i> (False fleabane)	Flower, leaf, stem	AgCl	460	28.6	Spherical	C=O, C–Cl, C=C	(Sharifi-Rad and Pohl 2020)
<i>A. turcomanica</i> (Mugwort)	Leaf	Ag	430	20–60	Spherical	O–H, C–H, C=O, C–O–C	(Mousavi et al. 2018)
<i>D. anomala</i> (Stomach bush)	Root	Ag	424	8.724	Round, rod-like, hexagonal, uneven shapes	–OH, –NH, C=C, C–O–C, =C–H, C=O, N–H	(Tripathy et al. 2020)
<i>C. intybus</i> (Chicory)	Leaf	Ag	Not reported	17.17	Spherical	O–H, C–H, C=C, C–H, C–O–C	(Behboodi et al. 2019)

**Table 2** (continued)

Plant name (common name)	Part	NPs	$\lambda_{max}$ (nm)	Particle size (nm)	Morphology	Chemical bonds	References
<i>S. rebaudiana</i> (Sugarleaf)	Leaf	CeO <sub>2</sub> -Ni	Not reported	10.56	Spherical	Not reported	(Khatami et al. 2019)
<i>T. officinale</i> (Common dandelion)	Leaf	Ag	546	5–30	Spherical	C=C, C=O, C-OH, -NH <sub>2</sub> , -OH	(Saratale et al. 2018)
<i>S. indicus</i> (East Indian globe thistle)	Leaf	Au	531	25	Spherical	-OH, C-H, -C=O, -C-O-C, C-H, N-H, C-Cl	(Balakshmi et al. 2017)
<i>S. marianum</i> (Blessed thistle)	Whole plant	ZnO, Ag-ZnO	420 (ZnO), 347 (Ag-ZnO)	31.2 (ZnO), 35.3 (Ag-ZnO)	Quasi-spherical (ZnO), spherical (Ag-ZnO)	-OH, Zn-O, C=C, C-N, C-H	(Hameed et al. 2019)
<i>E. odoratum</i> (Chromolaena odorata)	Leaf	Ag/Ag <sub>2</sub> O	424	23.6	Spherical	Not reported	(Elemike et al. 2017a, b)
<i>V. amygdalina</i> (Bitter leaf)	Leaf	Zn <sub>1-x</sub> Cu <sub>x</sub> O	441–635	34–39	Spherical, petal, rod-like	C=C, C=O, C-H, Zn-O	(Okeke et al. 2020)
<i>Zinnia elegans</i> (Common zinnia)	Whole plant	Au	530	<25	Spherical	O-H, C-H	(Kotcherakota et al. 2019)
<i>O. genistifolia</i> (Klein perdekaroo)	Leaf	Ag/AgCl	270–290	34.2	Spherical	N-H, O-H, C=O, -C-O-C, -C-O-	(Okaiyeto et al. 2019)
<i>C. tinctorius</i> (Safflower)	Flower	Ag	420	20–70	Spherical, regular polygons	n.a	(Aboutorabi et al. 2018)
<i>D. tombolens</i> (Yellowhead)	Aerial parts	MnO	240	38	Spherical	O-H, C=C, C=O	(Souri et al. 2018)
<i>X. strumarium</i> (Rough cocklebur)	Leaf	Ag	450	20–50	Spherical	O-H, C=C, C-F, C-N, -C-O	(Mittal et al. 2017)
<i>B. eriantha</i> (Blumea)	Whole plant	Ag, Fe	445 (Ag), Fe (365)	10–50	Spherical, irregular	O-H, C-O-C, C=O	(Chavan et al. 2020)
<i>A. pseudocotula</i> (Common chamomile)	Aerial parts	Fe <sub>3</sub> O <sub>4</sub>	Not reported	11–19	Spherical	CH <sub>3</sub> , CH <sub>2</sub> , -NH, -OH, -C=O, Fe-O, C=C	(Abdullah et al. 2018)
<i>E. purpurea</i> (Purple coneflower)	Whole plant	TiO <sub>2</sub>	280	120	Spherical	C-O, C-H, C=C, O-H	(Dobrucka 2017)
<i>A. annua</i> (Sweet wormwood)	Stem bark	ZnO	330	20	Spherical	C-O, N-H, C=C, C=O	(Wang et al. 2020)
<i>T. procumbens</i> (Coat-buttons)	Leaf	Ag	425	54.34	Oval, spherical	C-H, C=C=C, C=O, N-O, S=O	(Rani et al. 2020)
<i>P. leubnitziae</i> (Stinkbush)	Whole plant	Ag	400	100	Spherical	C-H, O-H, C=C, C-N, =CH	(Mofolo et al. 2020)
<i>A. millefolium</i> (Yarrow)	Whole plant	Ag	460	14.27–20.77	Spherical, rectangular, cubical	C-C, O-H, C-H, C=O	(Yousaf et al. 2020)



Table 2 (continued)

Plant name (common name)	Part	NPs	$\lambda_{\max}$ (nm)	Particle size (nm)	Morphology	Chemical bonds	References
<i>W. chinensis</i> (Sphagneticola calendulecea)	Leaf	Ag	408	31.68	Spherical	–OH, C=O	(Paul Das et al. 2018)
<i>T. procumbens</i> (Coat-buttons)	Leaf	CuO	236	16	Rod, spherical	N–H, C–H, C=O	(Muthamil Selvan et al. 2018)
<i>C. benedicti</i> (Blessed thistle)	Whole plant	Au–CuO, CuO–ZnO	350	13 (Au–CuO), 28 (CuO–ZnO)	Spherical	C–H, –NH, C–C, O–H	(Dobrucka et al. 2019)
<i>A. factorovskyi</i>	Leaf	Ag	430	< 100	Spherical	O–H, C=C, C–Cl, N=C=S	(Al-Otibi et al. 2020)
<i>K. grandiflora</i>	Leaf	Ag	429	20–50	Spherical	–OH, –NH, C–H, C–O, C–H, C–C, C–N	(Kanagamani et al. 2019)
<i>A. ciniformis</i>	Leaf	Ag	430	4–77	Spherical	O–H, N–H, C=C, N–H	(Aslany et al. 2020)
<i>V. amygdalina</i> (Bitter leaf)	Leaf	MnO <sub>2</sub>	320	20–22	Spherical	–OH, H–O–H, C–H, O–Mn–O, C=O	(Dessie et al. 2020)
<i>S. costus</i> (Putchuk)	Root	MgO	250	30–34	Spherical	–OH, C–H, C=O, Mg–O	(Alavi and Karimi 2017a)
<i>A. arborescens</i> (Ragweed)	Leaf	Ag	414	14	Spherical	C=C, C–O, O–H	(Morejón et al. 2018)
<i>A. tournefortiana</i>	Whole plant	Ag	420	22.89	Spherical	O–H, C–H, P–H, –COO, C=C, C–O–C	(Baghbani-Arani et al. 2017)
<i>C. scolymus</i> (Globe artichoke)	Leaf	ZnO	371	65.9	Spherical	O–H, N–H, –C–H, C–O, C=C, =C–H	(Rajapriya et al. 2020)
<i>A. abrotanum</i> (Southern wormwood)	Whole plant	MgO	300	10	Spherical	O–H, C=O, C–H	(Dobrucka 2018)
<i>O. vulgare</i> (Oregano)	Leaf	Pd	320	2–20	Spherical	O–H, C=O, C–O, C–H	(Shaik et al. 2017)
<i>R. puerariae</i> (Gegen)	Root	Ag	400–430	10–35	Spherical, oval	Not reported	(Balwe et al. 2017)
<i>P. guajava</i> (Guava)	Leaf	CuO	282	2–6	Spherical	Cu–O, C=O	(Singh et al. 2019d)
<i>C. paradisi</i> (Paradise citrus)	Peel	Ag	405	14.84	Spherical	O–H, –NH <sub>2</sub> , C=O, C=C	(Naseem et al. 2020)
<i>G. arborea</i> (Verbenaceae)	Fruit	Ag	418	8–32	Spherical	Not reported	(Saha et al. 2017)
<i>R. tuberosa</i> (Minnieroot)	Whole plant	CuO	327	20–100	Spherical, cylindrical, cubical	O–H, C=C, C–O, Cu–O	(Vasantharaj et al. 2019)
<i>C. ramiflora</i> (Katong laut)	Fruit	Fe <sub>2</sub> O <sub>3</sub>	n.a	58.5–78.13	Spherical	–C–NH, C–H, C=O, C–H	(Bishnoi et al. 2018)
<i>A. procera</i> (White siris)	Leaf	Ag	460	6.18	Spherical	Not reported	(Raftique et al. 2019)

Table 2 (continued)

Plant name (common name)	Part	NPs	$\lambda_{\max}$ (nm)	Particle size (nm)	Morphology	Chemical bonds	References
<i>P. granatum</i> (Pomegranate)	Seed	Fe <sub>2</sub> O <sub>3</sub>	Not reported	25–55	Variable	Not reported	(Bibi et al. 2019)
<i>D. mezereum</i> (February daphne)	Leaf	IO (Iron oxide)	465	6.5–14.9	Spherical	–OH, FeO, C=C	(Beheshkhoo et al. 2018)
<i>P. farcta</i> (Syrian mesquite)	Fruit	Ag	441	30	Spherical	Not reported	(Medda et al. 2015)
<i>M. koenigii</i> (Curry tree)	Leaf	CuO	670	8.4	Prism, pentagon, hexagon	–OH, –CHO, –COO, Cu–O, C=O	(Nordin and Shamsudin 2019)
<i>L. cubeba</i> (Aromatic litsea)	Fruit	Au	535	8–18	Spherical	O–H, C–H, C=C, C–O	(Doan et al. 2020)
<i>A. indica</i> (Neem tree)	Leaf	Ag	438	10–15	Spherical	–NH, –OH, –C=O, –C–OC–, –C–O–	(Singh et al. 2019b)
<i>M. indica</i> (Mango)	Flower	Au	532	10–60	Spherical	O–H, C=O, C–C	(Nayan et al. 2018)
<i>C. coccineum</i> (Maltese fungus)	Whole plant	Cu	Not reported	14.2	Spherical	C–O–C, O–H, C=C, C–O	(Sebeia et al. 2020)

is a powerful tool to explore their two-dimensional surface morphology. SEM investigation is applied to characterize the shape, size, morphology, and size distribution of the bio-synthesized nanoparticles. For example, Yousaf et al. (2020) showed Ag nanoparticles from *A. millefolium* extract owning diverse shapes such as spherical, rectangular, and cubical. Vasantharaj et al. (2019) reported CuO nanoparticles from *R. tuberosa* extract with spherical, cylindrical, and cubical morphologies. Meanwhile, MgO and ZnO nanoparticles from plant extracts can exhibit both spherical shapes (Dobrucka 2018; Rajapriya et al. 2020). However, this technique may be less significant to discovery the structure of nanoparticles, particularly their particle sizes.

### Transmission electron microscopy

Transmission electron microscopy (TEM) technique records the electron images of nanoparticle using the electron beam. It gives a very high-resolution to explore the inherent structure of nanoparticles. This technique is not only used to observe the aggregation or clustering of the nanoparticles but also to identify the size distribution of nanoparticles (Fig. 8c). Indeed, Fig. 8d–g shows a marked change in the degree of dispersion of nanoparticles (Ag, Cu, ZnO, MgO). Specifically, almost all Ag nanoparticles are discrete and evenly well-distributed while the slight clustering of Cu, ZnO nanoparticles can occur, and MgO nanoparticles show the strongest aggregation. The inherent morphological difference of mentioned nanoparticles can be attributed to the effect of temperature during their synthesis. Ag and Cu nanoparticles offer a lower degree of clustering possibly because the synthesis occurs at room temperature or slightly higher than room temperature (60–80 °C). Meanwhile, the strong aggregation of ZnO and MgO nanoparticles may relate to the calcination process at high temperature (400–700 °C).

The size of nanoparticles is one of the most important structural features that strongly influences their properties and applications. Many works used TEM technique to calculate the average sizes. For example, Lee et al. (2019) synthesized Au and Ag nanoparticles from *T. farfara* flower bud extract with the particles size in a range from 13.57 to 18.20 nm. Nazar et al. (2018) reported that the average size of Cu nanoparticles from *P. granatum* seeds extract was 43.9 nm. Meanwhile, Hii et al. (2018) synthesized MgO nanoparticles from *C. gigantea* extract with an average size of 53.37 nm. Rajapriya et al. (2019) showed the highest particle size of ZnO nanoparticles from *C. scolymus* extract, at 65.9 nm. This may be due to the clustering of the nanoparticles depending on the synthesis temperature, resulting in different sizes. Indeed, (Siddiqui et al. 2013) synthesized Ag nanoparticles at room temperature, while Lee et al. (2011) produced Cu nanoparticles at about 95 °C. ZnO and MgO nanoparticles could be formed by the calcination of raw

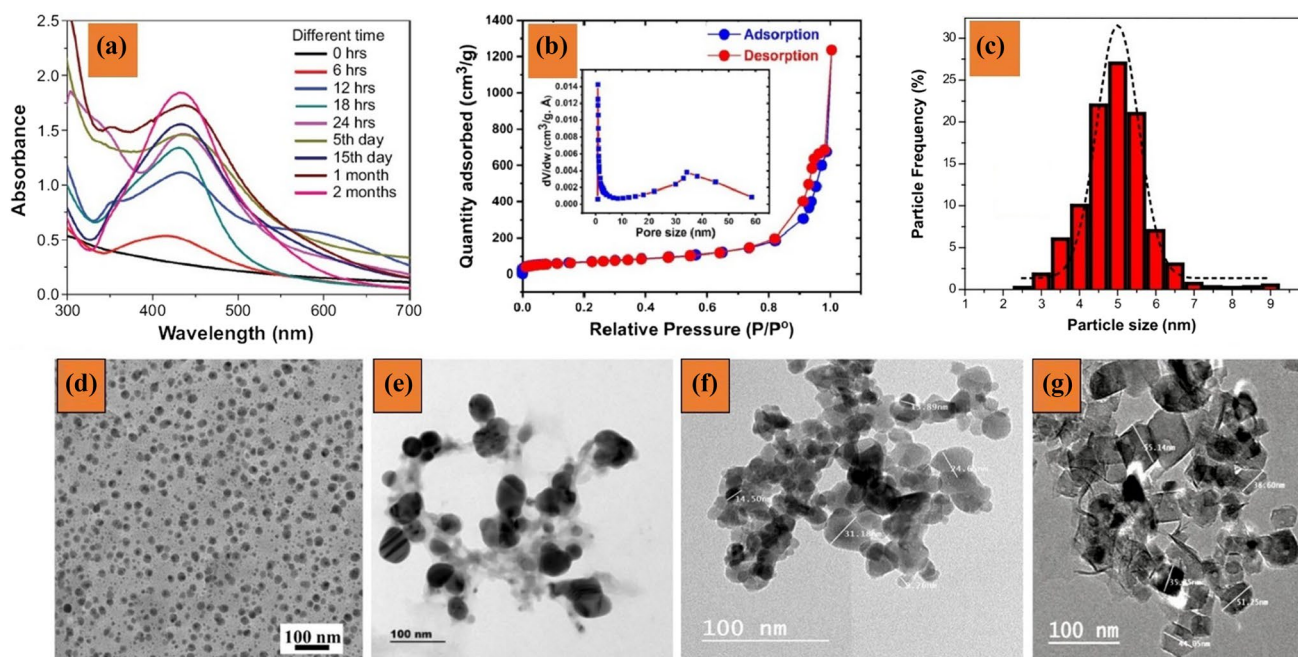


**Fig. 8** **a** Ultraviolet–visible absorption spectra for checking stability of Ag nanoparticles from *C. roxburghii* extract at different times, reproduced from the reference (Balashanmugam and Pudupalayam Thangavelu 2015). **b**  $N_2$  adsorption/desorption isotherm of  $Fe_3O_4$  nanoparticles from *A. comosus* extract, reproduced from the reference (Akpomie et al. 2021). **c** Histogram of particle size of Ag nanoparticles from *M. indica* extract, reproduced with the permission of Springer from the reference (Horta-Piñeres et al. 2020). Transmis-

sion electron microscope images of **(d)** Ag nanoparticles from *M. recuita* extract, reproduced with the permission of Elsevier from the reference (Uddin et al. 2017); **e** Cu nanoparticles from *H. abyssinica* extract, reproduced from the reference (Murthy et al. 2020); **f** ZnO nanoparticles from *D. tortuosa* extract, reproduced from the reference (Selim et al. 2020); and **g** MgO nanoparticles from *R. floribunda* extract, reproduced from the reference (Younis et al. 2021)

materials at 200 and 450 °C, respectively (Alavi and Karimi 2017a; Rajapriya et al. 2020).

## X-ray diffraction

X-Ray diffraction (XRD) pattern is the characteristic technique to analyze the crystal structure, crystal plane and calculate the crystal size of a nanomaterial (Thamaphat et al. 2008). X-rays can penetrate deeply through materials and provide information about their crystal structure (Huang et al. 2007). If the material has a crystalline structure, diffraction peaks at different angles will be observed by the XRD. The Debye–Scherrer equation measures the particle size from the XRD data by determining the width of the (111) Bragg reflection according to the following equation (Eq. 1).

$$d = \frac{K \cdot \lambda}{\beta \cos \theta} \quad (1)$$

where  $d$  is the particle size (nm),  $K$  is the Scherrer constant,  $\beta$  is the full width half maximum,  $\theta$  is half of Bragg angle and  $\lambda$  is the wavelength of X-ray (Kumar Petla et al. 2012). Alavi and Karimi (2018) reported that the XRD sample

showed characteristic diffraction peaks of 38.5°, 50.7°, 65.2°, 78.4°, and 81.2°, corresponding to the planes at (111), (200), (220), (311), and (222), determine the face-centered cubic structure of Ag nanoparticles from the extract of *A. haussknechtii*. In addition, the crystal size of Ag nanoparticles is estimated to be around 47 nm by the above formula. In another study, Pansambal et al. (2017) observed that the XRD patterns of CuO nanoparticles from *A. hispidum* showed diffraction peaks at (110), (002), (111), (202), (020), (113), and (311) of face-centered cubic structure. Okeke et al. (2020) confirmed that the Cu-doped ZnO nanoparticles from *V. amygdalina* bring the crystalline structure with the hexagonal wurtzite form. This is confirmed by observing the XRD pattern with the appearance of diffraction peaks at the planes (100), (002), (101), (102), (110), (103), (112), and (201).

## Applications of nanoparticles synthesized from plants

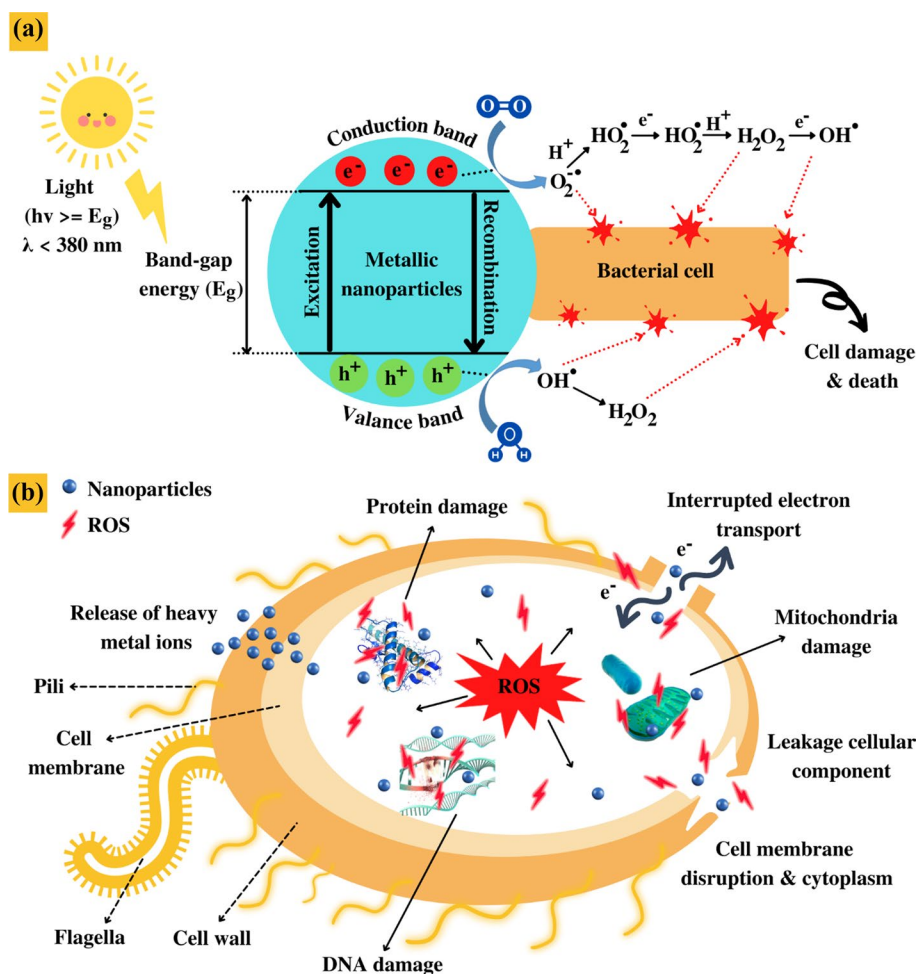
### Antibacterial activity

Bacteria exist prevalently in the living environment, and some harmful bacteria can enter the body and cause harm to human health. The overuse of antibiotics can induce the rapid development of the drug resistance in bacterial species (Llor and Bjerrum 2014). This raises the concerns about the treatment of infections caused by bacteria. Metallic nanoparticles have demonstrated their great effectiveness in antibacterial activity (Singh et al. 2020). Accordingly, the nanoparticles simultaneously target many biomolecules in bacteria, increasing the stress of bacterial cells to intercept their resistance. Besides, the nanoparticles have outstanding properties such as the small size of particles, large surface area, and good mechanical stability, which are suitable for clinical applications such as antibacterial (Sharma et al. 2020; Yin et al. 2020). Chemically synthesized nanoparticles may raise the toxic degree to the

environment and human health. Moreover, the production cost of nanoparticles is likely to be expensive, and hence, it is difficult to attain the critically green chemistry criteria (Chen et al. 2020). Meanwhile, the synthesis of biogenic nanoparticles based on plant extracts is one of the most optimal and environmentally friendly routes. In particular, the presence of a large amount of phytochemicals (e.g., polyphenols, reducing sugars, flavonoids, and alkaloids) in the extract can increase the stability and activity of nanoparticles against microorganisms (Bharathi et al. 2020).

The plausible mechanisms of the antibacterial activity of nanoparticles are still being investigated. Kumar et al. (2020) suggested that the nanoparticles possibly contact with cell walls and membranes of bacteria through the metabolic pathway. Then, the nanoparticles bind with the basic ingredients of bacteria cells such as deoxyribonucleic acid, enzymes, and ribosomes. They are more likely to deactivate the essential functions of enzymes, and proteins. Rajeshkumar and Bharath (2017) offered the hypothesis of the inhibition of transcription and translation by metal ions, causing the destruction of genetic materials inside bacterial cells. Figure 9a illustrates the mechanism of producing

**Fig. 9** **a** Mechanism of photocatalytic activity of metal metallic and mechanism producing reactive oxygen species under solar light irradiation, **b** antibacterial mechanistic process of metallic nanoparticles producing from the plants





reactive oxygen species in the presence of nanoparticles under solar light irradiation and their damage to bacterial cells. Specifically, when metallic nanoparticles are exposed to solar light, photons with the excitation energy larger than the band gap of the nanoparticles will shift electrons from the valence band (VB) to the conduction band (CB), creating electron–hole pairs ( $e^-$  and  $h^+$ ). Both entities migrate to the nanoparticle surface and perform the photocatalytic reactions, i.e.,  $h^+$  reacts with  $OH^-$  or  $H_2O$  to produce  $OH^\bullet$ ;  $e^-$  reacts with  $O_2$  to form  $O_2^{\bullet-}$ . The result of these processes is to produce reactive oxygen species that can exhibit a wide range of activities such as cell membrane disruption, leakage of cytoplasm and cellular components, damage of DNA, protein and mitochondria, and finally cells death (Khezerlou et al. 2018). Figure 9b articulates the antibacterial mechanistic process of metallic nanoparticles.

Table 3 displays the antibacterial activity of nanoparticles synthesized from various plant extracts. Accordingly, Ag nanoparticles is the most used nanomaterial in the publications. In fact, Ag ions and Ag-based compounds are immensely noxious to microorganisms and exhibit great antibacterial properties (Khalil et al. 2014). The good bioactivity of Ag nanoparticles can be ascribed to their tiny sizes and high surface area (Franci et al. 2015). Because of such reasons the scientists have also exploited the ability of Ag nanoparticles against infectious diseases in recent decades. For example, commercial products derived from silver nitrate and silver sulfadiazine are used to terminate bacteria such as disinfecting drinking water and caring for burns (Baker et al. 2005). Ag exhibits the best antibacterial properties and has been used in food preservation, novel pesticides, and cosmetics.

Khatoun et al. (2015) informed the synthesis of spherical Ag nanoparticles from *Artemisia annua* leaf extract with particles size about 7–27 nm. In this study, the most prominent application is the antimicrobial activity against *E. coli*, *S. aureus*, *P. aeruginosa*, *S. epidermidis* and *B. subtilis* with wide inhibition zones between 6 and 16.5 mm. This proved a great potential of *A. annua* as a precursor to form Ag nanoparticles for better antimicrobial activities. Baghbani-Arani et al. (2017) notified the synthesis of Ag nanoparticles from *A. tournefortiana* extract. In particular, Ag nanoparticles were created with smaller size of about 22.89 nm than the study by Khatoun et al. (2015). Compared with the same bacterial subjects, minimum inhibitory concentration (MIC) values were in this study obtained from 0.39 to 12.5  $\mu\text{g/mL}$ , which were lower than those (3–21  $\mu\text{g/mL}$ ) by Khatoun et al. (2015). This phenomenon can be attributable to the easier penetration of smaller-size nanoparticles into the cell wall of bacteria. Therefore, the production of smaller-size Ag nanoparticles may be more optimal.

Besides, the lowest minimum bactericidal concentration (MBC) values for *S. pyogenes* were 1.56  $\mu\text{g/mL}$ . *P.*

*aeruginosa* and *B. subtilis* have co-values of MBC of about 25  $\mu\text{g/mL}$ . Finally, *E. coli* was the bacteria with the highest MBC values about 50  $\mu\text{g/mL}$ . Thus, it can be concluded that Ag nanoparticles are more resistant to gram-positive bacteria than gram-negative bacteria. Similarly, many works were commensurate with the reported results of better antibacterial activity of nanoparticles to gram-positive bacteria (Raut et al. 2014; Khalil et al. 2014). However, some studies reported the opposite and suggested that Ag is more resistant to gram-negative bacteria (Mukunthan et al. 2011; Dehnavi et al. 2013; Zhang et al. 2014). Indeed, Zhang et al. (2014) noticed that the MIC value of *E. coli* (Gram-negative, 7.8 mg/l) was significantly lower than that of *S. aureus* (Gram-positive, 50 mg/l). Singh et al. (2020) explained that in gram-negative bacteria *E. coli*, there was the formation of negatively charged lipopolysaccharides bonded to positively charged Ag. Gram-positive bacteria are enclosed with a thick layer of peptidoglycans and straight-chain polysaccharides that are cross-linked with embedded proteins, giving the cell stiffness and making it difficult for the nanoparticles to bind to the cell surface. This mechanism is still being questioned, suggesting that more investigations of the impact of Ag nanoparticles on negative- and positive-gram bacteria need to be articulated.

Apart from the synthesis and utilization of Ag nanoparticles, several nanoparticles such as CuO, Au, and ZnO fabricated from various plant extracts were also addressed (Rajakumar et al. 2016; Pansambal et al. 2017; Wang et al. 2020; Rajapriya et al. 2020). For example, Pansambal et al. (2017) have synthesized CuO nanoparticles with particles size range 5–25 nm which has brought high efficiency against *M. tuberculosis*. According to this study, CuO nanoparticles exhibited the termination (99%) of *M. tuberculosis* with the MIC value of 100  $\mu\text{g/mL}$ . Rajakumar et al. (2016) focused on the synthesis of Au nanoparticles from false daisy plants. The results showed the inhibition zone at the nanoparticle concentration of 25  $\mu\text{L/mg}$  toward *E. coli* (~ 24 nm), followed by *S. aureus* (~ 16 nm), and *B. subtilis* (~ 12 nm). In another study, Wang et al. (2020) carried out the synthesis of ZnO nanoparticles from *A. annua* stem barks extract. The inhibition zones were in range from 7.4 to 22.3 mm for *E. coli*, *S. typhi*, *S. aureus* and *V. cholerae*. Recently, Ananda Murthy et al. (2021) used *V. amygdalina* leaves as the main raw material to synthesize CuO nanoparticles for antibacterial performance. The results showed that *S. aureus*, *E. coli* and *P. aeruginosa* had an inhibition zone of about 12 mm while that of *E. aerogenes* was 15 mm. As such, the plant extracts can be promising sources to synthesize the types of metallic nanoparticles and pave the way for the diverse anti-bacterial applications.



**Table 3** Antibacterial activity of nanoparticles synthesized from various plant extracts

Plant name (common name)	Part	NPs	Main findings	References
<i>A. haussknechtii</i>	Leaf	Ag, Cu, TiO <sub>2</sub>	Inhibition zone (mm) at the concentrations of 0.5–60 µg/mL: + Ag NPs: <i>E. coli</i> (14–36), <i>S. aureus</i> (8–12) + Cu NPs: <i>E. coli</i> (10–34), <i>S. aureus</i> (4–8), <i>S. marcescens</i> (4) + TiO <sub>2</sub> NPs: not found	(Alavi and Karimi 2017b)
<i>A. marschalliana</i> (Mugwort)	Aerial parts	Ag	Inhibition zone (mm) at the concentrations of 100 µg/mL: <i>S. aureus</i> (0–15.50), <i>P. aeruginosa</i> (0–13.38), <i>A. baumannii</i> (0–11.45), <i>B. cereus</i> (0–8.66)	(Ardestani et al. 2016)
<i>H. trichophylla</i>	Flower	Ag	Inhibition zone (mm) at the concentrations of 0–250 µg/mL: <i>E. coli</i> (9.1), <i>P. aeruginosa</i> (8.5), <i>B. subtilis</i> (8.2), <i>S. aureus</i> (10.2)	(Yazdi et al. 2019)
<i>T. erecta</i> (Marigold)	Flower	Ag	Inhibition zone (mm) at concentration of 5–1280 µg/mL: <i>E. coli</i> (9–25.5), <i>P. aeruginosa</i> (13.5–31.5), <i>S. aureus</i> (9–38)	(Padalia et al. 2015)
<i>C. tinctorius</i> (Safflower)	Flower	Ag	Bacterial removal percentage (%): + Ag–fabric treated at 40 °C: 98 + Ag–fabric treated at 80 °C: 85	(Aboutorabi et al. 2018)
<i>T. farfara</i> (Coltsfoot)	Flower bud	Ag	Minimum inhibitory concentration (µg/mL) against: <i>E. coli</i> (10), <i>E. faecalis</i> (> 40), <i>P. aeruginosa</i> (10), <i>S. aureus</i> (40)	(Lee et al. 2019)
<i>T. collinus</i> (Goatsbeard)	Whole plant	Ag	Inhibition zone (mm) at the concentrations of 6000–7000 µg/mL: <i>S. aureus</i> (2–10), <i>E. coli</i> (4–8)	(Seifipour et al. 2020)
<i>A. tournefortiana</i>	Whole plant	Ag	Minimum inhibitory concentration (µg/mL) against: <i>S. pyogenes</i> (0.39), <i>B. subtilis</i> (3.12), <i>P. aeruginosa</i> (12.5)	(Baghbani-Arani et al. 2017)
<i>A. millefolium</i> (Yarrow)	Whole plant	Ag	Inhibition zone (mm) at the concentrations of 100 µg/mL: <i>S. aureus</i> (14.33), <i>P. aeruginosa</i> (13.67), <i>E. coli</i> (10.33), <i>S. enterica</i> (11.95), <i>B. subtilis</i> : (6.75)	(Yousaf et al. 2020)
<i>S. quettense</i> (Podlech)	Whole plant	Ag	Minimum inhibitory concentration (µg/mL) against: <i>E. coli</i> , <i>K. pneumonia</i> and <i>B. subtilis</i> (11.1–33.3)	(Qasim Nasar et al. 2019)
<i>E. scaber</i> (Elephant's foot)	Leaf	Ag	Inhibition zone (*) (mm) against: <i>B. subtilis</i> (14–16), <i>L. lactis</i> (21–24), <i>P. fluorescens</i> (18–23), <i>P. aeruginosa</i> (21–22), <i>A. flavus</i> (9–12), <i>A. penicillioides</i> (6–139)	(Francis et al. 2018)
<i>W.chinensis</i> (Sphagneticola calendulacea)	Leaf	Ag	Inhibition zone (mm) at the concentration of 12.25–200 µg/mL: <i>E. coli</i> (17.2– 35.1), <i>L. monocytogenes</i> (11.9– 27.3)	(Paul Das et al. 2018)

**Table 3** (continued)

Plant name (common name)	Part	NPs	Main findings	References
<i>X. strumerium</i> (Rough cocklebur)	Leaf	Ag	Minimum inhibitory concentration (µg/mL) at concentrations of 1–100 ppm against: <i>E. coli</i> (35), <i>S. aureus</i> (40), <i>P. aeruginosa</i> (45)	(Mittal et al. 2017)
<i>A. factorovskyi</i>	Leaf	Ag	Inhibition zone (mm) against <i>S. aureus</i> (19), <i>F. solani</i> : (1.5)	(Al-Otibi et al. 2020)
<i>A. annua</i> (Sweet wormwood)	Leaf	Ag	Inhibition zone (mm) at concentration of 5–20 µg/mL: <i>E. coli</i> (6–13), <i>S. aureus</i> (9–16.5), <i>P. aeruginosa</i> (8–16), <i>S. epidermidis</i> (10–19), <i>B. subtilis</i> (7.5–15)	(Khattoon et al. 2015)
<i>K. grandiflora</i>	Leaf	Ag	Inhibition zone (mm) at concentration of 10–100 µg/mL: <i>P. aeruginosa</i> (17), <i>E. coli</i> (22)	(Kanagamani et al. 2019)
<i>T. officinale</i> (Common dandelion)	Leaf	Ag	Inhibition zone (mm) at concentration of 20 µg/mL: <i>X. axonopodis</i> (22), <i>P. syringae</i> (19.5)	(Saratale et al. 2018)
<i>S. nodiflora</i> (Nodeweed)	Leaf	Ag, Au	Inhibition zone (mm) against bacteria: + Ag NPs: <i>B. subtilis</i> (9.1), <i>Streptococcus</i> spp. (8.8), <i>Pseudomonas</i> spp. (11), <i>E. coli</i> (14) + Au NPs: <i>B. subtilis</i> (7.5), <i>Streptococcus</i> spp. (6.9), <i>Pseudomonas</i> spp. (8.1), <i>E. coli</i> (9)	(Vijayan et al. 2018)
<i>T. procumbens</i> (Coatbuttons)	Leaf	Ag	Inhibition zone (mm) against bacteria: <i>E. coli</i> (15.33), <i>S. aureus</i> (15.33), <i>P. aeruginosa</i> (14.33)	(Rani et al. 2020)
<i>A. hispidum</i> (Bristly starbur)	Leaf	Ag	Inhibition zone (mm) at concentration of 18–19 µg/mL: <i>S. pyogenus</i> (23 mm), <i>E. coli</i> (12 mm)	(Ghotekar et al. 2019)
<i>A. hispidum</i> (Bristly starbur)	Leaf	CuO	Percent inhibition (%) of <i>M. tuberculosis</i> : 99	(Pansambal et al. 2017)
<i>P. vulgaris</i> (False fleabane)	Flower, leaf, stem	AgCl	Inhibition zone (mm) at concentration of 20–40 µg/mL: 25–38	(Sharifi-Rad and Pohl 2020)
<i>A. scoparia</i> (Virgate wormwood)	Aerial part	Au, Ag, Cu, Au–Ag, Au–Cu, Ag–Cu	The minimum inhibitory concentration /minimum bactericidal concentration values (µM): + AuNPs: <i>E. coli</i> (> 500/> 500), <i>S. epidermis</i> (> 500/500) + AgNPs: <i>E. coli</i> (15.6/31.2), <i>S. epidermis</i> (31.2/125) + CuNPs: <i>E. coli</i> (250/500), <i>S. epidermis</i> (> 500/> 500) + Au–AgNPs: <i>E. coli</i> (7.8/31.2), <i>S. epidermis</i> (7.8/62.5) + Au–CuNPs: <i>E. coli</i> (> 500/> 500), <i>S. epidermis</i> (> 500/> 500) + Ag–CuNPs: <i>E. coli</i> (31.2/125), <i>S. epidermis</i> (31.2/62.5)	(Shankar et al. 2016)

**Table 3** (continued)

Plant name (common name)	Part	NPs	Main findings	References
<i>S. marianum</i> (Blessed thistle)	Whole plant	ZnO, Ag–ZnO	Minimum inhibitory concentration ( $\mu\text{g/mL}$ ) against bacteria: + ZnO NPs: <i>B. subtilis</i> (50), <i>S. epidermis</i> (250), <i>P. aeruginosa</i> (250), <i>K. pneumonia</i> (150), <i>E. coli</i> (100) + Ag–ZnO NPs: <i>B. subtilis</i> (50), <i>S. epidermis</i> (150), <i>P. aeruginosa</i> (150), <i>K. pneumonia</i> (250), <i>E. coli</i> (150)	(Hameed et al. 2019)
<i>S. altissima</i> (Lategoldenrod)	Leaf	Ag	The optical density values at 600 nm ( $\text{OD}_{600}$ ) at 5–20 $\mu\text{g/mL}$ against <i>E. coli</i> and <i>B. subtilis</i> were 0.1 and 9, respectively	(Kumar et al. 2016)
<i>O. genistifolia</i> (Klein perdekaroo)	Leaf	Ag/AgCl	Minimum inhibitory concentration ( $\mu\text{g/mL}$ ) against: <i>L. ivanovic</i> (1), <i>E. cloacae</i> (0.5), <i>S. uberis</i> (0.5), <i>S. aureus</i> (0.5), <i>M. smergatis</i> (0.25), <i>Vibrio</i> spp. (0.25)	(Okaiyeto et al. 2019)
<i>V. amygdalina</i> (Bitter leaf)	Leaf	$\text{Zn}_{1-x}\text{Cu}_x\text{O}$	Minimum inhibitory concentration ( $\mu\text{g/mL}$ ) against <i>S. aureus</i> and <i>E. coli</i> (10–2.5), <i>P. aeruginosa</i> (5)	(Okeke et al. 2020)
<i>B. eriantha</i> (Blumea)	Whole plant	Ag, Fe	Inhibition zone (mm) at the concentrations of 0.5–60 $\mu\text{g/mL}$ : + Ag NPs: <i>B. cereus</i> (35.2), <i>B. subtilis</i> (30.12), <i>S. aureus</i> (20.17), <i>E. Coli</i> (25.24) + Fe NPs: <i>B. cereus</i> (24.12), <i>B. subtilis</i> (26.45), <i>S. aureus</i> (17.06), <i>E. Coli</i> (11.55)	(Chavan et al. 2020)
<i>A. annua</i> (Sweet wormwood)	Stem bark	ZnO	Inhibition zone (mm) at concentration of 20–80 $\mu\text{g/mL}$ : <i>E. coli</i> (8.6–11.3), <i>S. typhi</i> (7.6–12.3), <i>S. aureus</i> (7.4–22.3), <i>V. cholerae</i> (7.9–22.1)	(Wang et al. 2020)
<i>C. benedicti</i> (Blessed thistle)	Whole plant	Au–CuO, CuO–ZnO	Minimum inhibition concentration (%) against bacteria: + CuO–ZnO NPs: <i>S. aureus</i> (0.3125), <i>P. aeruginosa</i> (2.5), <i>E. coli</i> (0.625), <i>C. albicans</i> (1.25) + Au–CuO NPs: <i>S. aureus</i> (2.5), <i>P. aeruginosa</i> (2.5), <i>E. coli</i> (1.25), <i>C. albicans</i> (2.5)	(Dobrucka et al. 2019)
<i>E. prostrata</i> (False daisy)	Leaf	Au	Inhibition zone (mm) at the concentrations of 25 $\mu\text{g/mL}$ : <i>E. coli</i> (24), <i>S. aureus</i> (16), <i>B. subtilis</i> (12)	(Rajakumar et al. 2016)
<i>S. costus</i> (Putchuk)	Root	MgO	Inhibition zone (mm) at the concentrations of 5–1280 $\mu\text{g/mL}$ : <i>E. coli</i> (15 mm), <i>P. aeruginosa</i> (16 mm), <i>S. aureus</i> (14 mm), <i>B. subtilis</i> (10 mm)	(Alavi and Karimi 2017a)
<i>C. scolymus</i> (Globe artichoke)	Leaf	ZnO	Minimum inhibition concentration ( $\mu\text{g/mL}$ ) against: <i>S. aureus</i> (>0.7), <i>E. coli</i> (25), <i>P. aeruginosa</i> (>100)	(Rajapriya et al. 2020)

## Anticancer activity

Cancer diseases are increasingly detected in many recent years, affecting the physical and mental health of patients. They can cause many anxiety, distress, and depression behaviors. According to the International Cancer Research Organization, there are about 18.1 million new cases of cancer and 9.6 million cases of death each year around the world (Bray et al. 2018). It is forecasted that by 2025, this number will increase to 19.3 million, of which patients are mainly from developing countries. Therefore, the treatments and therapies against cancer diseases have paid special attention from scientists. Some cancer treatments involve hormone therapy and immunotherapy, but these often result in some abnormalities in the patient body. Specifically, they possibly damage normal cells and vital organs, exacerbating the patient health, and causing the reduction in life quality (Han et al. 2019). Metallic nanoparticles have a huge potential in the detection, diagnosis and treatment of cancer diseases (Ikram et al. 2021). Their high selectivity between diseased and normal cells minimizes the risks of side effects and limits the damage to normal cells (Saravanan et al. 2020). The reason may be owing to different electrostatic interactions between nanoparticles and these cells (Javed et al. 2021).

The anticancer mechanism of metallic nanoparticles is quite complex and still under investigation. Lee et al. (2019) suggested that the plausible anticancer mechanism of metallic nanoparticles could be due to the reactive oxygen species-dependent apoptosis and caspase-mediated apoptosis in cancer cell lines (Fig. 10). When metallic nanoparticles come into contact with cancer cell membranes, cell surface provokes the invagination of nanoparticles by endocytosis to generate the intracellular membrane-bounded vesicles (Doherty and McMahon 2009). This allows endocytosed nanoparticles to enter the intracellular space without elimination. They are then released to produce reactive oxygen species which can perform the tasks of malfunctioning a variety of mitochondria and enzymes, protein oxidation, deoxyribonucleic acid (DNA) damage, nuclear destruction, and decreasing major non-protein free-radical scavengers (Bethu et al. 2018). In particular, reactive oxygen agents are likely to induce cell cycle arrest in the growth and preparation for mitosis phase as well as meiosis phase (Patil and Kim 2017). They are ascribed to increasing the ratio between B-cell lymphoma protein 2-associated X and B-cell lymphoma protein, which determines cell susceptibility to apoptosis. This process is finalized through the stimulation of caspase -3, -8, -9 (proteins related to apoptosis). Many works also indicated that reactive oxygen species increase the level of tumor protein P53 as known to inhibit cancer cells (Kordezangeneh et al. 2015; Patil and Kim 2017; Kim et al. 2019). Based on the mentioned mechanisms, nanoparticles

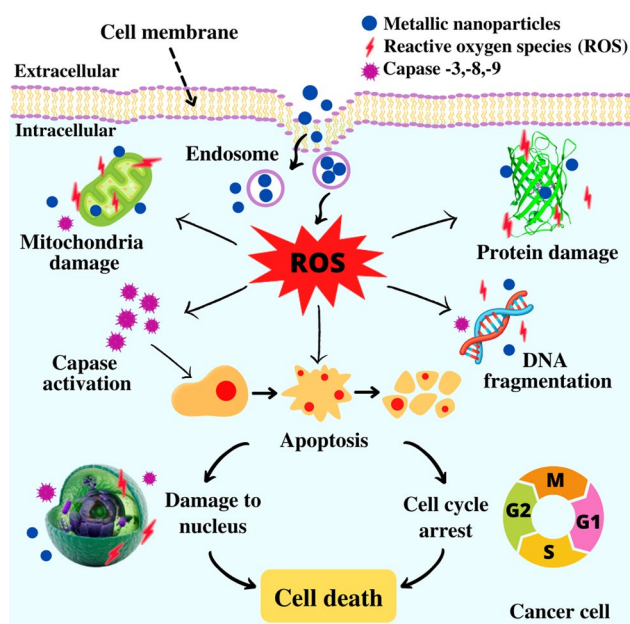


**Fig. 10** Anticancer mechanistic process of metallic nanoparticles producing from the plants. The formation of reactive oxygen species may play a main role in protein damage, DNA fragmentation, and so forth, finally causing apoptosis inhibition, cell death. Abbreviations: ROS, reactive oxygen species; DNA, deoxyribonucleic acid; cell cycle (as shown in bottom right corner): G1 (growth), S (DNA synthesis), G2 (growth and preparation for mitosis), M (mitosis or cell division)

through reactive oxygen agents can contribute greatly to killing cancer cells.

Table 4 summarizes the anticancer activity of nanoparticles synthesized from various plant extracts. For example, Lee et al. (2019) reported that *T. farfara* flower bud extracts could be used to synthesize Ag nanoparticles and Au nanoparticles. Through the structural characterization by the atomic force microscopy images, the average particle sizes of Ag nanoparticles and Au nanoparticles were determined, at 56.24, and 41.96 nm, respectively. Both Au nanoparticles and Ag nanoparticles presented good anticancer abilities to cells including human gastric adenocarcinoma (AGS), human colorectal adenocarcinoma (HT-29), and human pancreas ductal adenocarcinoma (PANC-1). However, the minimum inhibitory concentration values of Au nanoparticles were between 2 and 4 times lower than Ag nanoparticles for all cells, indicating that Au nanoparticles were more likely to be resistant against cancer line cells than Ag nanoparticles. It could be explained due to the smaller particle size of Au nanoparticles, leading to better penetration into the cell membrane. Agreeing with this finding, Patil and Kim (2017) confirmed that the higher surface area of the gold nanoparticles allows the presence of more surface atoms, hence more exposure of nanoparticles in cancer cells.

Qasim Nasar et al. (2019) noticed that Ag nanoparticles synthesized from *S. quettense* extracts could be against liver

**Table 4** Anticancer activity of nanoparticles synthesized from various plant extracts

Plant name (common name)	Part	NPs	Optimal conditions and results	References
<i>T. farfara</i> (Coltsfoot)	Flower	Ag, Au	Minimum inhibition concentration ( $\mu\text{M}$ ) against human gastric adenocarcinoma cell line (Ag NPs: 338.0, Au NPs: 77.9), human colon cancer cell line (Ag NPs: 275.3, Au NPs: 87.0), human pancreatic cancer cell line (Ag NPs: 166.1, Au NPs: 71.2)	(Lee et al. 2019)
<i>C. cernuum</i>	Whole plant	Ag	The percentage of cellular uptake (%) at the concentration of 0.025–0.1 $\mu\text{g}/\text{mL}$ against on murine melanoma cell line (17.3), epithelial carcinoma cell line (22.6)	(Ahn et al. 2019)
<i>P. leubnitziae</i> (Stinkbush)	Whole plant	Ag	Half-maximal inhibitory concentration value ( $\mu\text{g}/\text{mL}$ ) against: the glioma cell line (0.64–0.71)	(Mofolo et al. 2020)
<i>S. quettense</i> (Podlech)	Whole plant	Ag	Half-maximal inhibitory concentration value ( $\mu\text{g}/\text{mL}$ ) against: human liver cancer cell line (62.5)	(Qasim Nasar et al. 2019)
<i>A. turcomanica</i> (Mugwort)	Leaf	Ag	Half-maximal inhibitory concentration value ( $\mu\text{g}/\text{mL}$ ) against: murine fibroblast cell line (14.56), human gastric adenocarcinoma cell line (4.88)	(Mousavi et al. 2018)
<i>E. scaber</i> (Elephant's foot)	Leaf	Ag	Half-maximal inhibitory concentration value ( $\mu\text{g}/\text{mL}$ ) against: human skin carcinoma cells (15.68), fibroblast cells (65.49)	(Francis et al. 2018)
<i>C. intybus</i> (Chicory)	Leaf	Ag	Half-maximal inhibitory concentration value ( $\mu\text{g}/\text{mL}$ ) against: breast cancer cell line (507.58)	(Behboodi et al. 2019)
<i>T. officinale</i> (Common dandelion)	Leaf	Ag	Cell viability (%) at the concentrations of range 10–200 $\mu\text{g}/\text{mL}$ against: human liver cancer cell line: 2–99	(Saratale et al. 2018)
<i>W. chinensis</i> (Sphagneticola calendulacea)	Leaf	Ag	Half-maximal inhibitory concentration value ( $\mu\text{g}/\text{mL}$ ) against: human liver cancer cell line (25)	(Paul Das et al. 2018)
<i>K. grandiflora</i>	Leaf	Ag	Percentage cytotoxicity cells (%) at the concentration of 200 $\mu\text{g}/\text{mL}$ against: Dalton's lymphoma ascites cell line (100)	(Kanagamani et al. 2019)
<i>A. ciniformis</i>	Leaf	Ag	Cell viability estimated (%) at the concentrations of range 0.78–100 $\mu\text{g}/\text{mL}$ against: human gastric adenocarcinoma cell line (2–99)	(Aslany et al. 2020)
<i>A. biebersteinii</i> (Yellow milfoil)	Flower	Ag	Half-maximal inhibitory concentration value ( $\mu\text{g}/\text{mL}$ ) against: breast cancer cell line (20–99)	(Baharara et al. 2015)
<i>A. marschalliana</i> (Mugwort)	Aerial parts	Ag	Half-maximal inhibitory concentration value ( $\mu\text{g}/\text{mL}$ ) against: human gastric adenocarcinoma cell line (21.05)	(Ardestani et al. 2016)
<i>E. prostrata</i> (False daisy)	Leaf	ZnO	The percentage necrosis of cell (%) at the concentrations of 1–500 $\mu\text{g}/\text{mL}$ against human liver carcinoma cell line (14.5–86.5)	(Chung et al. 2015)
<i>E. prostrata</i> (False daisy)	Leaf	Pd	Percentage cytotoxicity cells (%) at the concentration of 1–500 $\mu\text{g}/\text{mL}$ against: human liver cancer cell line (7.5–76.5)	(Rajakumar et al. 2015)
<i>C. benedicti</i> (Blessed thistle)	Whole plant	Au–CuO, CuO–ZnO	Dead cells percentage (%) against the rat glioma cell line: 0.2–90 (Au–CuO NPs), 0.1–80 (CuO–ZnO NPs)	(Dobrucka et al. 2019)
<i>S. costus</i> (Putchuk)	Root	MgO	Half-maximal inhibitory concentration value (%) against: human breast cancer line cell (52.1–67.3)	(Alavi and Karimi 2017a)



cancer cells A375. Half-maximal inhibitory concentration value (IC<sub>50</sub>) of Ag nanoparticles (62.5 µg/mL) was significantly lower than that of *S. quettense* extract (251 µg/mL). Consequently, Ag nanoparticles were more likely to destroy human liver cancer (HepG2) cells than the crude extract. This finding demonstrated that Ag nanoparticles presented higher cytotoxicity than plant extracts. Similarly, Francis et al. (2018) showed Ag nanoparticles produced from *E. scaber* extract attained a superior anticancer property than *E. scaber* extract. Indeed, IC<sub>50</sub> value to liver cancer cells A375 obtained for Ag nanoparticles produced from *E. scaber* significantly was threefold lower than that of *E. scaber*. This result proves that metallic nanoparticles (Au and Ag) acquired a significant potential to human cancer therapies.

Amina et al. (2020) focused on the synthesis of MgO nanoparticles from patchouli root extract for the resistance of breast cancer cell lines (MCF-7). According to the results, 67.3% of cancer cells were destroyed, showing that the synthesized MgO nanoparticles may contribute significantly to the cancer treatment field. In another study, Ahn et al. (2019) have successfully synthesized Ag nanoparticles from *C. cernuum* extracts. Obtained nanoparticles had an average size of about 13.0 nm, and spherical morphology, which plays a key role in the enhancement against mouse melanoma cells (17.3%) and human lung cancer cells (22.6%) at concentrations between 25 and 100 ng/mL. To sum up, the synthesized MgO nanoparticles may be beneficial as promising anticancer agents.

## Antifungal activity

Currently, acquired immunodeficiency syndrome (AIDS) and organ transplants provide the ideal environment for the infection of opportunistic fungi, which are becoming one of the main originators of mortality and morbidity (Webster et al. 2008). In addition, the fungi also affect the agricultural economy, cause seasonal diseases, and reduce the quality of crops. Therefore, antifungal researches using biogenic nanoparticles are being interested enormously. Synthesis of nanoparticles from plant extracts is one of the most potential and environmentally friendly methods for expanding the antifungal applications in the medicinal and agricultural fields.

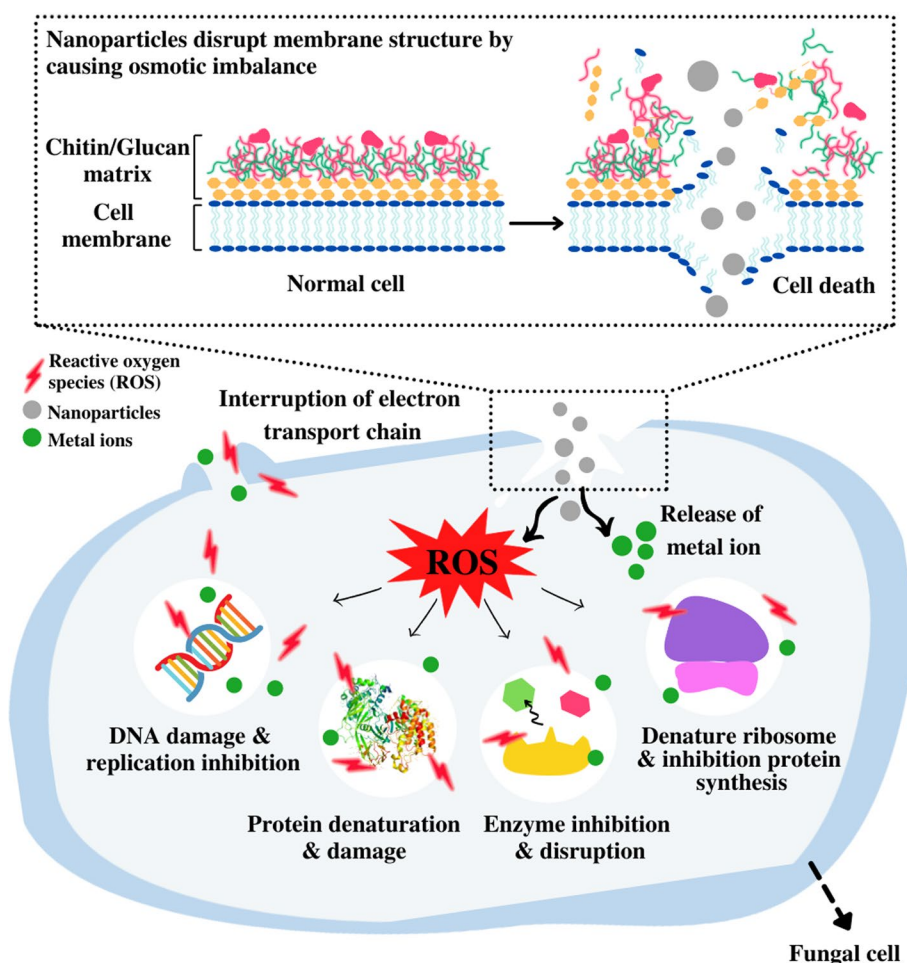
Similar to mentioned antibacterial and anticancer mechanisms, metallic nanoparticles also adopt the same mechanism of producing reactive oxygen species and free radicals by releasing metal ions from their nanostructure to exterminate fungal species (Lipovsky et al. 2011). As illustrated in Fig. 11, nanoparticles approach the surface of microorganisms and cause many damaging interactions with the cell wall, leaking out intracellular components (Reddy et al. 2015). Specifically, they disrupt cell walls by altering redox homeostasis and oxidative stress. This deconstruction leads to the homeostatic imbalance and loss of membrane

integrity, from which nanoparticles enter the cells (Kumari et al. 2019). Through the mechanism of reactions with the phosphorus or sulfur moieties of DNA, nanoparticles can also prevent DNA replication, ceasing the growth of microorganisms, leading to cell death (Shanmugam et al. 2016). In addition, they induce a variety of activities, e.g., protein denaturation and damage, enzyme inhibition and disruption, denature ribosome, and inhibition of ribosome synthesized proteins. In particular, metallic nanoparticles are also capable of inhibiting glutathione-producing enzymes (GSH)—an enzyme that plays an antioxidant role, which reduces the resistance of fungi (Sun et al. 2018).

Table 5 shows the good antifungal performance of nanoparticles synthesized from various plant extracts. Indeed, Vijayan et al. (2018) carried out the fabrication of Ag and Au nanoparticles from *S. nodiflora* leaf extract for the performance of antifungal activities. Accordingly, the inhibition zone of Ag nanoparticles against *Aspergillus* spp. and *Penicillium* spp. obtained about 12.9 mm, and 10.9 mm, respectively. Under the same conditions, Au nanoparticles have the smaller zone inhibition for both *Aspergillus* spp. and *Penicillium* spp. (~9 mm). These outcomes clarified that Ag nanoparticles acquired a better relatively antifungal potential than that of Au nanoparticles. The reasonable interpretation possibly relies on the particle size of Ag nanoparticles (19.4 nm) smaller than that of Au nanoparticles (22.01 nm), making them easier to enter cell membranes and destroy fungal cells. In another study, Qasim Nasar et al. (2019) have synthesized Ag nanoparticles from *S. quettense* extract with the significantly larger particle size between 48.40 and 55.35 nm compared with that by Vijayan et al. (2018). However, the antifungal results against *Aspergillus* spp. seemed to be more promising since the inhibition zone was wider, at 13.2 mm. As a result, Ag nanoparticles biosynthesized from *S. quettense* extract achieved better antifungal results than those biosynthesized from *S. nodiflora*. This finding is attributable to the significant presence of phenolic and flavonoid compounds found in the plant extracts of *S. quettense*, i.e., with their amount of 40–56 µg per mg dried extract. Hence, the antifungal behaviors of metallic nanoparticles are not only reliant on the particle size but also on bioactive compounds present in the plant extracts during the synthesis.

Apart from the use of precious metallic nanoparticles such as Au, Ag, and ZnO nanoparticles could be used for the antifungal performance against *C. albicans*, *C. tropicalis*, and *F. oxysporum*. Indeed, Rajapriya et al. (2019) have successfully synthesized ZnO nanoparticles from *C. scolymus* (globe artichoke) leaf extract. In this study, the minimum inhibitory concentration of ZnO nanoparticles against *C. albicans* and *C. tropicalis* was ~100 and 0.35 µg/mL, respectively. This result demonstrated that ZnO attained a considerably higher antifungal behavior against *C. tropicalis* (approximately 300 times) than that against *C. albicans*.

**Fig. 11** Antifungal mechanism of metallic nanoparticles producing from the plants. The reactive oxygen species are responsible for protein damage, DNA replication inhibition, enzyme inhibition, and so forth, causing fungal cell death. Abbreviations: ROS, reactive oxygen species; DNA, deoxyribonucleic acid



Jebril et al. (2020) conducted an investigation on the antifungal activity of Ag nanoparticles from *M. azedarach* leaf extracts. Accordingly, the percentage of inhibition against *V. dahliae* of Ag nanoparticles were 18, 33, and 51% at the range concentrations of 20, 40, and 60 ppm, respectively. It could be concluded that higher the concentration of Ag nanoparticles, better the antifungal activity. In another study, Narendhran and Sivaraj. (2016) carried out the production of ZnO nanoparticles from *L. aculeata* extract for the antifungal effect. The results indicated that the inhibition zones against *A. flavus* and *F. oxysporum* were found at 21, and 19 mm, respectively. For other nanoparticles, Pagar et al. (2020) reported a promising antifungal activity of green CuO nanoparticles produced by using leaves extract of *Moringa oleifera*. In general, metallic nanoparticles (majorly, Au, Ag, and ZnO) biofabricated from plant extracts acquire great potentials in inhibiting a wide range of fungal species.

### Antioxidant activity

For a long time, researchers have concluded that free radicals are one of the causes of human disease and aging

processes (Chen et al. 2012). Cells that perform functional activities such as immunity and respiration in the body can produce free radicals. When free radicals are, however, overproduced, they will pair with other biomolecules such as proteins, nucleic acids, lipids and carbohydrates in the body. This phenomenon can cause a wide range of negative effects on humans such as atherosclerosis, aging, cardiovascular disease, inflammation. More seriously, free radicals are responsible for cancer diseases (Javed et al. 2021). In addition, the chemical compounds in foods exposed under air are likely to react with oxygen, which loses nutritional value, and increases rancidity as well as discoloration (Das et al. 2013). Free radicals in foods can be harmful to human health. Although butylated hydroxytoluene, n-propyl gallate, and butylated hydroxyanisole are effective antioxidants, they are highly carcinogenic agents, hence not widely used (Das et al. 2013). Some nanoparticles (ZnO, Ag) incorporated into food packaging membranes have played the potentials for antimicrobial activities and applications against free radicals (Al-Naamani et al. 2016; Yu et al. 2019).

Biogenic nanoparticles have recently been known for their high antioxidant capacity, biocompatibility, and

**Table 5** Antifungal activity of nanoparticles synthesized from various plant extracts

Plant name (common name)	Part	NPs	Optimal conditions and results	References
<i>S. nodiflora</i> (Nodeweed)	Leaf	Ag, Au	Inhibition zone (mm) against fungal: + Ag NPs: <i>Aspergillus</i> spp. (12.9) <i>Penicillium</i> spp. (10.9) + Au NPs: <i>Aspergillus</i> spp. (9) <i>Penicillium</i> spp. (9)	(Vijayan et al. 2018)
<i>S. quettense</i> (Podlech)	Whole plant	Ag	Inhibition zone (mm) against <i>A. niger</i> (13.2), <i>A. fumigatus</i> (12), <i>A. flavus</i> (10), <i>Mucor</i> spp. (11)	(Qasim Nasar et al. 2019)
<i>C. scolymus</i> (Globe artichoke)	Leaf	ZnO	Minimum inhibition concentration ( $\mu\text{g}/\text{mL}$ ) at the concentration of 100 $\mu\text{g}/\text{mL}$ against: <i>C. albicans</i> (> 100), <i>C. tropicalis</i> (0.35)	(Rajapriya et al. 2020)
<i>A. retroflexus</i> (Redroot pigweed)	Leaf	Ag	Minimum inhibition concentration ( $\mu\text{g}/\text{mL}$ ) at the concentration of 50–400 $\mu\text{g}/\text{mL}$ against: <i>M. phaseolina</i> (159.80), <i>A. alternata</i> (337.09), <i>F. oxysporum</i> (328.05)	(Bahrami-Teimoori et al. 2017)
<i>M. azedarach</i> (Chinaberry)	Leaf	Ag	The percent inhibition (%) at the concentration of 20–60 $\mu\text{g}/\text{mL}$ against: <i>V. dahliae</i> (18–51)	(Jebri et al. 2020)
<i>N. arbor-tristis</i> (Night-flowering jasmine)	Flower	ZnO	Minimum inhibition concentration ( $\mu\text{g}/\text{mL}$ ) at the concentration of 256 $\mu\text{g}/\text{mL}$ against: <i>A. alternata</i> (64), <i>A. niger</i> (16), <i>B. cinerea</i> (128), <i>F. oxysporum</i> (64), <i>P. expansum</i> (128)	(Jamdagni et al. 2018)
<i>L. aculeata</i> (West Indian lantana)	Whole plant	ZnO	Inhibition zone (mm) against: <i>A. flavus</i> (21), <i>F. oxysporum</i> (19)	(Narendhran and Sivaraj 2016)
<i>A. vera</i>	Leaf	Ag	Minimum inhibition concentration ( $\mu\text{g}/\text{mL}$ ) against both <i>Aspergillus</i> spp. and <i>Rhizopus</i> spp. (21.8)	(Medda et al. 2015)
<i>C. sparsiflorus</i> (Bonpland's croton)	Leaf	Ag	Inhibition zone (mm) against <i>Mucor</i> spp. (0.1), <i>Trichoderma</i> spp. (0.1), <i>A. nigar</i> (0.1)	(Kathiravan et al. 2015)
<i>T. majus</i> (Common nasturtium)	Leaf	Ag	Minimum inhibition concentration ( $\mu\text{g}/\text{mL}$ ) against: <i>P. notatum</i> (31.2), <i>A. niger</i> (125), <i>C. albicans</i> (250), <i>T. viridiae</i> (62.5), <i>Mucor</i> spp.(29)	(Valsalam et al. 2019)
<i>C. paniculatus</i> (Intellect plant)	Leaf	Cu	The percent inhibition (%) against: <i>F. oxysporum</i> (59.25–76,29)	(Mali et al. 2020)
<i>Z. nummularia</i> (Jujube)	Leaf	ZnO	Minimum inhibition concentration ( $\mu\text{g}/\text{mL}$ ) at the concentration of 25–125 $\text{mg}/\text{mL}$ against both <i>C. albicans</i> and <i>C. glabrata</i> (1,25), <i>C. neoformans</i> (10)	(Padalia and Chanda 2017)
<i>S. arvensis</i> (Wild mustard)	Seed	Ag	The percent inhibition (%) at the concentration of 2.5–40 $\mu\text{g}/\text{mL}$ against <i>N. parvum</i> (15–83)	(Khatami et al. 2015)

stability (Mohanraj and Chen 2007; Naahidi et al. 2013). These properties may be derived from plant extracts, which contain various bioactive compounds known as phytochemicals including isoflavones, alkaloids, and polyphenols. They not only supply a good platform to produce nanoparticles but also improve their properties in terms of surface area, particle size, and surface functionality. As a result, they are used to serve as promising antioxidants against free radicals which are beneficial in the medical fields and food preservation (Fig. 12). The green synthesis of nanoparticles from

plant extract is recognized as one of the most economical and environment-friendly methods. Table 6 summarizes the results of antioxidant activities of biosynthesized nanoparticles from recent works.

The methods of determining the antioxidant activities of nanoparticles have been studied. 2-diphenyl-1-picrylhydrazyl (DPPH) is a free radical scavenging trap for other radicals, allowing to monitor antioxidant properties. This is owing to its ability in inhibiting free radicals (Zhaleh et al. 2019). The DPPH-based method presents as one of the most widely used

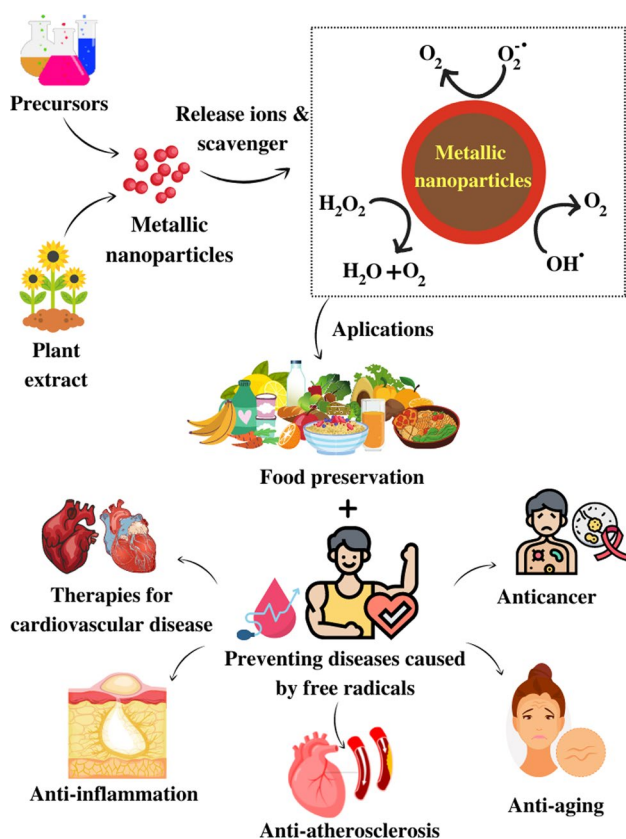


Fig. 12 Nanoparticles in the medical field and food preservation

ones because it provides a simple protocol, screening results rapidly and high reliability (Javed et al. 2021). Nelson et al. (2016) suggested a possible mechanism how metallic nanoparticles worked out antioxidant activity of metallic nanoparticles. The nanoparticles firstly eliminate  $\bullet\text{O}_2^-$  to  $\text{O}_2$ ,  $\text{H}_2\text{O}_2$  reduced to  $\text{H}_2\text{O}$  and  $\text{O}_2$ , and followed by the formation of  $\text{O}_2$  from  $\text{OH}^\bullet$  or  $\text{H}_2\text{O}_2$ . Specific for  $\text{CeO}_2$  nanoparticles, the chain initiates a series of reactions to remove free radicals, i.e., (1) and (2) are the reduction reaction of  $\bullet\text{O}_2^-$ , (3) is reduction in  $\text{H}_2\text{O}_2$ , (4) and (5) is the reduction in  $\text{OH}^\bullet$ .

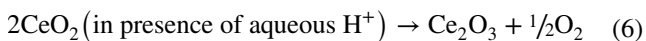
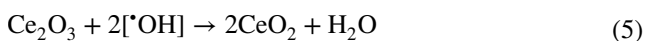
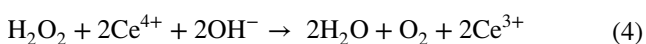
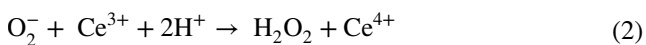


Table 6 exhibits the antioxidant performance of nanoparticles synthesized from various plant extracts. As an example, Kharat and Mendhulkar (2016) have reported that Ag nanoparticles synthesized from *Elephantopus scaber* leaf extracts. In this literature, the IC<sub>50</sub> values of Ag nanoparticles from *E. scaber* extract were between 41.86 and 126.6  $\mu\text{g}/\text{mL}$ . By using the same leaf extract, Francis et al. (2018) successfully produced Ag nanoparticles with a small average particle size of  $\sim 37.86$  nm. In addition, IC<sub>50</sub> value of Ag nanoparticles from *E. scaber* extract was found at 6.629  $\mu\text{g}/\text{mL}$  which was considerably lower than that of Ag nanoparticles reported by Kharat and Mendhulkar (2016). This indicated the antioxidant activity of Ag nanoparticles has been improved. The underlying reason might be the microwave-assisted synthesis procedure, enhancing the better stability of Ag nanoparticles (Francis et al. 2018). Ag nanoparticles from *E. scaber* extract also showed a comparative antioxidant activity better than crude extract. As a result, the use of microwaves may contribute to the enhancement of the antioxidant activity of Ag nanoparticles.

Other plant extracts were reportedly used to synthesize and test antioxidant activity of Ag nanoparticles. Indeed, Ahn et al. (2019) investigated the potential of *C. cernuum* extract for such purposes. Accordingly, IC<sub>50</sub> value against DPPH radical scavenging of Ag Nanoparticles was obtained at 121  $\mu\text{g}/\text{mL}$ . Park et al. (2020) explained that several bio-compounds such as sesquiceneole,  $\alpha$ -bisabolol, and myrtenal compounds in *C. cernuum* extract supported the superior antioxidant activity. Yousaf et al. (2020) pointed out Ag nanoparticles synthesized from *A. millefolium* extract had an excellent antioxidant performance. Accordingly, the IC<sub>50</sub> value of Ag nanoparticles against DPPH (7.03  $\mu\text{g}/\text{mL}$ ) was higher than that of ascorbic acid (vitamin C, 4.29  $\mu\text{g}/\text{mL}$ ), a popular natural antioxidant. In other words, as-mentioned results demonstrated that Ag nanoparticles produced from *A. millefolium* extract exhibited even more antioxidant effectiveness than vitamin C. This finding suggests a prospective future for the researches on bio-based Ag nanometallic antioxidants.

Apart from the synthesis of Ag nanoparticles, many studies also carried out the synthesis of other metallic nanoparticles (e.g. Au, ZnO, CuO) from different plant species and measure their antioxidant activities (Rajeshkumar et al. 2018, 2019; Zhaleh et al. 2019). Indeed, Zhaleh et al. (2019) synthesized Au nanoparticles from *G. tournefortii* leaf extract, and the IC<sub>50</sub> value against DPPH was about 194  $\mu\text{g}/\text{mL}$ . Likewise, Rajeshkumar et al. (2018) implicated that ZnO nanoparticles from leaf mango extract acquired outstanding antioxidant activity. As evidenced by the percentage of inhibition toward DPPH, the value for ZnO Nanoparticles was in range from 22 to 93%. Rajeshkumar et al. (2019) performed another study on the antioxidant ability of CuO nanoparticles from *C. arnotiana* extract. Accordingly,



**Table 6** Antioxidant activity of nanoparticles synthesized from various plant extracts

Plant name (common name)	Part	NPs	Optimal conditions and results	References
<i>E. scaber</i> (Elephant's foot)	Leaf	Ag	Half-maximal inhibitory concentration value ( $\mu\text{g}/\text{mL}$ ) against DPPH: 6.629	(Francis et al. 2018)
<i>E. scaber</i> (Elephant's foot)	Leaf	Ag	Half-maximal inhibitory concentration value ( $\mu\text{g}/\text{mL}$ ) against DPPH: 41.86–126.6	(Kharat and Mendhulkar 2016)
<i>S. nodiflora</i> (Nodeweed)	Leaf	Ag, Au	Half-maximal inhibitory concentration value ( $\mu\text{g}/\text{mL}$ ) against DPPH: 54.3–215	(Vijayan et al. 2018)
<i>A. millefolium</i> (Yarrow)	Whole plant	Ag	Half-maximal inhibitory concentration value ( $\mu\text{g}/\text{mL}$ ) against DPPH: 7.03	(Yousaf et al. 2020)
<i>C. cernuum</i>	Whole plant	Ag	Half-maximal inhibitory concentration value ( $\mu\text{g}/\text{mL}$ ) against DPPH: 0.121	(Ahn et al. 2019)
<i>G. tournefortii</i> (Tumbleweed)	Leaf	Au	Half-maximal inhibitory concentration value ( $\mu\text{g}/\text{mL}$ ) against DPPH: 194–330	(Zhaleh et al. 2019)
<i>C. arnotiana</i>	Leaf	CuO	The percentage of radical scavenging (%) against DPPH: 18–21	(Rajeshkumar et al. 2019)
<i>M. indica</i> (Mango)	Leaf	ZnO	The percent inhibition (%) against DPPH: 22–93	(Rajeshkumar et al. 2018)
<i>A. millefolium</i> (Common yarrow)	Whole plant	Ag	Half-maximal inhibitory concentration value ( $\mu\text{g}/\text{mL}$ ) against DPPH: 7.03	(Yousaf et al. 2020)
<i>C. nocturnum</i> (Queen of the night)	Leaf	Ag	The percentage of radical scavenging (%) against DPPH: 29.55	(Keshari et al. 2020)
<i>P. guajava</i> (Guava)	Leaf	Ag	Half-maximal inhibitory concentration value ( $\mu\text{g}/\text{mL}$ ) against DPPH: 52.53	(Wang et al. 2018)
<i>P. anisum</i> (Anise)	Seed	Au, Ag	Half-maximal inhibitory concentration value ( $\mu\text{g}/\text{mL}$ ) against DPPH: 45.53 (Ag NPs), 191.58 (Au NPs)	(Zayed et al. 2020)
<i>A. katsumadai</i> (Hainan galangal)	Seed	Ag	The percent inhibition estimated (%) against DPPH: 22–89.9	(He et al. 2017)
<i>N. oleander</i> (Nerium)	Leaf	Au	The percent inhibition estimated (%) against DPPH: 42–78	(Tahir et al. 2015)
<i>B. ciliata</i> (Fringed bergenia)	Rhizomes	Ag	The percentage of radical scavenging estimated (%) against DPPH: 60	(Phull et al. 2016)

the percentage of radical scavenging activity of CuO nanoparticles was about 21%. It can be concluded that diverse metallic nanoparticles (Ag, Au, CuO, ZnO) from various plant extracts have great potentials for antioxidant activities. Also, the common antioxidants can be replaced by such biogenic nanoparticles in health therapies, and medical technologies.

### Drug delivery

Treatments for diseases in biomedical fields are being investigated to address a wide range of restraints of normal drug delivery systems including nonspecific biological delivery and targeting, poor oral bioavailability, and insufficient water solubility (Rahman et al. 2020). Nanotechnology has long been attractive to researchers due to its affordable applications in delivering drugs to target organs, tissues or cells in cancer treatment or biocarriers by crossing the blood–brain barrier (Lockman et al. 2002; Haley and Frenkel 2008). Nanoparticles represent the surface functionalization and exhibited large surface area to

facilitate the drug loading (Faraji and Wipf 2009). In addition, nanoparticles show high biocompatibility and lessen drug resistance because they can accumulate in the body without being detected by the resistance protein P-glycoprotein (Cho et al. 2008). Specifically, the biosynthesis of nanoparticles using plant extract can be the optimal resolution due to the presence of phytochemicals that contribute to their stability and benignity (Yew et al. 2020).

The blood–brain barrier known as the "tough guardian" is the barrier that covers the inner nerve cells (Fig. 13). They play an important role in protecting the brain and regulating homeostasis, minimizing the penetration of foreign substances (Chen and Gao 2017). Therefore, it is difficult to transform drugs inside and support early treatment of nerve cell damage. Nanoparticles can bypass the blood–brain barrier without altering their integrity thanks to the small size and the process of endocytosis. As a result, neuroleptic drugs can be transported into neuron cells to support treatment by pathways such as through endocytosis or transport through the tight junction (Nair et al. 2012).



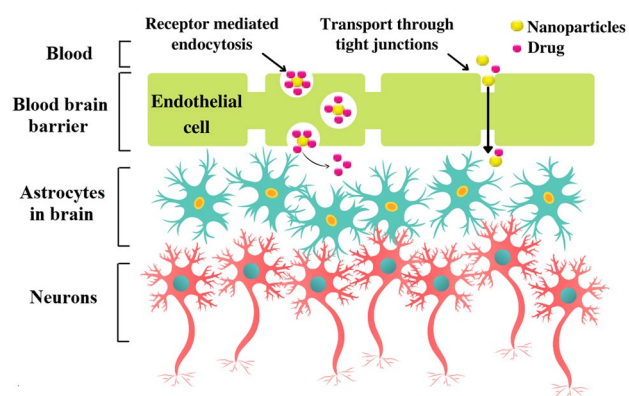


**Fig. 13** Transport mechanism of nanoparticles across the blood–brain barrier for drug delivery application

In recent researches on cancer treatment, nanoparticles from plant extracts exhibit the potential to act as the distribution system of anticancer drugs to tumors of patients (Table 7). Because conventional chemotherapeutic agents may not deliver specifically to target organs, potentially causing damage to other healthy cells, a reduction in their dose may result in ineffective treatment (Cho et al. 2008). Therefore, nanoparticles have solved the above problems, especially magnetic nanoparticles (Fig. 14). First, the drug will be loaded on nanoparticles and injected into the blood capillaries, then locate the sites of cancer cells and tumors using external magnetism. This access can pinpoint the

exact site of drug delivery without affecting other non-target organs (Yew et al. 2020). Then, the nanoparticles will approach cancer cells through the endocytosis pathway and release the drug, and thus, kill the cancer cells (Haley and Frenkel 2008). For example, Taghavi et al. (2016) synthesized  $\text{Fe}_3\text{O}_4$  nanoparticles to deliver the drug deferasirox, resulting in a cell death percentage of about 69.3% human leukemia cell lines. In another study, Pham et al. (2016) produced  $\text{Fe}_3\text{O}_4$  nanoparticles coated with curcumin to inhibit lung cancer cells, acquiring an  $\text{IC}_{50}$  value of 73.03  $\mu\text{g}/\text{mL}$ . Sriramulu et al. (2018) carried out the synthesis  $\text{ZnFe}_2\text{O}_4$  nanoparticles from *A. marmelos* leaf extract to carfilzomib drug delivery. Accordingly, 95% of carfilzomib was released by nanoparticles in 360 min.

In addition to magnetic nanoparticles, other nanoparticles (e.g. Ag, Au nanoparticles) are also capable of delivering drugs for cancer treatment effectively. Specifically, Ganeshkumar et al. (2013) reported that Au nanoparticles from *P. granatum* peel extract could load fluorouracil drug (78%) for breast cancer treatment. This study also indicated that 22.92% of the drug was released after 48 h. More interestingly,  $\text{IC}_{50}$  value of fluorouracil–Au nanoparticles against breast cancer cells was 4 times lower than that of the free fluorouracil. Similarly, Pooja et al. (2015) showed that Au nanoparticles from gum of *Sterculia* genus extract could deliver gemcitabine hydrochloride to human lung cancer cells. According to the results,  $\text{IC}_{50}$  value of drug–Au nanoparticles was about twofold lower than the free drug.

**Table 7** Applications of green nanoparticles synthesized from plant extract for drug delivery

Plant (common name)	Part	NPs	Drug	Result	Ref
<i>P. granatum</i> (Pomegranate)	Peel	Au	Fluorouracil	+ Percentage of drug (%) bound to nanoparticles: 78 + Percentage of drug (%) release after 2 days: 22.92 + Half-maximal inhibitory concentration value ( $\mu\text{g}/\text{mL}$ ) against breast cancer cells: 0.15–0.50	(Ganeshkumar et al. 2013)
<i>P. annua</i> (Annual meadowgrass)	Leaf	Ag	<i>E. dracunculoides</i>	+ Percentage of drug (%) bound to nanoparticles: 85 + Percentage of drug (%) release after 30 days: 96 + The percentage inhibiting estimated (%) against squamous cell carcinoma: 40	(Gul et al. 2021)
<i>Sterculia</i> genus	Gum	Au	Gemcitabine hydrochloride	+ The percentage drug loading (%): 19.2 + Half-maximal inhibitory concentration value ( $\mu\text{g}/\text{mL}$ ) against human lung cancer cells: 0.67	(Pooja et al. 2015)
<i>A. marmelos</i>	Leaf	$\text{ZnFe}_2\text{O}_4$	Carfilzomib	Percentage of drug (%) release after 6 h: 95	(Sriramulu et al. 2018)
<i>J. regia</i> (Walnut)	Bark	Au	Zonisamide	+ Percentage of drug (%) release after 11 days: 76,167 + Percentage of treatment (%) for acute spinal cord injury: 80	(Fang et al. 2019)

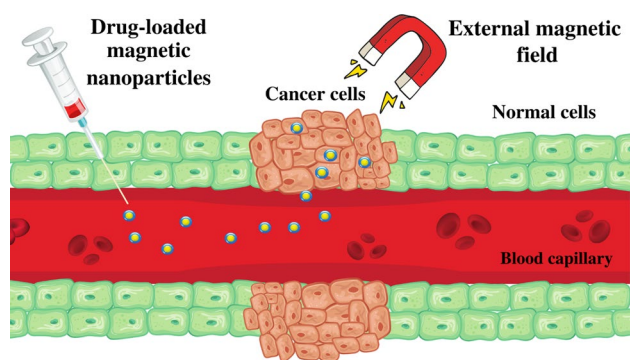


**Fig. 14** Targeted drug delivery mechanism using magnetic nanoparticles

Such outcomes showed the high affinity of nanoparticles to drug molecules in drug delivery systems for cancer treatment. Similarly, Fang et al. (2019) investigated the use of Au nanoparticles from walnut bark extract as a promising zonisamide biocarrier with 80% efficiency of acute spinal cord injury. Gul et al. (2021) performed the loading of herbal drug *E. dracunculoides* on Ag nanoparticles produced from *P. annua* extract. As a result, 96% of the drug was released after 30 days whereas the percentage of inhibiting squamous cell carcinoma was ~40%. In conclusion, both magnetic and metallic non-magnetic nanoparticles bring high drug delivery potentials, greatly benefiting medical technology.

### Medical diagnostics

Recent advances in medical nanotechnology are expanding in the early diagnosis of dangerous diseases such as cancer and stroke. Typically, some methods such as computed tomography (CT), and magnetic resonance imaging (MRI) are prevalently used. These diagnostic methods are, however, limited because they can only detect tumors and diseased tissues with a size of more than a few millimeters or equivalent to 10 million cells (Singh et al. 2018). The nanoparticles exhibit unique optical and surface plasmon resonance properties, whereas their scattering ability is five times greater than that of conventional dyes used in diagnostic techniques (Radwan and Azzazy 2009). Moreover, their small size and high biocompatibility bring them an easy approach to the tissues or organs to perform probe functions. Therefore, nanoparticles are used in diagnostic methods such as photoimaging, signal, fluorescence, and surface-enhanced Raman scattering (Boisselier and Astruc 2009).

Cancer is a dangerous disease, the second leading cause of human death in the world (Singh et al. 2018). The normal diagnostic methods can only detect the tumors at the grown periods, causing difficulty in cancer treatment. Therefore, early diagnosis is necessary to prevent these diseases. Mukherjee et al. (2013) noticed the synthesis of Au

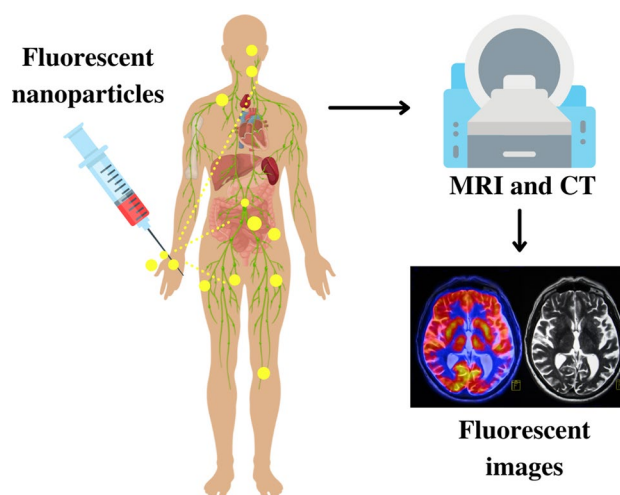


**Fig. 15** Fluorescent diagnostic techniques using nanoparticles for magnetic resonance imaging (MRI) and computed tomography (CT) scans

nanoparticles from *O. scandens* leaf extract for the diagnosis of lung and breast cancers. The results were observed by the olympus fluorescence microscope that nanoparticles can spontaneously emit red fluorescence toward both cancer cells. The authors also suggested the red emission phenomenon was ascribed to the encapsulating phytochemicals and the light scattering of nanoparticles. As an example, Fig. 15 describes the fluorescent diagnostic technique using nanoparticles for photo-imaging and computed tomography scans. In another study, Chanda et al. (2011) reported the cancer diagnostic ability of Au nanoparticles from cinnamon extract. Accordingly, the photoacoustic signal for prostate cancer cell lines was stronger in the presence of Au nanoparticles than the other.

In addition to supporting cancer diagnosis, nanoparticles can also diagnose various diseases, i.e., ischemic stroke is a disease with a high mortality rate. Whereas an ischemic attack occurs, the quantity of neurons lost is equivalent to the number of neurons lost in 36 years of normal aging. This would accelerate the rate of death in short time (Lakhan et al. 2009). Biomarkers such as S100 calcium binding protein B and glial fibrillary acidic protein have long been known to be used for the diagnosis of strokes, but unable to detect them early and clearly. Sarmah et al. (2017) showed the more pronounced signals of these biomarkers associated with Au nanoparticles and iron oxide nanoparticles in the detection of strokes by computed tomography scans, and MRI techniques. Fazal et al. (2014) investigated Au nanoparticles from cocoa bean extract for X-ray contrast in computed tomography scan. At the same concentration, Au nanoparticles gave a signal intensity about 1.5 times larger than Omnipaque, which is well known as a contrast agent used for X-ray imaging. Beside the cell diagnosis, Kumar Sur et al.

(2018) proved Ag nanoparticles from reetha and shikakai leaf extracts could detect *M. tuberculosis* bacteria for early diagnosis of tuberculosis. Through surface-enhanced Raman spectroscopy technique, the authors observed the signal of laser fluorescence from this bacterial species when they were exposed to Ag nanoparticles. With the encouraging vision, nanoparticles-based technologies promote the development of diagnostic methods for early detection of dangerous diseases such as cancer, strokes, tumors, and tuberculosis.

## Antiaging

Skin aging can affect aesthetics and raise the risks for skin cancers. Skin aging is caused by many factors, i.e., internal factors by age or genetic and external factors by constant exposure under ultraviolet irradiation or pollutants in daily life (Puizina-Ivic 2008). The free radicals are underlying to activate collagenase, elastase, and tyrosinase enzymes to digest collagen in the triple helix region, breaking down the elastin, and synthesizing toxic melanin (Eun Lee et al. 2019). Mostafa et al. (2019) showed that Ag nanoparticles from *C. pumilio* plant extract may be against enzymes that cause skin aging. The interaction between the hydroxyl groups of phenol in plant extract with the enzymes functional groups or the hydrophobic interaction between the benzene ring of phenol and enzyme may change the structure, reducing the enzyme activity. The inhibition percentages of anti-elastase, anti-collagenase and anti-tyrosinase enzymes in the keratinocyte cell line were 91, 76, and 79%, respectively. Likewise, nanoparticles can also be used as a shield against ultraviolet rays. Khatami et al. (2019) discovered Ni-doped CeO<sub>2</sub> nanoparticles synthesized from *S. rebaudiana* extract were a promising filter against ultraviolet agents. Sunscreen's ability to absorb ultraviolet rays is measured based on sun protection factor. If this factor is above 30, the filter can prevent 98% of ultraviolet rays from skin surface (Jose and Netto 2019). The results of sun protection factor from three samples are acceptable: CeO<sub>2</sub> (38.98) < Ni 1%-doped CeO<sub>2</sub> (40.15) < Ni 3%-doped CeO<sub>2</sub> (42.54). The authors explained that the smaller the nanoparticle size is, the narrower the band-gap, the better the ultraviolet-absorbing material. It can be seen that nanoparticles from plant extracts support potential anti-aging products for human health and the environment.

## Other biomedical treatments

Bionanotechnology has long been studied and applied in various biomedical fields from diagnosis to treatment. Conventional specialty drugs can have many side effects, prompting researchers to find more optimal treatments. The characteristic of nanoparticles such as small size,

large surface area, high stability and biocompatibility brings them great potential as effective agents in diseases treatment (Dutta et al. 2015).

Malaria is still a worrisome disease for mankind, every year there are about 283 million cases and 755,000 deaths over the world according to the annual report of the World Health Organization (Kumar et al. 2015). As infected with malaria, the disease-causing parasite (e.g., *P. falciparum*) binds with red blood cells to form parasitized red blood cells. Although chemotherapy is widely used to cure malaria, it possibly causes a high resistance to drugs and affects nonspecific parasites. Meanwhile, green synthesized nanoparticles exhibit the ability to combine with drugs and targeted treatment (Mohammadi et al. 2021). For example, Tripathy et al. (2020) demonstrated that *Dicoma anomala* roots biosynthesized Ag nanoparticles can reduce the number of red blood cells from 2.5% of the total red blood cells to 0.5% after 48 h.

Diabetes mellitus is characteristic of glucose homeostasis caused by defects in insulin secretion and action, leading to the impairment of glucose metabolism (Prajapati et al. 2008). It is reported that the number of people with diabetes has been worldwide increasing at an alarming rate. It was forecasted to be new 366 million cases by 2030 (Wild et al. 2004). However, hypoglycemic agents to treat diabetes are thought to have side effects such as lactic acidosis, liver problems, and diarrhea (Rajalakshmi et al. 2009). Daisy and Saipriya (2012) reported that nanoparticles from *C. fistula* bark extract could participate in hypoglycemic activity. According to the results, the total proportion of hemoglobin in the blood of diabetic rats treated with Au nanoparticles decreased from 13.59% to 10.40%.

Alzheimer is a form of disease dementia resulting in problems regarding memory, cognition, and behavior (Hajipour et al. 2017). To treat Alzheimer's, drugs are recommended to use against acetylcholinesterase, an enzyme that breaks down acetylcholine, causing a reduction in nerve cell communication (Soreq and Seidman 2001). Youssif et al. (2019) synthesized Ag nanoparticles from *Lampranthus coccineus* and *Malephora lutea* extracts against acetylcholinesterase. The results revealed that *L. coccineus*-Ag nanoparticles had higher anti-acetylcholinesterase activity (1.95 ng/mL) than that of *M. lutea*-Ag nanoparticles (1.23 ng/mL). More interestingly, both Ag Nanoparticles were more effective than rivastigmine, an anti-acetylcholinesterase drug used in the treatment of Alzheimer. To sum up, green nanoparticles have shown promising applications in the treatment of diseases such as skin aging, malaria, diabetes, Alzheimer, both cancers and various types of infections. They may probably contribute to other diseases treatment in biomedical technologies.

## Challenges

Nanotechnology is evolving and has bright future prospects. In particular, the use of plant extracts for nanofabrication is increasingly being developed and gradually replacing chemical or physical production technologies with the economic, ecological, and safety benefits. In the near future, nanoparticles biofabricated from plant extracts can be incorporated into large-scale production from locally available plant species. These strengths can open new commercialized opportunities for biogenic nanoparticles; and hence, lowering the production cost. This possibly leads to boosting the density of bionanomaterials in the material sciences. In addition to their outstanding biomedical and environmental applications, nanoparticles can also have great prospects in many other technologies. For example, the bio-based nanoparticles can act as green catalysts for the synthesis of novel bioactive compounds (Balwe et al. 2017). They have many potentials for antioxidant and free radical scavenging activities (Yousaf et al. 2020). These antioxidants can firmly link to food preservation, antiaging, and other biomedical applications. In particular, some of the outstanding applications of nanoparticles are to produce biopesticides, biofertilizers, and even bionanosensors applying for smart agricultural fields (Shang et al. 2019).

However, paralleling with the advanced technologies of nanoparticles, there can have many challenges and potential drawbacks. *Firstly*, these nanomaterials can have potentially affected human health. While many studies have performed in vitro and reported on antibacterial, anti-cancer as well as the treatment of many diseases, the effects of administering nanoparticles directly into the body still need a satisfactory answer (Zhang et al. 2014; Bethu et al. 2018; Youssif et al. 2019). *Secondly*, their special physicochemical properties need to be monitored for better understanding of underlying influential mechanisms because the nano-scaled materials exhibit more significantly variable behaviors than the macroscopic ones (Ojha 2020). *Thirdly*, for environmental and agricultural applications, the aspects of negative effects on living organisms are also of great concern. Animals, and aquatic organisms may be exposed directly or indirectly from residues of post-use nanomaterials discharged in soil and water environments (Marambio-Jones and Hoek 2010). *Fourthly*, the actual efficiency of biomedical and environmental applications of bio-based nanoparticles needs to be addressed as many studies are carried out in the simulated or theoretical mode. *Fifthly*, the adoption of plants to synthesize nanoparticles on a large scale will lead to worrying concerns about caring for well-grown

plants to accommodate conditions containing the necessary biological compounds. These undesirable effects require further insights and advancements with many specified researches. *Sixthly*, the biggest obstacle limiting the applications of nanoparticles is the lack of a standardized set of regulations necessary for their utilization. Their uncontrolled use without unified regulations will cause many inevitable effects. *Ultimately*, the field of nanotoxicology is still in its infancy to ensure the safety of nanoparticles (Baruah et al. 2016). These challenges need to be addressed before large-scale commercialization and development of nanoparticles from plant extracts can be made.

## Conclusion

Here, we systematically illuminated the formation, antimicrobial activity, and biomedical performance of green nanoparticles synthesized from plant extracts. Besides, this review assessed the significance of phytochemicals in the formation and properties of green resultant nanoparticles. These compounds act as reducing, capping, stabilizing and chelating agents during biosynthesis. The antimicrobial and antifungal activities of green nanoparticles were vigorously discussed with emphasis on the promising therapeutics against infectious diseases. The role of nanoparticles in drug delivery, disease diagnosis and treatment were also shed light on. Pathways using plant-based nanoparticles are opening new potential frontiers to treat diseases such as diabetes, malaria or Alzheimer.

**Acknowledgements** The authors would love to appreciate the effort of researchers all over the world in the fight against the COVID-19 pandemic. We also acknowledge Mina Rees Library, The Graduate Center of the City University of New York (CUNY) for granting access to databases, Freepik company projects at [www.freepik.com](http://www.freepik.com), and Canva® graphic design platforms at [www.canva.com](http://www.canva.com) for many graphic resources reproduced in this work.

**Authors contributions** NTTN contributed to conceptualization, data curation, investigation, methodology, writing—original draft. LMN contributed to data curation, investigation, validation, writing—original draft. TTTN contributed to writing—review & editing, data curation, validation. TTN contributed to writing—review & editing, data curation, validation. DTCN contributed to conceptualization, writing—review & editing, validation, data curation, supervision. TVT contributed to conceptualization, writing—review & editing, validation, data curation, supervision, project administration. All authors read and approved the final manuscript.

**Funding** There was no external funding for this study.

**Availability of data and material** The authors declare that all data and materials support their published claims and comply with field standards.



**Code availability** The authors declare that software application or custom code supports their published claims and comply with field standards.

## Declarations

**Conflict of interest** The authors declare that there are no conflicts of interest.

**Compliance with Ethical Standards** The authors declare that. The manuscript has not been published anywhere nor submitted to another journal.

The manuscript is not currently being considered for publication in any another journal.

All authors have been personally and actively involved in substantive work leading to the manuscript and will hold themselves jointly and individually responsible for its content.

Research does not involve any Human Participants and/or Animals.

**Ethics approval** Not applicable.

**Consent to participate** Not applicable.

**Consent for publication** Not applicable.

## References

- Abbasi E, Milani M, Fekri Aval S et al (2014) Silver nanoparticles: synthesis methods, bio-applications and properties. *Crit Rev Microbiol* 42:1–8. <https://doi.org/10.3109/1040841X.2014.912200>
- Abdullah FH, Bakar NHHA, Bakar MA (2021) Comparative study of chemically synthesized and low temperature bio-inspired Musa acuminata peel extract mediated zinc oxide nanoparticles for enhanced visible-photocatalytic degradation of organic contaminants in wastewater treatment. *J Hazard Mater* 406:124779. <https://doi.org/10.1016/j.jhazmat.2020.124779>
- Abdullah M, Atta A, Allohedan H et al (2018) Green synthesis of hydrophobic magnetite nanoparticles coated with plant extract and their application as petroleum oil spill collectors. *Nanomaterials* 8:855. <https://doi.org/10.3390/nano8100855>
- Abinaya S, Kavitha HP, Prakash M, Muthukrishnaraj A (2021) Green synthesis of magnesium oxide nanoparticles and its applications: a review. *Sustain Chem Pharm* 19:100368. <https://doi.org/10.1016/j.scp.2020.100368>
- Aboutorabi SN, Nasiriboroumand M, Mohammadi P et al (2018) Biosynthesis of silver nanoparticles using safflower flower: structural characterization, and its antibacterial activity on applied wool fabric. *J Inorg Organomet Polym Mater* 28:2525–2532. <https://doi.org/10.1007/s10904-018-0925-5>
- Agarwal H, Venkat Kumar S, Rajeshkumar S (2017) A review on green synthesis of zinc oxide nanoparticles—an eco-friendly approach. *Resour Technol* 3:406–413. <https://doi.org/10.1016/j.refit.2017.03.002>
- Ahmed S, Ahmad M, Swami BL, Ikram S (2016) A review on plants extract mediated synthesis of silver nanoparticles for antimicrobial applications: a green expertise. *J Adv Res* 7:17–28. <https://doi.org/10.1016/j.jare.2015.02.007>
- Ahn E-Y, Jin H, Park Y (2019) Green synthesis and biological activities of silver nanoparticles prepared by *Carpesium cernuum* extract. *Arch Pharm Res* 42:926–934. <https://doi.org/10.1007/s12272-019-01152-x>
- Akpomie KG, Ghosh S, Gryzenhout M, Conradie J (2021) Ananas comosus peel-mediated green synthesized magnetite nanoparticles and their antifungal activity against four filamentous fungal strains. *Biomass Convers Biorefinery*. <https://doi.org/10.1007/s13399-021-01515-9>
- Al-Naamani L, Dobretsov S, Dutta J (2016) Chitosan-zinc oxide nanoparticle composite coating for active food packaging applications. *Innov Food Sci Emerg Technol* 38:231–237. <https://doi.org/10.1016/j.ifset.2016.10.010>
- Al-Otibi F, Al-Ahaidib RA, Alharbi RI et al (2020) Antimicrobial potential of biosynthesized silver nanoparticles by *Aaronsohnia factorovskyi* extract. *Molecules* 26:130. <https://doi.org/10.3390/molecules26010130>
- Alavi M, Karimi N (2017a) Characterization, antibacterial, total antioxidant, scavenging, reducing power and ion chelating activities of green synthesized silver, copper and titanium dioxide nanoparticles using *Artemisia haussknechtii* leaf extract. *Artif Cells Nanomedicine Biotechnol* 15:1–16. <https://doi.org/10.1080/21691401.2017.1408121>
- Alavi M, Karimi N (2017b) Characterization, antibacterial, total antioxidant, scavenging, reducing power and ion chelating activities of green synthesized silver, copper and titanium dioxide nanoparticles using *Artemisia haussknechtii* leaf extract. *Artif Cells Nanomedicine Biotechnol* 46:1–16. <https://doi.org/10.1080/21691401.2017.1408121>
- Amooghaie R, Saeri MR, Azizi M (2015) Synthesis, characterization and biocompatibility of silver nanoparticles synthesized from *Nigella sativa* leaf extract in comparison with chemical silver nanoparticles. *Ecotoxicol Environ Saf* 120:400–408. <https://doi.org/10.1016/j.ecoenv.2015.06.025>
- Ananda Murthy HC, Zeleke TD, Tan KB et al (2021) Enhanced multifunctionality of CuO nanoparticles synthesized using aqueous leaf extract of *Vernonia amygdalina* plant. *Results Chem* 3:100141. <https://doi.org/10.1016/j.rechem.2021.100141>
- Ardestani MS, Sadat Shandiz SA, Salehi S et al (2016) Phytosynthesis of silver nanoparticles using *Artemisia marschalliana* Sprengel aerial part extract and assessment of their antioxidant, anticancer, and antibacterial properties. *Int J Nanomedicine* 11:1835. <https://doi.org/10.2147/IJN.S99882>
- Aslany S, Tafvizi F, Naseh V (2020) Characterization and evaluation of cytotoxic and apoptotic effects of green synthesis of silver nanoparticles using *Artemisia Ciniformis* on human gastric adenocarcinoma. *Mater Today Commun* 24:101011. <https://doi.org/10.1016/j.mtcomm.2020.101011>
- Baghbani-Arani F, Movagharnia R, Sharifian A et al (2017) Photocatalytic, anti-bacterial, and anti-cancer properties of phyto-mediated synthesis of silver nanoparticles from *Artemisia tournefortiana* Rchb extract. *J Photochem Photobiol B Biol* 173:640–649. <https://doi.org/10.1016/j.jphotobiol.2017.07.003>
- Baharara J, Namvar F, Ramezani T et al (2015) Silver nanoparticles biosynthesized using *Achillea Biebersteinii* flower extract: apoptosis induction in MCF-7 Cells via Caspase activation and regulation of Bax and Bcl-2 gene expression. *Molecules* 20:2693–2706. <https://doi.org/10.3390/molecules20022693>
- Bahrami-Teimoori B, Nikparast Y, Hojatianfar M et al (2017) Characterisation and antifungal activity of silver nanoparticles biologically synthesised by *Amaranthus retroflexus* leaf extract. *J Exp Nanosci* 12:129–139. <https://doi.org/10.1080/17458080.2017.1279355>
- Baker C, Pradhan A, Pakstis L et al (2005) Synthesis and antibacterial properties of silver nanoparticles. *J Nanosci Nanotechnol* 5:244–249. <https://doi.org/10.1166/jnn.2005.034>
- Balalakshmi C, Gopinath K, Govindarajan M et al (2017) Green synthesis of gold nanoparticles using a cheap *Sphaeranthus indicus* extract: impact on plant cells and the aquatic crustacean



- Artemia nauplii. *J Photochem Photobiol B Biol* 173:598–605. <https://doi.org/10.1016/j.jphotobiol.2017.06.040>
- Balashanmugam P, Pudupalayam Thangavelu K (2015) Biosynthesis characterization of silver nanoparticles using *Cassia roxburghii* DC. Aqueous extract, and coated on cotton cloth for effective antibacterial activity. *Int J Nanomedicine* 10:87. <https://doi.org/10.2147/IJN.S79984>
- Balwe SG, Shinde VV, Rokade AA et al (2017) Green synthesis and characterization of silver nanoparticles (Ag NPs) from extract of plant *Radix Puerariae*: an efficient and recyclable catalyst for the construction of pyrimido[1,2-*b*]indazole derivatives under solvent-free conditions. *Catal Commun* 99:121–126. <https://doi.org/10.1016/j.catcom.2017.06.006>
- Bandeira M, Giovanela M, Roesch-Ely M et al (2020) Green synthesis of zinc oxide nanoparticles: a review of the synthesis methodology and mechanism of formation. *Sustain Chem Pharm* 15:100223. <https://doi.org/10.1016/j.scp.2020.100223>
- Baruah S, Najam Khan M, Dutta J (2016) Perspectives and applications of nanotechnology in water treatment. *Environ Chem Lett* 14:1–14. <https://doi.org/10.1007/s10311-015-0542-2>
- Behboodi S, Baghbani-Arani F, Abdalan S, Sadat Shandiz SA (2019) Green engineered biomolecule-capped silver nanoparticles fabricated from *cichorium intybus* extract: in vitro assessment on apoptosis properties toward human breast cancer (MCF-7) Cells. *Biol Trace Elem Res* 187:392–402. <https://doi.org/10.1007/s12011-018-1392-0>
- Beheshtkhoo N, Kouhbanani MAJ, Savardashtaki A et al (2018) Green synthesis of iron oxide nanoparticles by aqueous leaf extract of *Daphne mezereum* as a novel dye removing material. *Appl Phys A* 124:363. <https://doi.org/10.1007/s00339-018-1782-3>
- Bethu MS, Netala VR, Domdi L et al (2018) Potential anticancer activity of biogenic silver nanoparticles using leaf extract of *Rhynchosia suaveolens*: an insight into the mechanism. *Artif Cells, Nanomedicine, Biotechnol* 46:104–114. <https://doi.org/10.1080/21691401.2017.1414824>
- Bejene HD, Werkneh AA, Bezabh HK, Ambaye TG (2017) Synthesis paradigm and applications of silver nanoparticles (AgNPs), a review. *Sustain Mater Technol* 13:18–23. <https://doi.org/10.1016/j.susmat.2017.08.001>
- Bharathi D, Preethi S, Abarna K et al (2020) Bio-inspired synthesis of flower shaped iron oxide nanoparticles (FeONPs) using phytochemicals of *Solanum lycopersicum* leaf extract for biomedical applications. *Biocatal Agric Biotechnol* 27:101698. <https://doi.org/10.1016/j.bcab.2020.101698>
- Bibi I, Nazar N, Ata S et al (2019) Green synthesis of iron oxide nanoparticles using pomegranate seeds extract and photocatalytic activity evaluation for the degradation of textile dye. *J Mater Res Technol* 8:6115–6124. <https://doi.org/10.1016/j.jmrt.2019.10.006>
- Bishnoi S, Kumar A, Selvaraj R (2018) Facile synthesis of magnetic iron oxide nanoparticles using inedible *Cynometra ramiflora* fruit extract waste and their photocatalytic degradation of methylene blue dye. *Mater Res Bull* 97:121–127. <https://doi.org/10.1016/j.materresbull.2017.08.040>
- Boisselier E, Astruc D (2009) Gold nanoparticles in nanomedicine: preparations, imaging, diagnostics, therapies and toxicity. *Chem Soc Rev* 38:1759. <https://doi.org/10.1039/b806051g>
- Borase HP, Salunke BK, Salunke RB et al (2014) Plant extract: a promising biomatrix for ecofriendly, controlled synthesis of silver nanoparticles. *Appl Biochem Biotechnol* 173:1–29. <https://doi.org/10.1007/s12010-014-0831-4>
- Bray F, Ferlay J, Soerjomataram I et al (2018) Global cancer statistics 2018: GLOBOCAN estimates of incidence and mortality worldwide for 36 cancers in 185 countries. *CA Cancer J Clin* 68:394–424. <https://doi.org/10.3322/caac.21492>
- Chanda N, Shukla R, Zambre A et al (2011) An effective strategy for the synthesis of biocompatible gold nanoparticles using cinnamon phytochemicals for phantom CT imaging and photoacoustic detection of cancerous cells. *Pharm Res* 28:279–291. <https://doi.org/10.1007/s11095-010-0276-6>
- Chandraker SK, Lal M, Shukla R (2019) DNA-binding, antioxidant, H<sub>2</sub>O<sub>2</sub> sensing and photocatalytic properties of biogenic silver nanoparticles using *Ageratum conyzoides* L. leaf extract. *RSC Adv* 9:23408–23417. <https://doi.org/10.1039/C9RA03590G>
- Chavan RR, Bhinge SD, Bhutkar MA et al (2020) Characterization, antioxidant, antimicrobial and cytotoxic activities of green synthesized silver and iron nanoparticles using alcoholic *Blumea eriantha* DC plant extract. *Mater Today Commun* 24:101320. <https://doi.org/10.1016/j.matcomm.2020.101320>
- Chen L, Gao X (2017) The application of nanoparticles for neuroprotection in acute ischemic stroke. *Ther Deliv* 8:915–928. <https://doi.org/10.4155/tde-2017-0023>
- Chen L, Hu JY, Wang SQ (2012) The role of antioxidants in photoprotection: a critical review. *J Am Acad Dermatol* 67:1013–1024. <https://doi.org/10.1016/j.jaad.2012.02.009>
- Chen T-L, Kim H, Pan S-Y et al (2020) Implementation of green chemistry principles in circular economy system towards sustainable development goals: challenges and perspectives. *Sci Total Environ* 716:136998. <https://doi.org/10.1016/j.scitotenv.2020.136998>
- Cho K, Wang X, Nie S et al (2008) Therapeutic nanoparticles for drug delivery in cancer. *Clin Cancer Res* 14:1310–1316. <https://doi.org/10.1158/1078-0432.CCR-07-1441>
- Chung I-M, Rahuman A, Marimuthu S et al (2015) An Investigation of the cytotoxicity and caspase-mediated apoptotic effect of green synthesized zinc oxide nanoparticles using *Eclipta prostrata* on human liver carcinoma cells. *Nanomaterials* 5:1317–1330. <https://doi.org/10.3390/nano5031317>
- Cuong HN, Pansambal S, Ghotekar S et al (2022) New frontiers in the plant extract mediated biosynthesis of copper oxide (CuO) nanoparticles and their potential applications: a review. *Environ Res* 203:111858. <https://doi.org/10.1016/j.envres.2021.111858>
- Dabhane H, Ghotekar S, Tambade P et al (2021) A review on environmentally benevolent synthesis of CdS nanoparticle and their applications. *Environ Chem Ecotoxicol* 3:209–219. <https://doi.org/10.1016/j.enceco.2021.06.002>
- Daisy P, Saipriya (2012) Biochemical analysis of *Cassia fistula* aqueous extract and phytochemically synthesized gold nanoparticles as hypoglycemic treatment for diabetes mellitus. *Int J Nanomedicine* 7:1189. <https://doi.org/10.2147/IJN.S26650>
- Das D, Nath BC, Phukon P, Dolui SK (2013) Synthesis and evaluation of antioxidant and antibacterial behavior of CuO nanoparticles. *Colloids Surfaces B Biointerfaces* 101:430–433. <https://doi.org/10.1016/j.colsurfb.2012.07.002>
- Dehnavi AS, Raisi A, Aroujalian A (2013) Control size and stability of colloidal silver nanoparticles with antibacterial activity prepared by a green synthesis method. *Synth React Inorganic Met Nano-Metal Chem* 43:543–551. <https://doi.org/10.1080/15533174.2012.741182>
- Dessie Y, Tadesse S, Eswaramoorthy R (2020) Physicochemical parameter influences and their optimization on the biosynthesis of MnO<sub>2</sub> nanoparticles using *Vernonia amygdalina* leaf extract. *Arab J Chem* 13:6472–6492. <https://doi.org/10.1016/j.arabjc.2020.06.006>
- Dhand C, Dwivedi N, Loh XJ et al (2015) Methods and strategies for the synthesis of diverse nanoparticles and their applications: a comprehensive overview. *RSC Adv* 5:105003–105037. <https://doi.org/10.1039/C5RA19388E>
- Doan V-D, Thieu AT, Nguyen T-D et al (2020) Biosynthesis of gold nanoparticles using *litsea cubeba* fruit extract for catalytic reduction of 4-nitrophenol. *J Nanomater* 2020:1–10. <https://doi.org/10.1155/2020/4548790>

- Dobrucka R (2018) Synthesis of MgO nanoparticles using artemisia abrotanum herba extract and their antioxidant and photocatalytic properties. *Iran J Sci Technol Trans A Sci* 42:547–555. <https://doi.org/10.1007/s40995-016-0076-x>
- Dobrucka R (2017) Synthesis of titanium dioxide nanoparticles using Echinacea purpurea herba. *Iran J Pharm Res* 16:756. <https://doi.org/10.22037/IJPR.2017.2026>
- Dobrucka R, Kaczmarek M, Łagiedo M et al (2019) Evaluation of biologically synthesized Au-CuO and CuO-ZnO nanoparticles against glioma cells and microorganisms. *Saudi Pharm J* 27:373–383. <https://doi.org/10.1016/j.jsps.2018.12.006>
- Doherty GJ, McMahon HT (2009) Mechanisms of endocytosis. *Annu Rev Biochem* 78:857–902. <https://doi.org/10.1146/annurev.biochem.78.081307.110540>
- Dowlath MJH, Musthafa SA, Mohamed Khalith SB et al (2021) Comparison of characteristics and biocompatibility of green synthesized iron oxide nanoparticles with chemical synthesized nanoparticles. *Environ Res* 201:111585. <https://doi.org/10.1016/j.envres.2021.111585>
- Dubey M, Bhadauria S, Kushwah BS (2009) Green synthesis of nanosilver particles from extract of Eucalyptus hybrida (safeda) leaf. *Dig J Nanomater Biostruct* 4:537–543
- Dutta R, Ahmad N, Bhatnagar S, Ali SS (2015) Phytofabrication of bioinduced silver nanoparticles for biomedical applications. *Int J Nanomed* 10:7019. <https://doi.org/10.2147/IJN.S94479>
- Elemike E, Onwudiwe D, Ekennia A et al (2017a) Green synthesis of Ag/Ag<sub>2</sub>O nanoparticles using aqueous leaf extract of eupatorium odoratum and its antimicrobial and Mosquito Larvicidal activities. *Molecules* 22:674. <https://doi.org/10.3390/molecules22050674>
- Elemike EE, Onwudiwe DC, Arijeh O, Nwankwo HU (2017b) Plant-mediated biosynthesis of silver nanoparticles by leaf extracts of Lasienthra africanum and a study of the influence of kinetic parameters. *Bull Mater Sci* 40:129–137. <https://doi.org/10.1007/s12034-017-1362-8>
- Eun Lee K, Bharadwaj S, Yadava U, Gu Kang S (2019) Evaluation of caffeine as inhibitor against collagenase, elastase and tyrosinase using in silico and in vitro approach. *J Enzyme Inhib Med Chem* 34:927–936. <https://doi.org/10.1080/14756366.2019.1596904>
- Falsafi SR, Rostamabadi H, Assadpour E, Jafari SM (2020) Morphology and microstructural analysis of bioactive-loaded micro/nanocarriers via microscopy techniques. *CLSM/SEM/TEM/AFM Adv Colloid Interface Sci* 280:102166. <https://doi.org/10.1016/j.cis.2020.102166>
- Fang C, Ma Z, Chen L et al (2019) Biosynthesis of gold nanoparticles, characterization and their loading with zonisamide as a novel drug delivery system for the treatment of acute spinal cord injury. *J Photochem Photobiol B Biol* 190:72–75. <https://doi.org/10.1016/j.jphotobiol.2018.11.011>
- Faraji AH, Wipf P (2009) Nanoparticles in cellular drug delivery. *Bioorg Med Chem* 17:2950–2962. <https://doi.org/10.1016/j.bmc.2009.02.043>
- Fazal S, Jayasree A, Sasidharan S et al (2014) Green Synthesis of anisotropic gold nanoparticles for photothermal therapy of cancer. *ACS Appl Mater Interfaces* 6:8080–8089. <https://doi.org/10.1021/am500302t>
- Förster H (2004) UV/vis spectroscopy. In: *Characterization I*. Springer, pp 337–426
- Franci G, Falanga A, Galdiero S et al (2015) Silver nanoparticles as potential antibacterial agents. *Molecules* 20:8856–8874. <https://doi.org/10.3390/molecules20058856>
- Francis S, Joseph S, Koshy EP, Mathew B (2018) Microwave assisted green synthesis of silver nanoparticles using leaf extract of elephantopus scaber and its environmental and biological applications. *Artif Cells Nanomed Biotechnol* 46:795–804. <https://doi.org/10.1080/21691401.2017.1345921>
- Ganesan K, Jothi VK, Natarajan A et al (2020) Green synthesis of copper oxide nanoparticles decorated with graphene oxide for anticancer activity and catalytic applications. *Arab J Chem* 13:6802–6814. <https://doi.org/10.1016/j.arabjc.2020.06.033>
- Ganeshkumar M, Sathishkumar M, Ponrasu T et al (2013) Spontaneous ultra fast synthesis of gold nanoparticles using Punica granatum for cancer targeted drug delivery. *Colloids Surfaces B Biointerfaces* 106:208–216. <https://doi.org/10.1016/j.colsurfb.2013.01.035>
- Ghotekar S, Pagar T, Pansambal S, Oza R (2020) A review on green synthesis of sulfur nanoparticles via plant extract, characterization and its applications. *Adv J Chem B*, 128–143. <https://doi.org/10.33945/SAMI/AJCB.2020.3.5>
- Ghotekar S, Pansambal S, Bilal M et al (2021) Environmentally friendly synthesis of Cr<sub>2</sub>O<sub>3</sub> nanoparticles: characterization, applications and future perspective—a review. *Case Stud Chem Environ Eng* 3:100089. <https://doi.org/10.1016/j.cscee.2021.100089>
- Ghotekar S, Pansambal S, Pawar SP et al (2019) Biological activities of biogenically synthesized fluorescent silver nanoparticles using Acanthospermum hispidum leaves extract. *SN Appl Sci* 1:1342. <https://doi.org/10.1007/s42452-019-1389-0>
- Ghotekar S, Savale A, Pansambal S (2018) Phytofabrication of fluorescent silver nanoparticles from Leucaena leucocephala L. leaves and their biological activities. *J Water Environ Nanotechnol* 3:95–105. <https://doi.org/10.22090/JWENT.2018.02.001>
- Gul AR, Shaheen F, Rafique R et al (2021) Grass-mediated biogenic synthesis of silver nanoparticles and their drug delivery evaluation: a biocompatible anti-cancer therapy. *Chem Eng J* 407:127202. <https://doi.org/10.1016/j.cej.2020.127202>
- Hajipour MJ, Santoso MR, Rezaee F et al (2017) Advances in Alzheimer's diagnosis and therapy: the implications of nanotechnology. *Trends Biotechnol* 35:937–953. <https://doi.org/10.1016/j.tibtech.2017.06.002>
- Haley B, Frenkel E (2008) Nanoparticles for drug delivery in cancer treatment. *Urol Oncol Semin Orig Investig* 26:57–64. <https://doi.org/10.1016/j.urolonc.2007.03.015>
- Hameed S, Khalil AT, Ali M et al (2019) Greener synthesis of ZnO and Ag-ZnO nanoparticles using Silybum marianum for diverse biomedical applications. *Nanomedicine* 14:655–673. <https://doi.org/10.2217/nnm-2018-0279>
- Hammad DM, Asaad AA (2021) A comparative study: biological and chemical synthesis of iron oxide nanoparticles and their affinity towards adsorption of methylene blue dye. *Desalin WATER Treat* 224:354–366. <https://doi.org/10.5004/dwt.2021.27053>
- Han HJ, Ekweremadu C, Patel N (2019) Advanced drug delivery system with nanomaterials for personalised medicine to treat breast cancer. *J Drug Deliv Sci Technol* 52:1051–1060. <https://doi.org/10.1016/j.jddst.2019.05.024>
- He Y, Wei F, Ma Z et al (2017) Green synthesis of silver nanoparticles using seed extract of *Alpinia katsumadai*, and their antioxidant, cytotoxicity, and antibacterial activities. *RSC Adv* 7:39842–39851. <https://doi.org/10.1039/C7RA05286C>
- Hii YS, Jeevanandam J, Chan YS (2018) Plant mediated green synthesis and nanoencapsulation of MgO nanoparticle from *Calotropis gigantea*: Characterisation and kinetic release studies. *Inorg Nano-Metal Chem* 48:620–631. <https://doi.org/10.1080/24701556.2019.1569053>
- Horta-Piñeres S, Britto Hurtado R, Avila-Padilla D et al (2020) Silver nanoparticle-decorated silver nanowires: a nanocomposite via green synthesis. *Appl Phys A* 126:15. <https://doi.org/10.1007/s00339-019-3178-4>
- Huang J, Li Q, Sun D et al (2007) Biosynthesis of silver and gold nanoparticles by novel sundried *Cinnamomum camphora* leaf. *Nanotechnology* 18:105104. <https://doi.org/10.1088/0957-4484/18/10/105104>

- Huang J, Zhan G, Zheng B et al (2011) Biogenic silver nanoparticles by *caecumen platycladi* extract: synthesis, formation mechanism, and antibacterial activity. *Ind Eng Chem Res* 50:9095–9106. <https://doi.org/10.1021/ie200858y>
- Ikram M, Javed B, Raja NI, Mashwani Z-R (2021) Biomedical potential of plant-based selenium nanoparticles: a comprehensive review on therapeutic and mechanistic aspects. *Int J Nanomedicine* 16:249–268. <https://doi.org/10.2147/IJN.S295053>
- Ikram S (2015) Synthesis of gold nanoparticles using plant extract: an overview. *Nano Res* 1:5
- Iravani S, Korbekandi H, Mirmohammadi SV, Zolfaghari B (2014) Synthesis of silver nanoparticles: chemical, physical and biological methods. *Res Pharm Sci* 9:385
- Ivanković A (2017) Review of 12 Principles of green chemistry in practice. *Int J Sustain Green Energy* 6:39. <https://doi.org/10.11648/j.ijrse.20170603.12>
- Jadoun S, Arif R, Jangid NK, Meena RK (2021) Green synthesis of nanoparticles using plant extracts: a review. *Environ Chem Lett* 19:355–374. <https://doi.org/10.1007/s10311-020-01074-x>
- Jamdagni P, Khatri P, Rana JS (2018) Green synthesis of zinc oxide nanoparticles using flower extract of *Nyctanthes arbor-tristis* and their antifungal activity. *J King Saud Univ Sci* 30:168–175. <https://doi.org/10.1016/j.jksus.2016.10.002>
- Jameel MS, Aziz AA, Dheyab MA (2020) Comparative analysis of platinum nanoparticles synthesized using sonochemical-assisted and conventional green methods. *Nano-Struct Nano-Objects* 23:100484. <https://doi.org/10.1016/j.nanos.2020.100484>
- Jamkhande PG, Ghule NW, Bamer AH, Kalaskar MG (2019) Metal nanoparticles synthesis: an overview on methods of preparation, advantages and disadvantages, and applications. *J Drug Deliv Sci Technol* 53:101174. <https://doi.org/10.1016/j.jddst.2019.101174>
- Javed B, Ikram M, Farooq F et al (2021) Biogenesis of silver nanoparticles to treat cancer, diabetes, and microbial infections: a mechanistic overview. *Appl Microbiol Biotechnol* 105:2261–2275. <https://doi.org/10.1007/s00253-021-11171-8>
- Jebriil S, Khanfir Ben Jenana R, Dridi C (2020) Green synthesis of silver nanoparticles using *Melia azedarach* leaf extract and their antifungal activities: In vitro and in vivo. *Mater Chem Phys* 248:122898. <https://doi.org/10.1016/j.matchemphys.2020.122898>
- Jose J, Netto G (2019) Role of solid lipid nanoparticles as photoprotective agents in cosmetics. *J Cosmet Dermatol* 18:315–321. <https://doi.org/10.1111/jocd.12504>
- Kanagamani K, Muthukrishnan P, Shankar K et al (2019) Antimicrobial, cytotoxicity and photocatalytic degradation of Norfloxacin using *Kleinia grandiflora* mediated silver nanoparticles. *J Clust Sci* 30:1415–1424. <https://doi.org/10.1007/s10876-019-01583-y>
- Kathiravan V, Ravi S, Ashokkumar S et al (2015) Green synthesis of silver nanoparticles using *Croton sparsiflorus* morong leaf extract and their antibacterial and antifungal activities. *Spectrochim Acta Part A Mol Biomol Spectrosc* 139:200–205. <https://doi.org/10.1016/j.saa.2014.12.022>
- Keshari AK, Srivastava R, Singh P et al (2020) Antioxidant and antibacterial activity of silver nanoparticles synthesized by *Cestrum nocturnum*. *J Ayurveda Integr Med* 11:37–44. <https://doi.org/10.1016/j.jaim.2017.11.003>
- Kesharwani J, Yoon KY, Hwang J, Rai M (2009) Phytofabrication of silver nanoparticles by leaf extract of *Datura metel*: hypothetical mechanism involved in synthesis. *J Bionanoscience* 3:39–44. <https://doi.org/10.1166/jbns.2009.1008>
- Khalil MMH, Ismail EH, El-Baghdady KZ, Mohamed D (2014) Green synthesis of silver nanoparticles using olive leaf extract and its antibacterial activity. *Arab J Chem* 7:1131–1139. <https://doi.org/10.1016/j.arabjc.2013.04.007>
- Khan M, Al-hamoud K, Liaqat Z et al (2020) Synthesis of Au, Ag, and Au–Ag bimetallic nanoparticles using *pulicaria undulata* extract and their catalytic activity for the reduction of 4-Nitrophenol. *Nanomaterials* 10:1885. <https://doi.org/10.3390/nano10091885>
- Khan MM, Saadah NH, Khan ME et al (2019) Potentials of *Costus woodsonii* leaf extract in producing narrow band gap ZnO nanoparticles. *Mater Sci Semicond Process* 91:194–200. <https://doi.org/10.1016/j.mssp.2018.11.030>
- Kharat SN, Mendhulkar VD (2016) Synthesis, characterization and studies on antioxidant activity of silver nanoparticles using *Elephantopus scaber* leaf extract. *Mater Sci Eng C* 62:719–724. <https://doi.org/10.1016/j.msec.2016.02.024>
- Khatami M, Pourseyedi S, Khatami M et al (2015) Synthesis of silver nanoparticles using seed exudates of *Sinapis arvensis* as a novel bioresource, and evaluation of their antifungal activity. *Bioresour Bioprocess* 2:19. <https://doi.org/10.1186/s40643-015-0043-y>
- Khatami M, Sarani M, Mosazadeh F et al (2019) Nickel-doped cerium oxide nanoparticles: green synthesis using stevia and protective effect against harmful ultraviolet rays. *Molecules* 24:4424. <https://doi.org/10.3390/molecules24244424>
- Khatoun N, Ahmad R, Sardar M (2015) Robust and fluorescent silver nanoparticles using *Artemisia annua*: biosynthesis, characterization and antibacterial activity. *Biochem Eng J* 102:91–97. <https://doi.org/10.1016/j.bej.2015.02.019>
- Khezerlou A, Alizadeh-Sani M, Azizi-Lalabadi M, Ehsani A (2018) Nanoparticles and their antimicrobial properties against pathogens including bacteria, fungi, parasites and viruses. *Microb Pathog* 123:505–526. <https://doi.org/10.1016/j.micpath.2018.08.008>
- Kim Y-J, Perumalsamy H, Castro-Aceituno V et al (2019) Photoluminescent and self-assembled hyaluronic acid-zinc oxide-ginsenoside Rh2 nanoparticles and their potential caspase-9 apoptotic mechanism towards cancer cell lines. *Int J Nanomedicine* 14:8195–8208. <https://doi.org/10.2147/IJN.S221328>
- Kordezangeneh M, Irani S, Mirfakhraie R et al (2015) Regulation of BAX/BCL2 gene expression in breast cancer cells by docetaxel-loaded human serum albumin nanoparticles. *Med Oncol* 32:208. <https://doi.org/10.1007/s12032-015-0652-5>
- Kotcherlakota R, Nimushakavi S, Roy A et al (2019) Biosynthesized gold nanoparticles. In Vivo Study of near-infrared fluorescence (NIR)-based bio-imaging and cell labeling applications. *ACS Biomater Sci Eng* 5:5439–5452. <https://doi.org/10.1021/acsbiomaterials.9b00721>
- Król A, Railean-Plugaru V, Pomastowski P, Buszewski B (2019) Phytochemical investigation of *Medicago sativa* L. extract and its potential as a safe source for the synthesis of ZnO nanoparticles: the proposed mechanism of formation and antimicrobial activity. *Phytochem Lett* 31:170–180. <https://doi.org/10.1016/j.phytol.2019.04.009>
- Kumar B, Smita K, Cumbal L, Debut A (2014) Green approach for fabrication and applications of zinc oxide nanoparticles. *Bioinorg Chem Appl* 2014:1–7. <https://doi.org/10.1155/2014/523869>
- Kumar H, Bhardwaj K, Kuča K et al (2020) Flower-based green synthesis of metallic nanoparticles: applications beyond fragrance. *Nanomaterials* 10:766. <https://doi.org/10.3390/nano10040766>
- Kumar Petla R, Vivekanandhan S, Misra M et al (2012) Soybean (*Glycine Max*) Leaf extract based green synthesis of Palladium nanoparticles. *J Biomater Nanobiotechnol* 03:14–19. <https://doi.org/10.4236/jbnt.2012.31003>
- Kumar R, Ray PC, Datta D et al (2015) Nanovaccines for malaria using *Plasmodium falciparum* antigen Pfs25 attached gold nanoparticles. *Vaccine* 33:5064–5071. <https://doi.org/10.1016/j.vaccine.2015.08.025>
- Kumar Sur U, Ankamwar B, Karmakar S et al (2018) Green synthesis of Silver nanoparticles using the plant extract of *Shikakai* and *Reetha*. *Mater Today Proc* 5:2321–2329. <https://doi.org/10.1016/j.matpr.2017.09.236>
- Kumar VA, Uchida T, Mizuki T et al (2016) Synthesis of nanoparticles composed of silver and silver chloride for a plasmonic



- photocatalyst using an extract from a weed *Solidago altissima* (goldenrod). *Adv Nat Sci Nanosci Nanotechnol* 7:015002. <https://doi.org/10.1088/2043-6262/7/1/015002>
- Kumari M, Giri VP, Pandey S et al (2019) An insight into the mechanism of antifungal activity of biogenic nanoparticles than their chemical counterparts. *Pestic Biochem Physiol* 157:45–52. <https://doi.org/10.1016/j.pestbp.2019.03.005>
- Lakhan SE, Kirchgessner A, Hofer M (2009) Inflammatory mechanisms in ischemic stroke: therapeutic approaches. *J Transl Med* 7:97. <https://doi.org/10.1186/1479-5876-7-97>
- Lakshminarayanan S, Shereen MF, Niraimathi KL et al (2021) One-pot green synthesis of iron oxide nanoparticles from *Bauhinia tomentosa*: characterization and application towards synthesis of 1, 3 diolein. *Sci Rep* 11:8643. <https://doi.org/10.1038/s41598-021-87960-y>
- Lee H-J, Lee G, Jang NR et al (2011) Biological synthesis of copper nanoparticles using plant extract. *Nanotechnology* 1:371–374
- Lee J, Park EY, Lee J (2014) Non-toxic nanoparticles from phytochemicals: preparation and biomedical application. *Bioprocess Biosyst Eng* 37:983–989. <https://doi.org/10.1007/s00449-013-1091-3>
- Lee YJ, Song K, Cha S-H et al (2019) Sesquiterpenoids from *Tussilago farfara* flower bud extract for the eco-friendly synthesis of silver and gold nanoparticles possessing antibacterial and anticancer activities. *Nanomaterials* 9:819. <https://doi.org/10.3390/nano9060819>
- Lipovsky A, Nitzan Y, Gedanken A, Lubart R (2011) Antifungal activity of ZnO nanoparticles—the role of ROS mediated cell injury. *Nanotechnology* 22:105101. <https://doi.org/10.1088/0957-4484/22/10/105101>
- Llor C, Bjerrum L (2014) Antimicrobial resistance: risk associated with antibiotic overuse and initiatives to reduce the problem. *Ther Adv Drug Saf* 5:229–241. <https://doi.org/10.1177/2042098614554919>
- Lockman PR, Mumper RJ, Khan MA, Allen DD (2002) Nanoparticle technology for drug delivery across the blood-brain barrier. *Drug Dev Ind Pharm* 28:1–13. <https://doi.org/10.1081/DDC-120001481>
- Mali SC, Dhaka A, Githala CK, Trivedi R (2020) Green synthesis of copper nanoparticles using *Celastrus paniculatus* Willd. leaf extract and their photocatalytic and antifungal properties. *Biotechnol Reports* 27:e00518. <https://doi.org/10.1016/j.btre.2020.e00518>
- Marambio-Jones C, Hoek EMV (2010) A review of the antibacterial effects of silver nanomaterials and potential implications for human health and the environment. *J Nanoparticle Res* 12:1531–1551. <https://doi.org/10.1007/s11051-010-9900-y>
- Medda S, Hajra A, Dey U et al (2015) Biosynthesis of silver nanoparticles from *Aloe vera* leaf extract and antifungal activity against *Rhizopus* sp. and *Aspergillus* sp. *Appl Nanosci* 5:875–880. <https://doi.org/10.1007/s13204-014-0387-1>
- Mittal AK, Chisti Y, Banerjee UC (2013) Synthesis of metallic nanoparticles using plant extracts. *Biotechnol Adv* 31:346–356. <https://doi.org/10.1016/j.biotechadv.2013.01.003>
- Mittal J, Jain R, Sharma MM (2017) Phytofabrication of silver nanoparticles using aqueous leaf extract of *Xanthium strumarium* L. and their bactericidal efficacy. *Adv Nat Sci Nanosci Nanotechnol* 8:025011. <https://doi.org/10.1088/2043-6254/aa6879>
- Mofolo MJ, Kadhila P, Chinsebu KC et al (2020) Green synthesis of silver nanoparticles from extracts of *Pechuel-oeschea leubnitziae*: their anti-proliferative activity against the U87 cell line. *Inorg Nano-Metal Chem* 50:949–955. <https://doi.org/10.1080/24701556.2020.1729191>
- Mohamad NAN, Arham NA, Jai J, Hadi A (2013) Plant extract as reducing agent in synthesis of metallic nanoparticles: a review. *Adv Mater Res* 832:350–355. <https://doi.org/10.4028/www.scientific.net/AMR.832.350>
- Mohammadi L, Pal K, Bilal M et al (2021) Green nanoparticles to treat patients with Malaria disease: an overview. *J Mol Struct* 1229:129857. <https://doi.org/10.1016/j.molstruc.2020.129857>
- Mohanraj VJ, Chen Y (2007) Nanoparticles—a review. *Trop J Pharm Res* 5:561–573. <https://doi.org/10.4314/tjpr.v5i11.14634>
- Morejón B, Pilaquinga F, Domenech F et al (2018) Larvicidal activity of silver nanoparticles synthesized using extracts of *Ambrosia arborescens* (Asteraceae) to Control *Aedes aegypti* L. (Diptera: Culicidae). *J Nanotechnol* 2018:1–8. <https://doi.org/10.1155/2018/6917938>
- Mostafa E, Fayed MAA, Radwan RA, Bakr RO (2019) *Centaurea pumilio* L. extract and nanoparticles: a candidate for healthy skin. *Colloids Surfaces B Biointerfaces* 182:110350. <https://doi.org/10.1016/j.colsurfb.2019.110350>
- Mousavi-Khattat M, Keyhanfar M, Razmjou A (2018) A comparative study of stability, antioxidant, DNA cleavage and antibacterial activities of green and chemically synthesized silver nanoparticles. *Artif Cells Nanomedicine Biotechnol* 46:S1022–S1031. <https://doi.org/10.1080/21691401.2018.1527346>
- Mousavi B, Tafvizi F, Zaker Bostanabad S (2018) Green synthesis of silver nanoparticles using *Artemisia turcomanica* leaf extract and the study of anti-cancer effect and apoptosis induction on gastric cancer cell line (AGS). *Artif Cells Nanomedicine Biotechnol* 46:499–510. <https://doi.org/10.1080/21691401.2018.1430697>
- Mukherjee S, Vinothkumar B, Prashanthi S et al (2013) Potential therapeutic and diagnostic applications of one-step in situ biosynthesized gold nanoconjugates (2-in-1 system) in cancer treatment. *RSC Adv* 3:2318. <https://doi.org/10.1039/c2ra22299j>
- Mukunthan K, Elumalai E, Patel TN, Murty VR (2011) *Catharanthus roseus*: a natural source for the synthesis of silver nanoparticles. *Asian Pac J Trop Biomed* 1:270–274. [https://doi.org/10.1016/S2221-1691\(11\)60041-5](https://doi.org/10.1016/S2221-1691(11)60041-5)
- Murthy HCA, Desalegn T, Kassa M et al (2020) Synthesis of green copper nanoparticles using Medicinal Plant *Hagenia abyssinica* (Brace) JF. Gmel. leaf extract: antimicrobial properties. *J Nanomater* 2020:1–12. <https://doi.org/10.1155/2020/3924081>
- Muthamil Selvan S, Vijai Anand K, Govindaraju K et al (2018) Green synthesis of copper oxide nanoparticles and mosquito larvicidal activity against dengue, zika and chikungunya causing vector *Aedes aegypti*. *IET Nanobiotechnol* 12:1042–1046. <https://doi.org/10.1049/iet-nbt.2018.5083>
- Muthuvel A, Jothibas M, Manoharan C (2020a) Synthesis of copper oxide nanoparticles by chemical and biogenic methods: photocatalytic degradation and in vitro antioxidant activity. *Nanotechnol Environ Eng* 5:14. <https://doi.org/10.1007/s41204-020-00078-w>
- Muthuvel A, Jothibas M, Manoharan C (2020b) Effect of chemically synthesized compared to biosynthesized ZnO-NPs using *Solanum nigrum* leaf extract and their photocatalytic, antibacterial and in vitro antioxidant activity. *J Environ Chem Eng* 8:103705. <https://doi.org/10.1016/j.jece.2020.103705>
- Naahidi S, Jafari M, Edalat F et al (2013) Biocompatibility of engineered nanoparticles for drug delivery. *J Control Release* 166:182–194. <https://doi.org/10.1016/j.jconrel.2012.12.013>
- Naghdi S, Sajjadi M, Nasrollahzadeh M et al (2018) *Cuscuta reflexa* leaf extract mediated green synthesis of the Cu nanoparticles on graphene oxide/manganese dioxide nanocomposite and its catalytic activity toward reduction of nitroarenes and organic dyes. *J Taiwan Inst Chem Eng* 86:158–173. <https://doi.org/10.1016/j.jtice.2017.12.017>
- Nagore P, Ghotekar S, Mane K et al (2021) Structural properties and antimicrobial activities of *Polyalthia longifolia* leaf extract-mediated CuO nanoparticles. *Bionanoscience* 11:579–589. <https://doi.org/10.1007/s12668-021-00851-4>
- Nair SB, Dileep A, Rajanikant GK (2012) Nanotechnology based diagnostic and therapeutic strategies for neuroscience with special

- emphasis on Ischemic stroke. *Curr Med Chem* 19:744–756. <https://doi.org/10.2174/092986712798992138>
- Narendhran S, Sivaraj R (2016) Biogenic ZnO nanoparticles synthesized using *L. aculeata* leaf extract and their antifungal activity against plant fungal pathogens. *Bull Mater Sci* 39:1–5. <https://doi.org/10.1007/s12034-015-1136-0>
- Naseem K, Zia Ur Rehman M, Ahmad A et al (2020) Plant extract induced biogenic preparation of silver nanoparticles and their potential as catalyst for degradation of toxic dyes. *Coatings* 10:1235. <https://doi.org/10.3390/coatings10121235>
- Nayan V, Onteru SK, Singh D (2018) Mangifera indica flower extract mediated biogenic green gold nanoparticles: Efficient nanocatalyst for reduction of 4-nitrophenol. *Environ Prog Sustain Energy* 37:283–294. <https://doi.org/10.1002/ep.12669>
- Nazar N, Bibi I, Kamal S et al (2018) Cu nanoparticles synthesis using biological molecule of *P. granatum* seeds extract as reducing and capping agent: growth mechanism and photo-catalytic activity. *Int J Biol Macromol* 106:1203–1210. <https://doi.org/10.1016/j.ijbiomac.2017.08.126>
- Nelson B, Johnson M, Walker M et al (2016) Antioxidant cerium oxide nanoparticles in biology and medicine. *Antioxidants* 5:15. <https://doi.org/10.3390/antiox5020015>
- Nijalingappa TB, Veeraiah MK, Basavaraj RB et al (2019) Antimicrobial properties of green synthesis of MgO micro architectures via *Limonia acidissima* fruit extract. *Biocatal Agric Biotechnol* 18:100991. <https://doi.org/10.1016/j.bcab.2019.01.029>
- Nithya K, Kalyanasundharam S (2019) Effect of chemically synthesized compared to biosynthesized ZnO nanoparticles using aqueous extract of *C. halicacabum* and their antibacterial activity. *Open-Nano* 4:100024. <https://doi.org/10.1016/j.onano.2018.10.001>
- Nordin NR, Shamsuddin M (2019) Biosynthesis of copper (II) oxide nanoparticles using *Murayya koeniggi* aqueous leaf extract and its catalytic activity in 4-nitrophenol reduction. *Mal J Fund Appl Sci* 15:218–224
- Ojha A (2020) Nanomaterials for removal of waterborne pathogens. In: *Waterborne Pathogens*. Elsevier, Amsterdam, pp 385–432
- Okaiyeto K, Ojemaye MO, Hoppe H et al (2019) Phytosynthesis of silver/silver chloride nanoparticles using aqueous leaf extract of *Oedera genistifolia*: characterization and antibacterial potential. *Molecules* 24:4382. <https://doi.org/10.3390/molecules24234382>
- Okeke I, Agwu K, Ubachukwu A et al (2020) Impact of Cu doping on ZnO nanoparticles phyto-chemically synthesized for improved antibacterial and photocatalytic activities. *J Nanoparticle Res* 22:272. <https://doi.org/10.1007/s11051-020-04996-3>
- Ong CB, Ng LY, Mohammad AW (2018) A review of ZnO nanoparticles as solar photocatalysts: Synthesis, mechanisms and applications. *Renew Sustain Energy Rev* 81:536–551. <https://doi.org/10.1016/j.rser.2017.08.020>
- Padalia H, Chanda S (2017) Characterization, antifungal and cytotoxic evaluation of green synthesized zinc oxide nanoparticles using *Ziziphus nummularia* leaf extract. *Artif Cells Nanomedicine Biotechnol* 45:1751–1761. <https://doi.org/10.1080/21691401.2017.1282868>
- Padalia H, Moteriya P, Chanda S (2015) Green synthesis of silver nanoparticles from marigold flower and its synergistic antimicrobial potential. *Arab J Chem* 8:732–741. <https://doi.org/10.1016/j.arabjc.2014.11.015>
- Pagar K, Ghotekar S, Pagar T et al (2020) Antifungal activity of biosynthesized CuO nanoparticles using leaves extract of *Moringa oleifera* and their structural characterizations. *Asian J Nanosci Mater* 3:15–23. <https://doi.org/10.26655/AJNANOMAT.2020.1.2>
- Pakzad K, Alinezhad H, Nasrollahzadeh M (2020) <sc> *Euphorbia polygonifolia* </sc> extract assisted biosynthesis of Fe<sub>3</sub>O<sub>4</sub>@CuO nanoparticles: Applications in the removal of metronidazole, ciprofloxacin and cephalexin antibiotics from aqueous solutions under UV irradiat. *Appl Organomet Chem* 34:e5910. <https://doi.org/10.1002/aoc.5910>
- Palomo JM (2019) Nanobiohybrids: a new concept for metal nanoparticles synthesis. *Chem Commun* 55:9583–9589. <https://doi.org/10.1039/C9CC04944D>
- Pansambal S, Deshmukh K, Savale A, et al (2017) Phytosynthesis and biological activities of fluorescent CuO nanoparticles using *Acanthospermum hispidum* L. extract. *J Nanostructures* 7:165–174. <https://doi.org/10.22052/JNS.2017.03.001>
- Park Y-J, Cheon S-Y, Lee D-S et al (2020) Anti-inflammatory and antioxidant effects of *Carpesium cernuum* L. methanolic extract in LPS-stimulated RAW 264.7 macrophages. *Mediators Inflamm* 2020:1–14. <https://doi.org/10.1155/2020/3164239>
- Patil MP, Kim G-D (2017) Eco-friendly approach for nanoparticles synthesis and mechanism behind antibacterial activity of silver and anticancer activity of gold nanoparticles. *Appl Microbiol Biotechnol* 101:79–92. <https://doi.org/10.1007/s00253-016-8012-8>
- Paul Das M, Rebecca Livingstone J, Veluswamy P, Das J (2018) Exploration of *Wedelia chinensis* leaf-assisted silver nanoparticles for antioxidant, antibacterial and in vitro cytotoxic applications. *J Food Drug Anal* 26:917–925. <https://doi.org/10.1016/j.jfda.2017.07.014>
- Pham XN, Nguyen TP, Pham TN et al (2016) Synthesis and characterization of chitosan-coated magnetite nanoparticles and their application in curcumin drug delivery. *Adv Nat Sci Nanosci Nanotechnol* 7:045010. <https://doi.org/10.1088/2043-6262/7/4/045010>
- Phull A-R, Abbas Q, Ali A et al (2016) Antioxidant, cytotoxic and antimicrobial activities of green synthesized silver nanoparticles from crude extract of *Bergenia ciliata*. *Futur J Pharm Sci* 2:31–36. <https://doi.org/10.1016/j.fjps.2016.03.001>
- Pooja D, Panyaram S, Kulhari H et al (2015) Natural polysaccharide functionalized gold nanoparticles as biocompatible drug delivery carrier. *Int J Biol Macromol* 80:48–56. <https://doi.org/10.1016/j.ijbiomac.2015.06.022>
- Prajapati DD, Patel NM, Savadi RV et al (2008) Alleviation of alloxan-induced diabetes and its complications in rats by *Actinodaphne hookeri* leaf extract. *Bangladesh J Pharmacol* 3:102–106. <https://doi.org/10.3329/bjp.v3i2.946>
- Puizina-Ivic N (2008) Skin aging. *Acta Dermatovenerologica Alp Panon Adriat* 17:47
- Qasim Nasar M, Zohra T, Khalil AT et al (2019) Seripheidium quettense mediated green synthesis of biogenic silver nanoparticles and their theranostic applications. *Green Chem Lett Rev* 12:310–322. <https://doi.org/10.1080/17518253.2019.1643929>
- Radwan SH, Azzazy HM (2009) Gold nanoparticles for molecular diagnostics. *Expert Rev Mol Diagn* 9:511–524. <https://doi.org/10.1586/erm.09.33>
- Rafique M, Sadaf I, Rafique MS, Tahir MB (2017) A review on green synthesis of silver nanoparticles and their applications. *Artif Cells Nanomedicine Biotechnol* 45:1272–1291. <https://doi.org/10.1080/21691401.2016.1241792>
- Rafique M, Sadaf I, Tahir MB et al (2019) Novel and facile synthesis of silver nanoparticles using *Albizia procera* leaf extract for dye degradation and antibacterial applications. *Mater Sci Eng C* 99:1313–1324. <https://doi.org/10.1016/j.msec.2019.02.059>
- Rahman HS, Othman HH, Hammadi NI et al (2020) Novel drug delivery systems for loading of natural plant extracts and their biomedical applications. *Int J Nanomedicine* 15:2439–2483. <https://doi.org/10.2147/IJN.S227805>
- Rajakumar G, Gomathi T, Abdul Rahuman A et al (2016) Biosynthesis and biomedical applications of gold nanoparticles using *Eclipta prostrata* leaf extract. *Appl Sci* 6:222. <https://doi.org/10.3390/app6080222>
- Rajakumar G, Rahuman AA, Chung I-M et al (2015) Antiplasmodial activity of eco-friendly synthesized palladium nanoparticles



- using *Eclipta prostrata* extract against *Plasmodium berghei* in Swiss albino mice. *Parasitol Res* 114:1397–1406. <https://doi.org/10.1007/s00436-015-4318-1>
- Rajalakshmi M, Eliza J, Priya CE et al (2009) Anti-diabetic properties of *Tinospora cordifolia* stem extracts on streptozotocin-induced diabetic rats. *African J Pharm Pharmacol* 3:171–180. <https://doi.org/10.5897/AJPP.9000027>
- Rajapriya M, Sharmili SA, Baskar R et al (2020) Synthesis and characterization of zinc oxide nanoparticles using *cynara scolymus* leaves: enhanced hemolytic, antimicrobial, antiproliferative, and photocatalytic activity. *J Clust Sci* 31:791–801. <https://doi.org/10.1007/s10876-019-01686-6>
- Rajeshkumar S, Bharath LV (2017) Mechanism of plant-mediated synthesis of silver nanoparticles - A review on biomolecules involved, characterisation and antibacterial activity. *Chem Biol Interact* 273:219–227. <https://doi.org/10.1016/j.cbi.2017.06.019>
- Rajeshkumar S, Kumar SV, Ramaiah A et al (2018) Biosynthesis of zinc oxide nanoparticles using *Mangifera indica* leaves and evaluation of their antioxidant and cytotoxic properties in lung cancer (A549) cells. *Enzyme Microb Technol* 117:91–95. <https://doi.org/10.1016/j.enzmictec.2018.06.009>
- Rajeshkumar S, Menon S, Venkat Kumar S et al (2019) Antibacterial and antioxidant potential of biosynthesized copper nanoparticles mediated through *Cissus annotiana* plant extract. *J Photochem Photobiol B Biol* 197:111531. <https://doi.org/10.1016/j.jphotobiol.2019.111531>
- Rani R, Sharma D, Chaturvedi M, Yadav JP (2020) Green synthesis of silver nanoparticles using *Tridax procumbens*: their characterization, antioxidant and antibacterial activity against MDR and reference bacterial strains. *Chem Pap* 74:1817–1830. <https://doi.org/10.1007/s11696-019-01028-w>
- Rasheed T, Nabeel F, Bilal M, Iqbal HMN (2019) Biogenic synthesis and characterization of cobalt oxide nanoparticles for catalytic reduction of direct yellow-142 and methyl orange dyes. *Biocatal Agric Biotechnol* 19:101154. <https://doi.org/10.1016/j.cbab.2019.101154>
- Rath M, Panda SS, Dhal NK (2014) Synthesis of silver nanoparticles from plant extract and its application in cancer treatment: a review. *Int J Plant Anim Env Sci* 4:137–145
- Raut RW, Mendhulkar VD, Kashid SB (2014) Photosensitized synthesis of silver nanoparticles using *Withania somnifera* leaf powder and silver nitrate. *J Photochem Photobiol B Biol* 132:45–55. <https://doi.org/10.1016/j.jphotobiol.2014.02.001>
- Reddy GB, Madhusudhan A, Ramakrishna D et al (2015) Green chemistry approach for the synthesis of gold nanoparticles with gum kondagogu: characterization, catalytic and antibacterial activity. *J Nanostructure Chem* 5:185–193. <https://doi.org/10.1007/s40097-015-0149-y>
- Saha J, Begum A, Mukherjee A, Kumar S (2017) A novel green synthesis of silver nanoparticles and their catalytic action in reduction of Methylene Blue dye. *Sustain Environ Res* 27:245–250. <https://doi.org/10.1016/j.serj.2017.04.003>
- Saratale RG, Benelli G, Kumar G et al (2018) Bio-fabrication of silver nanoparticles using the leaf extract of an ancient herbal medicine, dandelion (*Taraxacum officinale*), evaluation of their antioxidant, anticancer potential, and antimicrobial activity against phytopathogens. *Environ Sci Pollut Res* 25:10392–10406. <https://doi.org/10.1007/s11356-017-9581-5>
- Saravanan M, Vahidi H, Medina Cruz D et al (2020) Emerging anti-neoplastic biogenic gold nanomaterials for breast cancer therapeutics: a systematic review. *Int J Nanomedicine* 15:3577–3595. <https://doi.org/10.2147/IJN.S240293>
- Sarmah D, Saraf J, Kaur H et al (2017) Stroke management: an emerging role of nanotechnology. *Micromachines* 8:262. <https://doi.org/10.3390/mi8090262>
- Sebeia N, Jabli M, Ghith A, Saleh TA (2020) Eco-friendly synthesis of *Cynomorium coccineum* extract for controlled production of copper nanoparticles for sorption of methylene blue dye. *Arab J Chem* 13:4263–4274. <https://doi.org/10.1016/j.arabjc.2019.07.007>
- Seifipour R, Nozari M, Pishkar L (2020) Green synthesis of silver nanoparticles using *tragopogon collinus* leaf extract and study of their antibacterial effects. *J Inorg Organomet Polym Mater* 30:2926–2936. <https://doi.org/10.1007/s10904-020-01441-9>
- Selim YA, Azb MA, Ragab I, Abd El-Azim M (2020) Green synthesis of zinc oxide nanoparticles using aqueous extract of *deverra tortuosa* and their cytotoxic activities. *Sci Rep* 10:3445. <https://doi.org/10.1038/s41598-020-60541-1>
- Sethy NK, Arif Z, Mishra PK, Kumar P (2020) Green synthesis of TiO<sub>2</sub> nanoparticles from *Syzygium cumini* extract for photocatalytic removal of lead (Pb) in explosive industrial wastewater. *Green Process Synth* 9:171–181. <https://doi.org/10.1515/gps-2020-0018>
- Shaik M, Ali Z, Khan M et al (2017) Green synthesis and characterization of palladium nanoparticles using *Origanum vulgare* L. Extract Catalytic Activity *Molecules* 22:165. <https://doi.org/10.3390/molecules22010165>
- Shang Y, Hasan MK, Ahammed GJ et al (2019) Applications of nanotechnology in plant growth and crop protection: a review. *Molecules* 24:2558. <https://doi.org/10.3390/molecules24142558>
- Shankar S, Jaiswal L, Selvakannan PR et al (2016) Gelatin-based dissolvable antibacterial films reinforced with metallic nanoparticles. *RSC Adv* 6:67340–67352. <https://doi.org/10.1039/C6RA10620J>
- Shanmugam C, Sivasubramanian G, Parthasarathi B et al (2016) Antimicrobial, free radical scavenging activities and catalytic oxidation of benzyl alcohol by nano-silver synthesized from the leaf extract of *Aristolochia indica* L.: a promenade towards sustainability. *Appl Nanosci* 6:711–723. <https://doi.org/10.1007/s13204-015-0477-8>
- Sharifi-Rad M, Pohl P (2020) Synthesis of biogenic silver nanoparticles (AgCl-NPs) using a *pulicaria vulgaris* gaertn. aerial part extract and their application as antibacterial, antifungal and antioxidant agents. *Nanomaterials* 10:638. <https://doi.org/10.3390/nano10040638>
- Sharma R, Garg R, Kumari A (2020) A review on biogenic synthesis, applications and toxicity aspects of zinc oxide nanoparticles. *EXCLI J* 19:1325. <https://doi.org/10.17179/excli2020-2842>
- Siddiqui MR, Khan M, Khan et al (2013) Green synthesis of silver nanoparticles mediated by *Pulicaria glutinosa* extract. *Int J Nanomedicine* 8:1507. <https://doi.org/10.2147/IJN.S43309>
- Singh A, Gautam PK, Verma A et al (2020) Green synthesis of metallic nanoparticles as effective alternatives to treat antibiotics resistant bacterial infections: a review. *Biotechnol Reports* 25:e00427. <https://doi.org/10.1016/j.btre.2020.e00427>
- Singh A, Joshi NC, Ramola M (2019a) Magnesium oxide Nanoparticles (MgONPs): green synthesis, characterizations and antimicrobial activity. *Res J Pharm Technol* 12:4644. <https://doi.org/10.5958/0974-360X.2019.00799.6>
- Singh J, Kukkar P, Sammi H et al (2019b) Enhanced catalytic reduction of 4-nitrophenol and congo red dye By silver nanoparticles prepared from *Azadirachta indica* leaf extract under direct sunlight exposure. *Part Sci Technol* 37:434–443. <https://doi.org/10.1080/02726351.2017.1390512>
- Singh J, Kumar V, Kim K-H, Rawat M (2019c) Biogenic synthesis of copper oxide nanoparticles using plant extract and its prodigious potential for photocatalytic degradation of dyes. *Environ Res* 177:108569. <https://doi.org/10.1016/j.envres.2019.108569>
- Singh P, Pandit S, Mokkaleti V et al (2018) Gold nanoparticles in diagnostics and therapeutics for human cancer. *Int J Mol Sci* 19:1979. <https://doi.org/10.3390/mi19071979>

- Soreq H, Seidman S (2001) Acetylcholinesterase—new roles for an old actor. *Nat Rev Neurosci* 2:294–302. <https://doi.org/10.1038/35067589>
- Souri M, Hoseinpour V, Shakeri A, Ghaemi N (2018) Optimisation of green synthesis of MnO nanoparticles via utilising response surface methodology. *IET Nanobiotechnol* 12:822–827. <https://doi.org/10.1049/iet-nbt.2017.0145>
- Soto-Robles CA, Luque PA, Gómez-Gutiérrez CM, et al (2019) Study on the effect of the concentration of Hibiscus sabdariffa extract on the green synthesis of ZnO nanoparticles. *Results Phys* 15:102807. <https://doi.org/10.1016/j.rinp.2019.102807>
- Srikar SK, Giri DD, Pal DB et al (2016) Green synthesis of silver nanoparticles: a review. *Green Sustain Chem* 06:34–56. <https://doi.org/10.4236/gsc.2016.61004>
- Sriramulu M, Shukla D, Sumathi S (2018) Aegle marmelos leaves extract mediated synthesis of zinc ferrite: Antibacterial activity and drug delivery. *Mater Res Express* 5:115404. <https://doi.org/10.1088/2053-1591/aadd88>
- Stan M, Lung I, Soran M-L et al (2017) Removal of antibiotics from aqueous solutions by green synthesized magnetite nanoparticles with selected agro-waste extracts. *Process Saf Environ Prot* 107:357–372. <https://doi.org/10.1016/j.psep.2017.03.003>
- Sudhasree S, Shakila Banu A, Brindha P, Kurian GA (2014) Synthesis of nickel nanoparticles by chemical and green route and their comparison in respect to biological effect and toxicity. *Toxicol Environ Chem* 96:743–754. <https://doi.org/10.1080/02772248.2014.923148>
- Sun Q, Li J, Le T (2018) Zinc Oxide nanoparticle as a novel class of antifungal agents: current advances and future perspectives. *J Agric Food Chem* 66:11209–11220. <https://doi.org/10.1021/acs.jafc.8b03210>
- Sundararajan B, Ranjitha Kumari BD (2017) Novel synthesis of gold nanoparticles using Artemisia vulgaris L. leaf extract and their efficacy of larvicidal activity against dengue fever vector Aedes aegypti L. *J Trace Elem Med Biol* 43:187–196. <https://doi.org/10.1016/j.jtemb.2017.03.008>
- Suresh J, Pradheesh G, Alexramani V et al (2018) Green synthesis and characterization of hexagonal shaped MgO nanoparticles using insulin plant ( Costus pictus D. Don) leave extract and its antimicrobial as well as anticancer activity. *Adv Powder Technol* 29:1685–1694. <https://doi.org/10.1016/j.apt.2018.04.003>
- Taghavi F, Saljooghi AS, Gholizadeh M, Ramezani M (2016) Deferasirox-coated iron oxide nanoparticles as a potential cytotoxic agent. *Medchemcomm* 7:2290–2298. <https://doi.org/10.1039/C6MD00293E>
- Tahir K, Nazir S, Li B et al (2015) Nerium oleander leaves extract mediated synthesis of gold nanoparticles and its antioxidant activity. *Mater Lett* 156:198–201. <https://doi.org/10.1016/j.matlet.2015.05.062>
- Thamaphat K, Limsuwan P, Ngotawornchai B (2008) Phase characterization of TiO<sub>2</sub> powder by XRD and TEM. *Agric Nat Resour* 42:357–361
- Tripathy S, Rademan S, Matsabisa MG (2020) Effects of silver nanoparticle from Dicoma anomala Sond. Root Extract on MCF-7 cancer cell line and NF54 parasite strain: an in vitro study. *Biol Trace Elem Res* 195:82–94. <https://doi.org/10.1007/s12011-019-01822-3>
- Uddin I, Ahmad K, Khan AA, Kazmi MA (2017) Synthesis of silver nanoparticles using Matricaria recutita (Babunah) plant extract and its study as mercury ions sensor. *Sens Bio-Sensing Res* 16:62–67. <https://doi.org/10.1016/j.sbsr.2017.11.005>
- Valsalam S, Agastian P, Arasu MV et al (2019) Rapid biosynthesis and characterization of silver nanoparticles from the leaf extract of Tropaeolum majus L. and its enhanced in-vitro antibacterial, antifungal, antioxidant and anticancer properties. *J Photochem Photobiol B Biol* 191:65–74. <https://doi.org/10.1016/j.jphotobiol.2018.12.010>
- Vasantharaj S, Sathiyavimal S, Saravanan M et al (2019) Synthesis of ecofriendly copper oxide nanoparticles for fabrication over textile fabrics: Characterization of antibacterial activity and dye degradation potential. *J Photochem Photobiol B Biol* 191:143–149. <https://doi.org/10.1016/j.jphotobiol.2018.12.026>
- Veisi H, Rashtiani A, Barjasteh V (2016) Biosynthesis of palladium nanoparticles using Rosa canina fruit extract and their use as a heterogeneous and recyclable catalyst for Suzuki-Miyaura coupling reactions in water. *Appl Organomet Chem* 30:231–235. <https://doi.org/10.1002/aoc.3421>
- Vijayan R, Joseph S, Mathew B (2018) Eco-friendly synthesis of silver and gold nanoparticles with enhanced antimicrobial, antioxidant, and catalytic activities. *IET Nanobiotechnol* 12:850–856. <https://doi.org/10.1049/iet-nbt.2017.0311>
- Virmani I, Sasi C, Priyadarshini E et al (2020) Comparative Anticancer Potential of Biologically and Chemically Synthesized Gold Nanoparticles. *J Clust Sci* 31:867–876. <https://doi.org/10.1007/s10876-019-01695-5>
- Vishnukumar P, Vivekanandhan S, Misra M, Mohanty AK (2018) Recent advances and emerging opportunities in phytochemical synthesis of ZnO nanostructures. *Mater Sci Semicond Process* 80:143–161. <https://doi.org/10.1016/j.mssp.2018.01.026>
- Vishnukumar P, Vivekanandhan S, Muthuramkumar S (2017) Plant-mediated biogenic synthesis of Palladium Nanoparticles: recent trends and emerging opportunities. *ChemBioEng Rev* 4:18–36. <https://doi.org/10.1002/cben.201600017>
- Wang D, Cui L, Chang X, Guan D (2020) Biosynthesis and characterization of zinc oxide nanoparticles from Artemisia annua and investigate their effect on proliferation, osteogenic differentiation and mineralization in human osteoblast-like MG-63 Cells. *J Photochem Photobiol B Biol* 202:111652. <https://doi.org/10.1016/j.jphotobiol.2019.111652>
- Wang L, Wu Y, Xie J et al (2018) Characterization, antioxidant and antimicrobial activities of green synthesized silver nanoparticles from Psidium guajava L. leaf aqueous extracts. *Mater Sci Eng C* 86:1–8. <https://doi.org/10.1016/j.msec.2018.01.003>
- Webster D, Taschereau P, Belland RJ et al (2008) Antifungal activity of medicinal plant extracts; preliminary screening studies. *J Ethnopharmacol* 115:140–146. <https://doi.org/10.1016/j.jep.2007.09.014>
- Wild S, Roglic G, Green A et al (2004) Global prevalence of diabetes: estimates for the year 2000 and projections for 2030. *Diabetes Care* 27:1047–1053. <https://doi.org/10.2337/diacare.27.5.1047>
- Wu J, Lin Z, Weng X et al (2020) Removal mechanism of mitoxantrone by a green synthesized hybrid reduced graphene oxide @ iron nanoparticles. *Chemosphere* 246:125700. <https://doi.org/10.1016/j.chemosphere.2019.125700>
- Yazdi MET, Amiri MS, Hosseini HA et al (2019) Plant-based synthesis of silver nanoparticles in Handelia trichophylla and their biological activities. *Bull Mater Sci* 42:155. <https://doi.org/10.1007/s12034-019-1855-8>
- Yew YP, Shameli K, Miyake M et al (2020) Green biosynthesis of superparamagnetic magnetite Fe<sub>3</sub>O<sub>4</sub> nanoparticles and biomedical applications in targeted anticancer drug delivery system: a review. *Arab J Chem* 13:2287–2308. <https://doi.org/10.1016/j.arabjc.2018.04.013>
- Yin IX, Zhang J, Zhao IS et al (2020) The antibacterial mechanism of silver nanoparticles and its application in dentistry. *Int J Nanomedicine* 15:2555–2562. <https://doi.org/10.2147/IJN.S246764>
- Younis IY, El-Hawary SS, Eldahshan OA et al (2021) Green synthesis of magnesium nanoparticles mediated from Rosa floribunda charisma extract and its antioxidant, antiaging and antibiofilm activities. *Sci Rep* 11:16868. <https://doi.org/10.1038/s41598-021-96377-6>

- Yousaf H, Mehmood A, Ahmad KS, Raffi M (2020) Green synthesis of silver nanoparticles and their applications as an alternative antibacterial and antioxidant agents. *Mater Sci Eng C* 112:110901. <https://doi.org/10.1016/j.msec.2020.110901>
- Youssef KA, Haggag EG, Elshamy AM et al (2019) Anti-Alzheimer potential, metabolomic profiling and molecular docking of green synthesized silver nanoparticles of *Lampranthus coccineus* and *Malephora lutea* aqueous extracts. *PLoS ONE* 14:e0223781. <https://doi.org/10.1371/journal.pone.0223781>
- Yu Z, Wang W, Kong F et al (2019) Cellulose nanofibril/silver nanoparticle composite as an active food packaging system and its toxicity to human colon cells. *Int J Biol Macromol* 129:887–894. <https://doi.org/10.1016/j.ijbiomac.2019.02.084>
- Zayed MF, Mahfoze RA, El-kousy SM, Al-Ashkar EA (2020) In-vitro antioxidant and antimicrobial activities of metal nanoparticles biosynthesized using optimized *Pimpinella anisum* extract. *Colloids Surfaces A Physicochem Eng Asp* 585:124167. <https://doi.org/10.1016/j.colsurfa.2019.124167>
- Zhaleh M, Zangeneh A, Goorani S, et al (2019) In vitro and in vivo evaluation of cytotoxicity, antioxidant, antibacterial, antifungal, and cutaneous wound healing properties of gold nanoparticles produced via a green chemistry synthesis using *Gundelia tournefortii* L. as a capping and reducing agent. *Appl Organomet Chem* 33:e5015. <https://doi.org/10.1002/aoc.5015>
- Zhang M, Zhang K, De Gusseme B et al (2014) The antibacterial and anti-biofouling performance of biogenic silver nanoparticles by *Lactobacillus fermentum*. *Biofouling* 30:347–357. <https://doi.org/10.1080/08927014.2013.873419>
- Zheng B, Kong T, Jing X et al (2013) Plant-mediated synthesis of platinum nanoparticles and its bioreductive mechanism. *J Colloid Interface Sci* 396:138–145. <https://doi.org/10.1016/j.jcis.2013.01.021>

**Publisher's Note** Springer Nature remains neutral with regard to jurisdictional claims in published maps and institutional affiliations.